FORSCHUNGSZENTRUM JÜLICH GmbH

Institut für Reaktorwerkstoffe

An Analysis of Creep Deformation and Rupture by the β-Envelope Method

V.M. Radhakrishnan, P.J. Ennis, H. Schuster

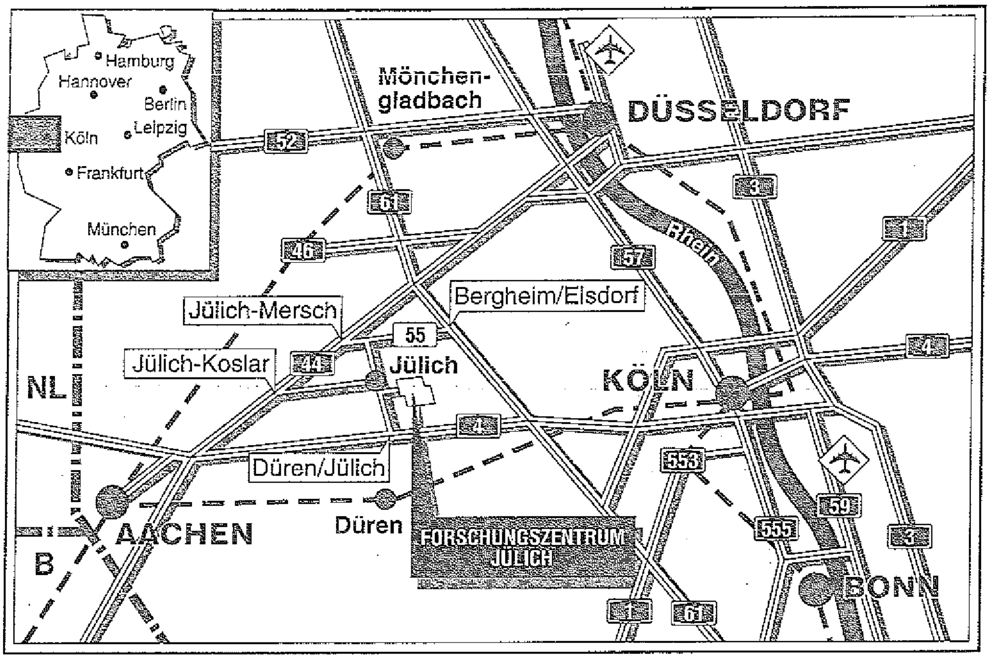

Berichte des Forschungszentrums Jülich ; 2535
ISSN 0366-0885
Institut für Reaktorwerkstoffe Jül-2535

Zu beziehen durch: Forschungszentrum Jülich GmbH · Zentralbibliothek
Postfach 1913 · D-5170 Jülich · Bundesrepublik Deutschland
Telefon: 02461/61-6102 · Telefax: 02461/61-6103 · Telex: 833556-70 kfa d

An Analysis of Creep Deformation and Rupture by the β-Envelope Method

V.M. Radhakrishnan*, P.J. Ennis, H. Schuster

* On Sabbatical Leave from the Department of Metallurgical Engineering, Indian Institute of Technology, Madras-600036, India.

AN ANALYSIS OF CREEP DEFORMATION AND RUPTURE BY THE ß-ENVELOPE METHOD

by

V.M. Radhakrishnan
P.J. Ennis
H. Schuster

Abstract

For several decades creep deformation and fracture have been analysed by parameters such as steady state creep rate $\dot{\varepsilon}_{min}$ and rupture time t_r. However, the relations based on these parameters contain a number of constants which are themselves dependent on the variables. For example, in Norton's equation for the steady state creep rate

$$\dot{\varepsilon}_{min} = A.\sigma^n$$

where A and n are constants, σ the applied stress, the exponent n may depend on the stress itself. Further, structural changes may take place during creep deformation which are not properly reflected in the relation.

Recently early approaches based on creep equations have been revived to describe the creep deformation and fracture. In this report creep equations of the type

$$\varepsilon_1 = \beta_1 t^{1/3}$$
$$\varepsilon_2 = \beta_2 t$$
and
$$\varepsilon_3 = \beta_3 t^3$$

where ε_1, ε_2, ε_3 are the creep strains in the primary, secondary and tertiary stages, β_i the respective coefficients and t the time, are used to envelope the creep strain data on the log-log plot of creep strain versus time. Based on this approach the creep behaviour of the following engineering materials has been analysed:

- X10 NiCrAlTi 32 20 (Alloy 800 H)
- 13 CrMo 4 4 (1 Cr- 0.5 Mo) steel in both new and service exposed conditions
- 14 CrMoV 6 3 (0.5 Cr- 0.5 Mo - 0.25 V) steel
- a Ni-base superalloy.

The analysis leads to an important modification of the Dobès-Milicka rule, namely, that the minimum creep rate $\dot{\varepsilon}_{min}$ and the rupture time t_r are related not only to the creep rupture strain ε_r but also to the creep strain at the end of the second stage ε_{23}, given in the form

$$\dot{\varepsilon}_{min}\, t_r = \sqrt[3]{\varepsilon_{23}^2 \cdot \varepsilon_r}$$

Eine Analyse der Kriechverformung und der Zeitstandfestigkeit mit Hilfe der "ß-Envelope"-Methode

von

V.M. Radhakrishnan
P.J. Ennis
H. Schuster

Kurzfassung

Während langer Zeit wurden für technische Anwendungen Kriechverformung und Kriechbruch allein durch die stationäre Dehnrate und die Bruchzeit beschrieben. Es zeigte sich dabei, daß die Gleichungen für diese Größen eine erhebliche Zahl von Koeffizienten enthalten, die selbst wieder von den Variablen abhängen. Es ist z. B. der Exponent n der Norton'schen Gleichung

$$\varepsilon_{min} = A \circ \sigma^n \qquad \text{(A: Konstante, } \sigma\text{: einwirkende Spannung)}$$

deutlich spannungsabhängig. Eine solche Gleichung kann auch die Einflüsse einer Gefügeänderung, die oft mit der Kriechverformung einhergeht, nicht beschreiben.

Nun sind in letzter Zeit wieder ältere Ansätze verwendet worden, um Kriechverformung und -bruch zu beschreiben. Von Interesse sind die einfachen Formulierungen, die eine leicht handhabbare mathematische Beschreibung der Basisdaten ermöglichen sollen.

In diesem Bericht werden Gleichungen algebraischen Types, wie z. B.

$$\varepsilon_1 = \beta_1 t^{1/3} \qquad \varepsilon_2 = \beta_2 t \qquad \varepsilon_3 = \beta_3 t^3$$

(ε_i: Kriechdehnungen, β_i: Koeffizienten, t: Einwirkungsdauer) verwendet, um gemessene Kriechkurven zu approximieren. Auf diesem Wege wurde das Kriechverhalten von

X10 NiCrAlTi 32 20 (Alloy 800H)
13 CrMo 4 4 (1Cr-0,5Mo-Stahl)
14 MoV 6 3 (0,5Cr-0,5Mo-0,25V-Stahl)
einer Ni-Basis-Legierung

formuliert.

Die Analyse zeigt, daß diese einfachen Gleichungen die Daten in weiten Bereichen gut beschreiben, und daß die funktionellen Abhängigkeiten der Koeffizienten eine vernünftige Extrapolation über den experimentell erfaßten Bereich hinaus gestatten.

Daneben läßt sich aus diesen Gleichungen eine neue Beziehung für die Konstante der Monkman-Grant-Gleichung definieren:

$$\varepsilon_{min}\, t_r = \sqrt[3]{\varepsilon_{23}^2 \circ \varepsilon_r}$$

wobei ε_{23} die Kriechdehnung am Ende des stationären Kriechens und ε_r die Kriechbruchdehnung sind.

CONTENTS

NOMENCLATURE

$A_1, A_2, A_3, \ldots$	Constants
$B_1, B_2, B_3, \ldots$	Constants
d	Grain size
F	Function
m, m_1, m_2	Exponents
n	Power law stress exponent
p, q	Exponents
Q_c, Q_1, Q_2, Q_3	Apparent activation energy for creep
R	Gas constant
T	Temperature
t	Time
t_r	Rupture time
z	Exponent
$\beta_i, \beta_1, \beta_2, \beta_3$	Coefficients in the ß-envelope method
$\beta'_1, \beta'_2, \beta'_3$	Coefficients in Graham-Walles equation
$\theta_i, \theta_1, \theta_2, \theta_3, \theta_4$	Coefficients in θ-Projection method
$\varepsilon, \varepsilon_1, \varepsilon_2, \varepsilon_3$	Creep strain
$\dot{\varepsilon}_{min}$	Minimum (secondary or steady state) creep rate
ε_r	Creep rupture strain
σ	True stress
σ_o	Initial stress in creep experiments under constant load

1. Introduction

1.1 Creep problems and anomalies

The classical form of the time dependent creep deformation exhibits three stages, namely primary, secondary, and tertiary creep. Typical variations of creep strain ε and creep strain rate $\dot{\varepsilon}$ with time t at constant stress are shown in Fig. 1. In the first stage from A to B (curve II) the creep rate decreases with time. As the second stage is approached, the creep rate becomes constant at $\dot{\varepsilon}_{min}$ in the region B to C. Then the tertiary stage (C to D) sets in where the creep strain and the creep strain rate increase with time. However, in some materials under certain conditions of loading, the steady state period from B to C may be absent and the creep deformation will consist of primary and tertiary stages only as shown by curve III in Figure 1. This happens under high stress levels. Under certain other conditions, the primary creep may be absent, as shown by curve I, the secondary creep may be very small and the creep deformation will be dominated by the tertiary creep. Thus, we find that steady state creep rate, characterized by the constant creep rate $\dot{\varepsilon}_{min}$, which is normally used to analyse creep deformation, may not be present in some cases. Usually $\dot{\varepsilon}_{min}$ cannot represent the complete deformation and may deviate significantly from the creep rate in the creep strain region permitted for technical use (i.e. less than 5 % strain).

The steady state creep regime is governed by different mechanisms depending on stress, σ, and temperature, T. These are

a) dislocation climb mechanism leading to a power law creep rate equation (Norton);

b) creep controlled by atomic diffusion through the grain interior or along the grain boundaries - Nabarro-Herring mechanism or Coble mechanism - leading to a linear creep rate equation. The steady state creep rate in general is given by

$$\dot{\varepsilon}_{min} = A_1 \sigma^n \left(\frac{1}{d}\right)^z \exp(-Q_c/RT) \qquad (1)$$

where d is the grain size, Q_c the activation energy and RT has its usual meaning. A_1, n and z are constants. In power law creep the stress exponent n takes values from 3 to 20 or even more. It does not depend on the grain size d and hence z = zero. In Nabarro-Herring creep, n = 1 and z = 2 and in Coble creep n = 1 and z = 3. Q_c will change accordingly.

Based on the creep rate equations governed by these mechanisms, the creep deformation regions can be represented on a σ-T plane and a typical "deformation map" is shown in Fig. 2 for titanium at three grain sizes /1/. As the grain size d is increased, it can be seen that the dislocation glide zone expands. Regions of Coble and Nabarro-Herring (N-H) diffusion creep shrink. Consider a point (A) at a given stress and temperature (σ-T) in the power law region with d = 20 μm. If the grain size is increased (σ and T remaining constant), the point (A) comes to the dislocation glide zone. If d is decreased, it comes to the N-H creep region. Thus we find that the grain size will very much affect the creep mechanism.

The constants A_1, n and Q_c in eqn(1) are constants for limited regions of temperature and the applied stress. Thus the above equation for the steady state creep rate is not a law with general applicability. At high stresses, the phenomenon of power law breakdown takes place and the steady state creep rate, changes from

$$\mathring{\varepsilon}_{min} = A_2 \ \sigma^n \ \exp(-Q_c/RT) \qquad (2)$$

to

$$\mathring{\varepsilon}_{min} = A_3 \ \exp(B\,\sigma)\ \exp(-Q_c/RT) \qquad (3)$$

At low stresses deformation by diffusional displacement of atoms governs the creep rate and n tends to one.

In alloys strengthened by dispersed particles or precipitates, such as thoria particles in TD Nickel, the activation energy Q_c and the stress exponent n are both increased. In TD Nickel, Q_c = 795 kJ/mole and n is extremely stress dependent with values up to 40, as compared to Q_c = 276 kJ/mole and n = 5 for nickel /2/. Similarly, fine carbide precipitates in a ferrite alloy matrix in Cr-Mo steel gives Q_c = 600 kJ/mole and n = 14 compared to the activation energy for lattice diffusion in the ferrite matrix which is about 250 kJ/mole /3/. The large Q_c values should be considered in relation to the fact that processes associated with Q_c values greater than about 400 kJ/mole would lead to very slow creep rates at 0.5 to 0.66 T_m. Thus, with sintered aluminium powder (SAP), the presence of a fine Al_2O_3 dispersion leads to n = 10 and Q_c = 625 to 1675 kJ/mole whereas n = 5 and Q_c = 142 kJ/mole is obtained for pure aluminium under comparable conditions.

Thus the anomalously high n and Q_c values at intermediate stresses are problems encountered when the creep characteristics of particle strengthened alloys are considered using conventional steady state approaches. Grain boundary diffusion is assumed to control the creep rate at low stress levels with $n = 1$. However, the $n = 1$ region can also be obtained in single crystals under appropriate conditions of stress and temperature.

The above anomalies can be better overcome by adopting a method based on a creep equation which will describe the complete creep curve over a wide range of stress and temperature.

1.2 Creep equations

A creep equation in its general form defines in terms of a mathematical formula the creep deformation and related phenomena. Many creep equations have been developed to describe the primary, secondary and tertiary stages. An early account of these equations is given by Garofalo /4/ and more recently by Miller /5/. Primary creep is given by equations of the type

$$\varepsilon = A_1 \; t^{m_1} \tag{4}$$

$$\varepsilon = A_2 \; (1 - \exp(-A_3.t)) \tag{5}$$

$$\varepsilon = A_4 \; \ln (1 + A_5.t) \tag{6}$$

where A_i are stress and temperature dependent constants. The exponent m_1 has values less than unity. Many of the theories behind these formulae describe the creep rate in the first stage considering stress induced strain hardening and thermal softening as the competing mechanisms.

For the secondary stage a steady state creep rate is assumed giving the creep strain ε directly proportional to time, so that

$$\varepsilon = A_6 \, t \tag{7}$$

As indicated earlier, a number of theories have been developed to establish the functional relationship of A_6 with stress and temperature. Tertiary creep is described by relations of the type

$$\varepsilon = A_7 \; t^{m_2} \tag{8}$$

$$\varepsilon = A_8 \ (\exp(A_9 t) - 1) \tag{9}$$

The exponent m_2 is greater than one.

1.3 Application and limitation

The application of generalized creep equations to describe the creep deformation behaviour of materials has been found to be useful in solving some problems where large tertiary creep strains are encountered and the conventional steady state creep rate approach is not suitable. Though there are a number of equations suggested in the literature, two among them are considered here - one due to Graham and Walles /6/ and the other due to Evans et al. /7/. They are given in the form

$$\varepsilon = \beta'_1 \, t^{1/3} + \beta'_2 \, t + \beta'_3 \, t^3 \tag{10}$$

and

$$\varepsilon = \theta_1(1 - \exp(-\theta_2 t)) + \theta_3 \ (\exp(\theta_4 t) - 1) \tag{11}$$

In both the equations the coefficients β'_i and θ_i are dependent on stress and temperature. In the first case, the temperature and stress dependence of each term has the general form

$$\beta_i = C \, \sigma^r \ (T' - T)^{-20k}$$

(12)

where σ, t and T are stress, time and temperature respectively. C, r, T', k and z are constants which may differ from term to term. The constant k takes the values from the sequence 1/3, 1 and 3 as shown in equation (10). In the second case the stress and temperature dependence of θ_i is given as

$$\log \theta_i = \theta_{io} + \theta_{i1}\sigma + \theta_{i2}T + \theta_{i3}\sigma \, . \, T \tag{13}$$

where i = 1, 2, 3, and 4. In all 15 to 16 equations have to be fitted to experimental data and the coefficients are determined by non-linear regression analysis.

The equation suggested by Graham and Walles is a very simple formulation to describe creep strain data. Computing time is minimised because the equation is linear in parameters. This algebraic formulation may furthermore be used to check the quality of more sophisticated constitutive equations and a formulation for multi-axial stresses is easily achievable. Evans and Wilshire /8/ while discussing the above equation mention that the coefficients β'_i do not always behave in a systematic manner with stress, so that they cannot form a reasonable basis even for creep curve interpolation. Thus, they pointed out that the value of β'_2 underestimates the measured minimum creep rate. They have also found, in one case, a negative value of β'_2, which is difficult to rationalize. This problem can be avoided by using a graphical procedure which defines the value of β'_2 as the minimum creep rate. Then the values of β'_1 and β'_3 are estimated from the expression

$$\varepsilon - \beta'_2 t = \beta'_1\, t^{1/3} + \beta'_3\, t^3 \tag{14}$$

With this approach the magnitudes of the coefficients scale with stress. However, the graphical method assumes that the steady state creep exists in all cases - which may not be true under certain conditions of loading.

In contrast, the θ-projection method (equation 11) suggested by Evans et al. assumes the creep strain to be composed of two terms , namely, a primary or decaying component represented by θ_1 and θ_2 and the tertiary or accelerating component defined by θ_3 and θ_4. The terms θ_1 and θ_3 act as scaling parameters describing the extent of primary and tertiary stages with respect to strain and θ_2 and θ_4 will characterize the shape of the primary and tertiary components. The steady state creep stage is taken to be absent in the θ-projection method.

The minimum creep rate, $\dot{\varepsilon}_{min}$, in the case of Graham-Walles can be given in the form

$$\dot{\varepsilon}_{min} = \frac{1}{3}\beta'_1 \left[\frac{1}{27}\frac{\beta'_1}{\beta'_3}\right]^{-1/4} + \beta'_2 + 3\beta'_3 \left[\frac{1}{27}\frac{\beta'_1}{\beta'_3}\right]^{3/4} \tag{15}$$

The above relation can be simplified and given in the form

$$\dot{\varepsilon}_{min} = 1.01 \sqrt[4]{\left(\beta'^3_1 \cdot \beta'_3\right)} + \beta'_2 \tag{15a}$$

This equation clearly points out that β'_2 is not equal to the minimum creep rate which is contributed by the other two coefficents β'_1 and β'_3. Thus if the first term on the

This equation clearly points out that β'_2 is not equal to the minimum creep rate which is contributed by the other two coefficents β'_1 and β'_3. Thus if the first term on the right hand side is greater than the minimum creep rate then this will result in a negative value of β'_2. This is what has been observed in the analysis of Evans and Wilshire /8/ as discussed above.

In the case of the θ-projection method, the minimum creep rate is given by the following equation

$$\dot{\varepsilon}_{min} = \theta_1 \theta_2 \left[\frac{\theta_3 \theta_4^2}{\theta_1 \theta_2^2} \right]^{\theta_2/(\theta_2+\theta_4)} + \theta_3 \theta_4 \left[\frac{\theta_1 \theta_2^2}{\theta_3 \theta_4^2} \right]^{\theta_4/(\theta_2+\theta_4)} \qquad (16)$$

Once the coefficients β'_i and θ_i have been determined, the minimum creep rate can be calculated from the above relations.

In terms of goodness of fit, there is little to choose between Graham-Walles equation (10) and Evans et al. equation (11), and, irrespective of the creep curve equation chosen, the problem of establishing the values of the coefficients remains.

In their analysis of creep behavioural models for gas turbine alloys, Candler and Winstone /9/ point out that both the above mentioned methods have similar success in predicting creep strain with similar limitations with respect to temperature range validity. In both cases the computer time involved is quite high. The cost of performing an analysis using the θ-projection technique is higher since it requires a powerful computer and extensive complex software. Further, incomplete data sets cannot be analysed. It is also important to ensure that the input data used for evaluating the coefficients is evenly distributed throughout the creep curve. Otherwise the coefficients calculated will lead to wrong predictions.

The Graham-Walles equation can be extended to cyclic creep, as the equation has a simple analytical solution and the cyclic creep curve can be constructed from static data /9/. The θ-projection does not have an analytical solution for time and hence is difficult to extend to cyclic creep. Both equations, naturally, cannot cover transient effects caused by a rapid stress increment.

1.4 Concept of ß-envelope method

The ß-envelope method is basically a graphical method. In general the creep strain versus time data on a log-log plot can be enveloped by three straight lines given by equations of the type

$$\varepsilon_1 = \beta_1 \, t^{x_1}$$

$$\varepsilon_2 = \beta \, t^{x_2}$$

$$\varepsilon_3 = \beta_3 \, t^{x_3} \tag{17}$$

The exponents x_i give the slope of the straight lines in the respective regions. Generally the assigned values of the exponent are $x_1 = 1/3$, $x_2 = 1$ and $x_3 = 3$ and the resulting components correspond to those suggested by Graham and Walles, though here each stage is considered separately by one equation.

The data points and the enveloping straight lines with slopes 1/3, 1 and 3 in the three stages of creep are schematically shown in Fig. 3. The data points in each region are taken separately and the formulae may be fitted by a least squares fit method.

The main advantages of this method are:

a) Since it is a "graphical" method it is easy to apply. Simple calculations will be sufficient to apply the least squares fit to the data.

b) Since each stage is considered separately, the data of one stage does not affect the analysis of the other. This leads to the important advantage that insufficient data, that is, data of experiments conducted only up to the second stage for example, can also be handled and analysed.

c) As will be given in a quantitative form later, the termination of the first or the second stage can be given in terms of the coefficients β_1, β_2 and β_3.

d) In a particular temperature-stress range, if any one stage is not present, the coefficient β_i corresponding to that stage may be taken to be zero. Thus the total strain up to a given time can be easily calculated in any range of stress and temperature.

e) Metallurgical changes contributing to strengthening or weakening of the material will automatically reflect on the coefficients.

The disadvantages are:

a) The method requires some skill on the part of the data analyst in fitting the data points in the respective stages.

b) As in any other type of creep equation, the final fracture strain cannot be described by this method. The fracture strain has to be defined so that the rupture time can be computed.

2. Data Acquisition

Four materials have been analysed for their creep and creep rupture behaviour, namely

a) X10 NiCrAlTi 32 20 (Alloy 800H)

b) 13 CrMo 4 4 (1 Cr- 0.5 Mo) steel (both new and service exposed)

c) 14 MoV 6 3 (0.5 Cr- 0.5 Mo- 0.25 V) steel

d) a Ni-base superalloy.

The experimental creep curves for the first two materials (a) and (b) were made available from the creep data bank, Institut für Reaktorwerkstoffe, KFA, Jülich. The stress and temperature ranges are given while discussing the results in the Data Analysis section. The data for the third material have been taken from /7/, who obtained them for the analysis applying the θ-projection method.

The data corresponding to the Ni-base superalloy have been obtained by carrying out creep tests in the temperature range of 1075K to 1125K. This alloy is used in the fabrication of hollow turbine blades. Creep experiments were carried out under constant load. The initial stresses were in the range of 177 to 255 MPa and the maximum rupture time obtained was around 1000 hours. The creep deformation was continuously monitored by an LVDT. The experimental details are given elsewhere /10/.

The nominal chemical compositions of the alloys used in this investigation are given in Table 1.

3. Data Analysis

3.1 Details of ß-envelope method

The ß-envelope method has been employed in the analysis of the creep data of the materials (a), (b) and (d). All fits are carried out with the creep data of these materials, obtained under constant load. For the material (c), for which the data were obtained under constant stress, the Graham-Walles equation was used.

As described earlier, the creep strain - time data points were enveloped by three straight lines on the log-log plot, each representing one stage, namely, the primary, secondary or the tertiary stage. The data points of each stage are considered separately and the creep strain in each is given as

$$\varepsilon_1 = \beta_1 t^{1/3}$$

$$\varepsilon_2 = \beta_2 . t$$

$$\varepsilon_3 = \beta_3 t^3 \qquad (18)$$

The coefficients β_1, β_2,and β_3 are obtained by a least squares fit method. They are dependent on the applied stress and temperature and the functions can be established considering the experimental data.

We denote the creep strain at the junction of stage 1 and stage 2 as ε_{12} and that at the junction of stage 2 and stage 3 as ε_{23}. The rupture strain and the rupture time are ε_r and t_r respectively.

At the transition from stage 1 to stage 2 we have

$$\beta_1 t_{12}^{1/3} = \varepsilon_{12} \quad \text{and} \quad \beta_2 t_{12} = \varepsilon_{12} \qquad (19a, b)$$

Thus we have

$$t_{12} = \sqrt[3/2]{\beta_1 / \beta_2} \qquad (20)$$

Similarly at the transition from stage 2 to stage 3 we have

$$\beta_2 t_{23} = \varepsilon_{23} \quad \text{and} \quad \beta_3 t_{23}^3 = \varepsilon_{23} \qquad (21a,b)$$

Thus we have

$$t_{23} = \sqrt{\beta_2/\beta_3} \tag{22}$$

If the second stage is absent, the transition from stage 1 to stage 3 is given by

$$t_{13} = \sqrt[3/8]{\beta_1/\beta_3} \tag{23}$$

Thus the boundary times of the first and the second stage, namely t_{12} and t_{23}, are defined in terms of the coefficients β_1, β_2, and β_3. Further taking the calculated creep rupture strain and the rupture time as ε_r and t_r, we have

$$\beta_3 \, t^3{}_r = \varepsilon_r \tag{24}$$

Noting that β_2 corresponds to minimum creep rate, ε_{min}, we obtain

$$\frac{\varepsilon_{min} \, t_r}{\sqrt[3]{\varepsilon^2{}_{23} \, \varepsilon_r}} = 1 \tag{25}$$

Thus the product $\varepsilon_{min} \cdot t_r$ is dependent on the creep strain at the end of the second stage and the creep rupture strain. If these strains are independent on the applied stress (or the strain rate), then we obtain the Monkman-Grant relation. In many cases investigated, both strains decrease with decreasing applied stress σ. One may cover this situation by writing

$$(\varepsilon_{min})^p \cdot t_r = \text{constant} \tag{26}$$

where the exponent p is less than one.

The coefficients β_1, β_2 and β_3 are functions of stress and temperature and can be expressed in the simple form as

$$\beta_1 = \beta_{10}\sigma^n \exp(-Q_1/RT)$$

$$\beta_2 = \beta_{2o}\sigma^n \exp(-Q_2/RT)$$

$$\beta_3 = \beta_{3o}\sigma^m \exp(-Q_3/RT) \qquad (27a,b,c)$$

Thus the transition times t_{12} and t_{23} and the transition creep strains ε_{12} and ε_{23} can be obtained in terms the applied stress and the temperature.

3.2 Application of ß-envelope method to creep of different engineering materials.

3.2.1 Validity of the creep equation

In order to check whether the ß-envelope method is applicable for different classes of high temperature alloys, creep data from different sources were collected and plotted on the log-log scale. These experimental data taken from references /11, 12, 13/ were limited in scope and hence the complete analysis could not be carried out on these materials. Nevertheless the data were used to see the applicability of the ß-envelope procedure. Figs. 4, 5 and 6 show the variation of creep strain with time of

1) 12 Cr- 1 Mo - 0.3 V steel

2) 1 Cr- 1 Mo - 0.25 V steel and

3) Type 316 stainless steel.

In the case of the first material, 12Cr-1Mo-0.3 V steel, it is reported that the experiments were conducted only up to the second stage. In the second material, 1Cr-1Mo-0.25 steel, data are given for one stress level only. The specimens were taken from the hot and cold parts of a steam pipe component. In the case of type 316 stainless steel, data for only one temperature are given. Although for the lower stresses the fit is somewhat forced, in general it can be seen that the data points can be well represented by the enveloping straight lines on the log-log plot with slopes equal to 1/3, 1 and 3. Thus it is concluded that the ß-envelope method assumed for the analysis can be successfully applied. However, care should be taken to discard data below, say, one hour duration which will come under hot tensile testing and dislocation glide will be the governing mechanism and hence $t^{1/3}$ law may not be obeyed.

3.2.2 Alloy 800 H

Figures 7, 8 and 9 show the creep strain versus time for Alloy 800 H on the log-log plot. In the temperature range of 800 °C to 900 °C the first stage is almost negligible. We have only the second and the third stages at the perceptible creep strains. The transition strain and time, ε_{23} and t_{23} depend on the stress level. ε_{23} decreases with decreasing stress or decreasing strain rate. Thus at low stress levels, the third stage is more dominant in the technically relevant range of creep strain. Fig. 10 shows the relation between the coefficients β_2 and β_3 and the applied stress σ for different temperatures on log-log plot. The relation is a straight line obeying the stress dependence of the equations

$$\beta_2 = \beta_{2o}\ \sigma^n\ \exp(-Q_2/RT) \qquad \text{and}$$

$$\beta_3 = \beta_{3o}\ \sigma^m\ \exp(-Q_3/RT)$$

The values of the exponents n, m and the constants β_{2o} $\exp(-Q_2/RT)$ and β_{3o} $\exp(-Q_3/RT)$ are given in Table 2.

It can be noted that it is power law creep which governs the deformation in the stress and temperature ranges used. The exponents n and m are dependent on temperature, as shown in Fig. 11. A straight line relationship may be fitted in the working range. Fig. 12 shows the relation between the minimum creep rate $\dot{\varepsilon}_{min}$ and the rupture time t_r on the log-log plot yielding the relation as

$$(\dot{\varepsilon}_{min})^p \cdot t_r = \text{constant}$$

with the exponent p = 1/1.3. It can be noted that the creep strain ε_{23} at the transition from the 2nd stage to the 3rd stage is dependent on the creep strain rate or on stress. It decreases with decreasing $\dot{\varepsilon}_{min}$. Further, the rupture strain ε_r also depends on the stress. Because of scatter an exact relation between these strains and the minimum creep rate could not be established. However, there is general indication that these strains decrease with decreasing creep strain rate or the applied stress. Thus in the generalized relation

$$\frac{\dot{\varepsilon}_{min} \cdot t_r}{\sqrt[3]{\varepsilon_{23}^2 \cdot \varepsilon_r}} = 1$$

the denominator is a function of ε_{min}. Hence we find the exponent p in eqn (26), instead of being equal to one as in the Monkman-Grant relation, is less than one and in this case it is 1/1.3 .

Fig. 13 shows the relation between stress and rupture time on the log-log plot. The full lines are derived from Figures 11 and 12. The data points fall well on the predicted lines. The relation between σ and t_r can be given as

$$(\sigma)^q \cdot t_r = \text{constant}$$

where the exponent q is found to be m/3. Normally it is taken that q is equal to n - the stress exponent in Norton's creep rate equation. But the above analysis clearly shows that it is not so, and the Monkman-Grant relation is not valid. Hence the exponent n should not be used in the stress - rupture time relation because the prediction based on this will overestimate the life extrapolated from short time creep tests. It is better to establish the relation between β_3 and σ and therefrom derive the stress rupture relation, especially when the tertiary creep is extensive and dominant.

Figs. 14(a), (b) and (c) show the creep curves at 900 °C, as given by the creep equation. The fit appears to be good. However, as the data points for determining the coefficients are taken only from these creep curves, a better fit is obtained from the creep equations. As a predictive method, the coefficients obtained are used and the creep curves at lower stress levels of 20 MPa and 15 MPa at 800 °C and 15 MPa and 10MPa at 850 °C are shown in Fig.15. These predicted curves at low stress levels, which may be the actual service condition, will be more useful to the designers of high temperature components.

3.2.3 1 Cr - 0.5 Mo steel

CrMo steels are widely used in the fabrication of steam pipes and other piping systems in power plants. Such parts often work in the temperature region of 530 to 550 °C and are normally designed for a life of above 10^5 hours. However, microstructural changes and environmental conditions might degrade the material resulting in loss of strength. Hence it is necessary to analyse the remaining life of the exposed material so as to have a reliable life prediction and suitable replacement of the component before failure.

Figures 16(a) (b) and (c) show the creep curves of the new 1Cr0.5Mo steel at 530 °C, 550 °C, 600 °C and 625 °C. At the latter two temperatures, the data points are limited and hence the discussion is mainly concentrated on the behaviour at 530 °C and 550 °C. Here again we can see that the three stages of creep can be well distinguished and described by the equations. Not all the data points are shown for the sake of clarity, but all the data points have been used obtain the coefficients. Fig. 17 shows the relation between the coefficients β_2 and β_3 and the applied stress σ on a semi-log plot. The data fit suggests relations of the type

$$\beta_2 = \beta_{20} \exp(B_2\sigma) \exp(-Q_2/RT)$$

$$\beta_3 = \beta_{30} \exp(B_3\sigma) \exp(-Q_3/RT) \qquad (28)$$

These types of exponential dependence on stress are observed in Cr-Mo steels. Noting that β_2 represents the minimum creep rate $\dot{\varepsilon}_{min}$ the relation between $\dot{\varepsilon}_{min}$ and the applied stress is shown in Fig. 18, on a log-log plot for temperatures of 530 °C and 550 °C. The relation is a curve with decreasing slope as the stress decreases. The slope is given by

$$\frac{\log \dot{\varepsilon}_{min}}{\log \sigma} = n \propto \sigma \qquad (29)$$

where n is the stress exponent in Norton's creep rate equation. It decreases with decreasing stress. At lower stress levels its value may tend to unity, indicating a creep mechanism controlled by grain boundary (Coble) diffusion.

Fig. 19 shows the relationship between $\dot{\varepsilon}_{min}$ and t_r on a log-log plot. Here also it can be observed that a relation of the type

$$(\dot{\varepsilon}_{min})^p \cdot t_r = \text{constant}$$

appears to be valid with $p = 1/1.3$. This is mainly because the creep strains ε_{23} and ε_r are dependent on the stress level, both decreasing as the stress is decreased.

The relation between log σ and log t_r as derived from Figures 18 and 19 is shown in Fig. 20. The relation at each temperature is not a straight line, but is curved. Extrapolation of short time data will result in overestimation of actual life at lower stress levels.

Materials from service - exposed components have also been creep tested. The component has faced a service temperature of 530 °C for a period of 2.6 x 10^5 hours. Specimens were made from the component material and tested at 530 °C and 550 °C. Limited experiments at 600 °C and 625 °C were also carried out.

Figs. 21(a), (b) and (c) show the creep strain variation with time on the log-log plot. Only limited data are shown on the graph to distinguish the three regions. At 530 °C and 550 °C the three stages are clearly seen. At 600 °C and 625 °C the first stage could not be obtained in the range of creep strain represented in the figure.

Fig. 22 shows the variation of log β_2 and log β_3 with applied stress. As in the case of new material, here also we have an exponential function of stress governing the variation of β_2 and β_3, given by the equations

$$\beta_2 = \beta_{2o} \exp(B_2\sigma) \exp(-Q_2/RT)$$

$$\beta_3 = \beta_{3o} \exp(B_3\sigma) \exp(-Q_3/RT)$$

As the data points at 600 and 625 °C are limited, the above relations are not attempted in these temperature regions. The relation between the minimum creep rate $\dot{\varepsilon}_{min}$ and the applied stress σ is shown in Fig. 23 on a log-log plot. For the sake of comparison the same relation for new material is included in the figure. As in the case of new material, the relation between log $\dot{\varepsilon}_{min}$ and log σ is a curve with decreasing slope as the stress is decreased. This implies that the creep stress exponent n decreases with the applied stress.

A comparison between the behaviour of new and service exposed materials is given below to show that the β-envelope method can take care of the structural changes in the materials if they happen in service.

Comparing the results of both the new and the service exposed materials, it can be seen that, in general, the minimum creep rate of service exposed material is higher than that of the new material, especially at high stress levels. At low stresses the difference is small.

Creep properties of ferritic steels are greatly affected by the size and distribution of the carbides. The fine carbide dispersion in the matrix, which will initially strengthen the material, coarsens on exposure to high temperature for a long duration. Metastable carbides of the type M_3C, MC and M_2C coarsen in the range of 500 to 700 °C obeying the Oswald $t^{1/3}$ kinetics. These agglomorated carbides will reduce the resistance to creep deformation. As a result the creep properties of new material will be superior to that of a service exposed material. Further the applied stress also plays a role in determining the nature of the internal resistance to deformation. In their analysis of the impact of structural instability on the extrapolation of short term creep test results, Steen and de Witte /14/ have shown two regions of stress levels, as indicated in Fig. 24(a); a high stress region in which Orowan looping around the incoherent carbide precipitates will be the dominant mechanism, and an intermediate stress region where the dislocations surmount the carbides by climb and so deformation is much less dependent on the precipitation characteristics. They have also shown that the boundary between high stress-low stress regions is dependent on the temperature as shown in Fig. 24(b).

It has been pointed out /15, 16/ that, at low stress levels in particle strengthened alloys with very dense dispersions, the dislocations may be completely immobilized by the particles resulting in very low strain rates during the primary creep. It is suggested /15/ that the remaining mechanism to cause perceptible creep is diffusion at the grain boundaries. The creep stress exponent is very low, almost equal to unity. However, as the true stress increases, the dislocation climb mechanism is activated and power law creep takes over. In contrast, the deformation at intermediate and high stress levels is by the continued movement of dislocations by climb process.

Both the changed structure due to service exposure and the different mechanisms of deformation due to high and low stress levels give rise to the different behaviour of the new and the service exposed materials. At low stress levels the difference between the creep lives of new and service exposed materials is not very large. The time to fracture is long enough to age and overage the new material, making its structure comparable to that of the service exposed material. But at high stress levels the difference in structures is important and creep rate of the exposed material will be higher than that of the new material. Such enhanced creep rate at high stress levels for service exposed material as compared to regenerated material can be seen in the analysis of Sklenicka et al. /17/.

Thus we find that the ß-envelope method can take care of the structural changes due to service conditions and will be able predict the behaviour according to the condition of the material.

Fig. 25 shows the relation between ε_{min} and the rupture time t_r. The full line is for the new material on which the data points of service exposed material are plotted. Thus, the relation

$$(\dot{\varepsilon}_{min})^{1/1.3}\ t_r = \text{constant}$$

is also valid for service exposed material.

Fig. 26 shows the σ - t_r relation on a log-log plot for both new and exposed materials. The full lines are for new materials. It can be seen that at low stress levels the rupture time of the exposed material approaches that of the new material. At high stresses the rupture life of exposed material is very much reduced. This is reflected in the ε_{min} - σ relation with higher values of ε_{min} at high stress levels as compared to that of new material.

In their comparison of Larson-Miller Parameter (LMP) for data of pre-exposed materials and the ASTM scatter band, Liaw et al /18/ found that the data points pertaining to high stress levels fell outside the scatter band and the LMP values were less than those of new material. Their results are shown in Fig. 27. Such a different behaviour could be understood based on the different dominant mechanisms that control the deformation.
Though the mechanisms are different, we find in the analysis that the ß-envelope method can be effectively applied to predict of the creep behaviour and rupture life of the materials both in the new and service exposed conditions and to make a comparison between the two.

3.2.4 0.5 Cr- 0.5 Mo - 0.25 V steel

This material has been investigated by Evans et al. /7/ to consider the applicability of the θ- projection method. The same data were analysed by Brown /19 / who has shown the merits and demerits of different creep equations. Without going into the details of the other creep equations, we can consider whether the data presented in the above literature could be analysed based on Graham Walles method which is a modified form of the ß-envelope method. As the base data are not available this indirect method is resorted to. The difference between the Graham Walles method and the ß-envelope method is that the coefficients β'_i in Graham Walles equation will be slightly smaller than those of the ß-envelope method, because in Graham Walles method it is a generalised equation and each term representing each stage of creep is affected by the other terms as well. In the ß-envelope method one strain-time relation is considered for each region separately and hence the coefficients β_i will not be influenced by other terms.

The coefficients β'_1 , β'_2 and β'_3 have been obtained by non-linear regression analysis and the variation of the coefficients with stress is expressed in the form

$$\log \beta'_i = C + D\,\sigma \tag{30}$$

where C and D are constants. The data pertain to the temperature of 565 °C. The relation between the coefficients and the stress is shown in Fig. 28. The time is expressed in seconds. Using these coefficients the creep curves were reconstructed and thus the calculated creep curve at a stress level of 200 MPa is shown in Fig. 29 /20 /. In this relation the upper limit for creep strain at rupture ε_r is assumed to be constant. Then the rupture time corresponding to this limit can be obtained. The creep rupture strain ε_r at 565 °C is around 0.15. Its variation with applied stress level is negligible. Thus taking $\varepsilon_r = 0.15$ at all stress levels, the rupture times t_r for different stress levels have been computed and the relation between log σ and log t_r is shown in Fig. 30. The rupture data points of the material at 550 °C and 575 °C are also shown in the figure. Although there is scatter in the experimental data, the predicted line for 565 °C lies between the data points of 550 °C and 575 °C. The relation in the double log plot is not a straight line and hence extrapolation of short time data is not valid.

The minimum creep rate $\dot{\varepsilon}_{min}$ has been calculated based on equation (15) and the relation between $\dot{\varepsilon}_{min}$ and the stress is shown in Fig. 31. The full line represents the calculated values and the experimental points are from /21/. As in the case of 1 Cr-0.5 Mo steel, here also the relation obtained on the double log plot is a curve with decreasing slope with decreasing stress level. Thus the creep stress exponent n decreases with decreasing stress in this CrMoV steel.

3.2.5 Ni-base superalloy

The Ni-base superalloy investigated in this work /22/ formed part of an M.Tech. Thesis /10/. The material is used in the fabrication of cooled turbine blades in aero-engines. The temperature range in service is from 800 °C to 1000 °C. Creep experiments have been carried out under constant load conditions and typical creep curves for different temperatures are shown in Fig. 32 on the log-log plot. The first stage is almost negligible in the range of stress and temperature used. The second and third stage creep strains obey the equations

$$\varepsilon_2 = \beta_2 \, t$$

$$\varepsilon_3 = \beta_3 \, t^3$$

The relation between the coefficients β_2 and β_{32} and the applied stress is shown in Fig. 33 on the log-log plot. The relations are given as

$$\beta_2 = \beta_{2o} \, \sigma^n \, \exp(-Q_2/RT)$$

$$\beta_3 = \beta_{3o} \, \sigma^m \, \exp(-Q_3/RT)$$

The relation on the log-log plot clearly indicates that a simple power law creep governs the creep deformation of this Ni-base superalloy in the stress and temperature range used. The variation of the stress exponents n and m with inverse temperature is shown in Fig.34. Based on these relations and the variation of β_{2o} and β_{3o} as a function of temperature, the dependence of β_2 and β_3 on the stress at the temperature of 775 °C has been computed and the relation is shown in the Figure 33.

The relation between the minimum creep rate and the rupture time is shown in Fig. 35. There is a systematic trend in the data and the slope of the line log $\dot{\varepsilon}_{min}$ versus log t_r has been found to be 1.37. Thus an equation of the type

$$\dot{\varepsilon}_{min}{}^{1/1.37} \circ t_r = \text{constant} \tag{31}$$

has been found to be the best fit.

The predicted variation of creep strain with time at 150 MPa and 100 MPa at temperatures of 802 and 777 °C is shown in Fig. 36. It can be seen that the strain at the end of the second stage, namely ε_{23}, decreases with decreasing stress level or temperature. At low stress level or temperature the tertiary stage appears to be more dominant.

The relation between the stress and rupture time is shown in Fig. 37. The data points are also shown in the figure. Taking the variation in rupture strain with stress level to be negligible in this case, it can be shown from the equations

$$\beta_3 \; t_r^3 \; = \varepsilon_r$$

and

$$\beta_3 \; \alpha \; \sigma^m$$

that the slope of log σ - log t_r will be equal to 1/(m/3). Thus, the predicted rupture relations describe well the experimental data points. The predicted relationship of log σ - log t_r for the temperature 777°C is also shown in the figure.

Thus the ß-envelope method has been found to describe well the experimental data and predict the stress rupture time relation in the case of the Ni-base superalloy.

4. General Discussion

In the development of ß-envelope method a number of relations have been derived in terms of the coefficients β_1, β_2 and β_3. It has also been noted that the creep strain at the end of the secondary stage, ε_{23}, and the creep rupture strain, ε_r, play a role in the Monkman - Grant relation. In this section the results of some published work are discussed in light of the derivations obtained in the ß-envelope method.

Normally the Monkman-Grant relation is given in the form

$$\dot{\varepsilon}_{min} \circ t_r = \text{constant} \tag{32}$$

It has not been found to be suitable for materials showing large tertiary creep. Hence it has been modified by Dobès and Milicka/23/ in the form

$$\frac{\dot{\varepsilon}_{min}\ t_r}{\varepsilon_r} = \text{constant} \tag{33}$$

Let us consider the application of the above relation for the data obtained by Molinie et al. /12/ for the material 1Cr-1Mo-0.25V steel. The material was taken from the cold and hot parts of the high temperature component in a power plant exposed for about 1.5×10^5 hours. It has been shown that the creep rupture strain ε_r decreases with the minimum creep strain rate ε_{min}. The results from cold part material have been found to give a systematic trend, whereas those from the hot part show some scatter. The results are replotted and shown in Fig.38 on a log-log plot which yield a straight line relation according to the equation

$$\varepsilon_r = A'\ \dot{\varepsilon}_{min}{}^{0.33} \tag{34}$$

where A' is a constant.

The relation between $\dot{\varepsilon}_{min}$ and t_r is given by Molinie et al. as

$$\dot{\varepsilon}_{min}{}^{p} \circ t_r = \text{constant} \tag{26}$$

where the exponent p = 1/1.18. Now applying the Dobès-Milicka relation with ε_r given by equation(34), we obtain

$$\dot{\varepsilon}_{min}{}^{0.67} \cdot t_r \;=\; \text{constant} \qquad (35)$$

In other words, the value of p is 1/ 1.5, which is different from what has been reported by Molinie et al.

Now let us consider the relation obtained based on the ß-envelope method. The relation obtained is in the form

$$\frac{\dot{\varepsilon}_{min} \cdot t_r}{\sqrt[3]{\varepsilon_{23}^2 \; \varepsilon_r}} \;=\; 1$$

The variation of the creep strain ε_{23}, either with the stress or with the minimum creep rate has not been reported in the paper. Hence for the time being we take that the strain ε_{23} is not strongly dependent on stress. Then we obtain the relation

$$\frac{\dot{\varepsilon}_{min} \cdot t_r}{\sqrt[3]{\varepsilon_r}} \;=\; \text{constant} \qquad (36)$$

Using the equation (34) for ε_r, we obtain

$$\dot{\varepsilon}_{min}{}^{0.89} \cdot t_r \;=\; \text{constant} \qquad (37)$$

This relation is shown in Fig. 39 on a log-log plot along with the data points of Molinie et al. The results are well described by the above equation. Thus we find that the value of the exponent p is 1/ 1.2 from the above analysis, instead of the value 1/1.8 reported by Molinie et al.

Therefore the relation obtained for the minimum creep rate and the rupture time by the ß-envelope method represents an improvement over the description of the data obtained by Molinie et al.

Additionally, we may consider the results of the service exposed 2.25Cr-1Mo weld material reported by Liaw et al. /18/. Typical relations between the minimum creep rate $\dot{\varepsilon}_{min}$, the rupture time t_r and the normalized rupture time are shown in Fig. 40. The relations of these lines (from bottom to top) as given by Liaw et al are

$$\dot{\varepsilon}_{min}^{0.825} \cdot t_r = \text{constant} \tag{38}$$

$$\frac{\dot{\varepsilon}_{min}^{0.983} \cdot t_r}{\varepsilon_r} = \text{constant} \tag{39}$$

$$\frac{\dot{\varepsilon}_{min}^{1.004} \cdot t_{23}}{\varepsilon_{23}} = \text{constant} \tag{40}$$

(Note the terminologies used by Liaw et al. which are given in the figure for the sake of easy comparison with the original work

$$t_r = t_h, \quad \varepsilon_r = \varepsilon_h, \quad t_{23} = t_p + t_s, \quad \varepsilon_{23} = \varepsilon_p + \varepsilon_s)$$

Equation (40) clearly shows that the relation of the type

$$\beta_2 \, t_{23} = \varepsilon_{23}$$

as obtained in the present ß-envelope method is valid.

Equation (39) is in the form

$$\frac{\dot{\varepsilon}_{min} \cdot t_r}{\varepsilon_r} = \text{constant}$$

Now we consider the relation obtained based on the ß-envelope method, namely,

$$\frac{\dot{\varepsilon}_{min} \cdot t_r}{\sqrt[3]{\varepsilon_{23}^2 \cdot \varepsilon_r}} = \text{constant}$$

Now let us consider the variation of the creep strain ε_{23} with the rupture strain ε_r. The data reported by Liaw et al. are replotted on log-log scale and shown in Fig.41. The results allow a straight line relation with a slope equal to unity and thus we have

$$\log \varepsilon_{23} = \log \varepsilon_r + \text{constant} \tag{41}$$

This means that the strain ε_{23} decreases with minimum creep rate much in the same way as does the rupture strain ε_r for the weld material investigated by Liaw et al. So we have

$$\frac{\dot{\varepsilon}_{min} \cdot t_r}{\sqrt[3]{\varepsilon_{23}^2 \cdot \varepsilon_r}} = \frac{\dot{\varepsilon}_{min} \cdot t_r}{\varepsilon_r} = \text{constant} \tag{42}$$

This is what has been obtained in equation (39)

Equation (38) clearly shows that the equation $\dot{\varepsilon}_{min} \cdot t_r$ = constant is not valid and a modified approach is required for the material used. This modified approach is provided by the ß-envelope method.

Now let us consider the creep data of 316 stainless steel at 600 °C as reported by Hyge /13/. The log - log plot shows that the creep strain at the end of the secondary stage ε_{23} and the rupture strain ε_r are not very much dependent on the creep rate, as can be seen from Figure 6. The minimum creep rate and the corresponding rupture time have been computed from the results reported in the paper by Hyge and this relation is plotted in Fig. 42. The relation obtained clearly shows that an equation of the type

$$\dot{\varepsilon}_{min} \cdot t_r = \text{constant}$$

is valid in this case.

From the above three case studies and discussions it is clear that the generalized relation is applicable to all the materials. The Monkman-Grant and Dobes-Milicka relations are only particular forms of this generalized relation.

Another important finding in this investigation is the fact that the creep stress exponent n in the relation

$$\dot{\varepsilon}_{min} \propto \sigma^{n} \tag{43}$$

and the stress exponent q in the creep rupture time relation

$$t_r \propto \sigma^{-q} \tag{44}$$

are not the same. n will be equal to q only in the particular case when the Monkman-Grant relation is valid. Otherwise the value of q will be smaller than the value of n and hence extrapolation of short time data on the log σ versus log t_r relation based on the value of n will overestimate the creep life at low stress levels. Hence care has to be exercised in using the value of n in evaluating the creep rupture properties of the material.

In service exposed materials the changed internal structure alters the creep properties and accelerates the creep rate and reduces the rupture life. These changed properties are reflected in the coefficients β_1, β_2 and β_3 in the β-envelope method. Thus while comparing the properties of new material with exposed material care has to be taken in evaluating proper values of the coefficients and their dependence on the structure.

5. Conclusions

At the outset it should be pointed out that there are a number of creep equations which can be applied with varying degrees of success to creep deformation and rupture life. The merit of a particular method can possibly be assessed by its coverage of the stress and temperature ranges, its simplicity and convenience. In considering these aspects the ß-envelope method proposed in the present investigation appears to be suitable for a number of materials over a wide range of stress and temperature.

From the analytical investigations carried out on Alloy 800H, a Ni-base superalloy and two CrMo steels, the following conclusions can be drawn.

1) The creep strain versus time relation on the log-log plot can be conveniently represented by three enveloping straight lines showing the regions of primary, secondary and tertiary creep. In some cases the first stage is absent and the second stage is small. The creep strain in each stage can be represented by

$$\varepsilon_1 = \beta_1 \; t^{1/3}$$

$$\varepsilon_2 = \beta_2 \; t$$

$$\varepsilon_3 = \beta_3 \; t^3$$

2) The coefficients β_i are determined by taking the data points in each stage and fitting them with the respective equations by least squares fit method. Thus each coefficient is not influenced by the other terms in the creep equation.

3) The above approach clearly demarcates the transition points from one stage to the other stage. The transition times t_{12} and t_{23} from the first to second stage and second to third stage are given as

$$t_{12} = \sqrt[3/2]{\beta_1/\beta_2} \quad \text{and} \quad t_{23} = \sqrt{\beta_2/\beta_3}$$

4) The coefficients β_i are dependent on the stress and temperature. The functional form depends on the material. Thus for the austenitic steels and alloys Ni-base alloys the coefficients β_2 and β_3 are given as

$$\beta_2 = \beta_{2o}\ \sigma^n\ \exp(-Q_2/RT)$$

$$\beta_3 = \beta_{3o}\ \sigma^m\ \exp(-Q_3/RT)$$

In the case of ferritic CrMo steels the relations are given as

$$\beta_2 = \beta_{2o}\ \exp(B_2\sigma)\ \exp(-Q_2/RT)$$

$$\beta_3 = \beta_{3o}\ \exp(B_2\sigma)\ \exp(-Q_3/RT)$$

The constants β_{2o}, β_{3o} and Q_2 and Q_3 take different values in each equation.

5) The minimum creep rate and rupture time relation is found to be a function of the creep strain at the end of the second stage and the creep rupture strain and is given by the equation

$$\frac{\dot{\varepsilon}_{min} \cdot t_r}{\sqrt[3]{\varepsilon_{23}^2 \cdot \varepsilon_r}} = 1$$

This equation has been found to describe well the experimental findings in the present investigation and the results reported in the literature. The Monkman-Grant and Dobès-Milicka relations are particular cases of this generalized relation.

6) In the Ni-base superalloy under the load conditions applied, a simple power law given in the form

$$\dot{\varepsilon}_{min} \propto \sigma^n$$

governs the creep rate. In the case of CrMo steels an exponential power law given in the form

$$\dot{\varepsilon}_{min} \propto \exp(B\sigma)$$

governs the minimum creep rate.

7) The minimum creep rate and the rupture time, t_r, can be related by an equation of the type

$$\dot{\varepsilon}_{min}{}^{p} \cdot t_r = \text{constant}$$

The exponent p is less than one. In the present case it is equal to 1/1.3. The above relation is a modification of the relation given in (5) when the creep strains ε_{23} and ε_r are dependent on the minimum creep rate.

8) For the austenitic steels, the stress-rupture time relation in the range of stress and temperature used, can be given in the form

$$t_r \propto \sigma^{-q}$$

The value of the exponent q is not equal to the creep stress exponent n. It is less than n and is equal to q = m/3 as the variation of rupture strain ε_r with stress is not very pronounced in these alloys in the temperature regions used for the testing. For materials where the Monkman-Grant relation is valid, q will be equal to n.

9) In the case of CrMo steels a plot of log σ and log t_r yields curves of drooping nature for different temperatures. Thus extrapolation of short time tests should not be carried out in these cases as it will overestimate the creep life at lower stress levels.

10) In service exposed materials of CrMo steels the changed internal structure due to exposure at elevated temperature alters the creep properties. It accelerates the creep rate and reduces the rupture life, especially at high stress levels. Hence, in evaluating the remaining life of the service exposed components, care has to be taken to quantify the contribution to creep deformation and

rupture life by the changed internal structure. The ß-envelope method can be successfully applied to evaluate the life of the exposed materials as well. The coefficients take different values according to changed structural conditions. The relation between the changed structure and the values of the coefficients can be properly quantified.

Acknowledgement

The first author (V.M.R.) is extremely thankful to Prof.Dr. N.V.C. Swamy, Director, I.I.T., Madras, India, for having granted him Sabbatical Leave during which period most of the above analytical work was carried out. He is also thankful to the Alexander von Humboldt Foundation for for their financial help. He places on record his sincere thanks to Prof.Dr. H. Nickel, Director, Insitutut für Reaktorwerkstoffe, KFA, Jülich, for having provided him all the necessary facilities to carry out the analytical work.

References

1. J.A. Ruppen, C.L. Hoffman, V.M. Radhakrishnan and A.J. McEvily
The effect of environment and temperature on the fatigue behaviour of titanium alloys. Fatigue - Environment and Temperature Effects. Proc. 27th Sagamore Army Materials Research Conference. Bolton Landing, Lake George, New York, Plenum Press, N.Y., (1980) p.265.

2. B.A. Wilcox and A.H. Clauer
Trans. AIME, 236, (1966), p.570.

3. R.J. Browne, B.J. Cane, J.D. Parker,and D.J. Walters
Creep of engineering materials and structures, (eds) B. Wilshire and D.R.J.Owen. Pineridge Press, Swansea, (1981), p.645.

4. F. Garofalo
Fundamentals of creep and creep rupture in metals. McMillan and Co., New York, (1965)

5. A.K. Miller
Unified constitutive equations for creep and plasticity. Elsevier Applied Science, London and New York, (1987).

6. A. Graham and K.F.A. Walles
JISI, 193, (1955), p.255.

7. R.W. Evans, J.D. Parker and B.Wilshire
Recent advances in creep and fracture of engineering materials and structures. (eds) B. Wilshire and D.R.J. Owen. Pineridge Press, Swansea, (1982), p.135.

8. R.W. Evans and B. Wilshire
Creep of Metals and Alloys. The Institute of Metals, (1985) p.192.

9. L.W. Candler and M.R. Winstone
An evaluation of creep behaviour models for gas turbine alloys. High Temperature Materials for Power Engineering, Part II. (eds) E. Bachelet et al. Kluwer Academic Publ., London (1990), p.1077.

10. S. Upadhyay
Characterization of creep fracture of a Ni-base superalloy by parametric methods. M.Tech. Thesis, Metallurgy Department, I.I.T., Madras. (1990).

11. K.H. Kloos, J. Granacher and M. Oehl
Beschreibung des Kriechverhaltens einiger warmfester stähle. Mat.-wiss u. Werkstofftech., 21, (1990) p.265.

12. E. Molinie, R. Piques and A. Pineau
Behaviour of a 1Cr-1Mo-0.25V steel after long-term exposure- Charpy impact toughness and creep properties. Fatigue Fract. Engng. Mater. Struct., 14(5), (1991), p.531.

13. T.H. Hyge
Creep crack growth in 316 stainless steel at 600 °C. J. High Temperature Tech., 6(2)(1988),p.51.

14. M. Steen and M. de Witte
Impact of structural instability on the extrapolation of short term creep test results. In Proc. 3rd Int Conf on Creep and Fracture of Engineering Mater. Struct., (eds) B. Wilshire and R.W. Evans. The Institute of Metals, London, (1987), p.773.

15. H.P. Lahodny
Mechanismenorientierte Dehnratenanalyse zur Lebesdauervorhersage kriechbelasteter Werkstoffe. Fortschritt - Berichte, VDI, Nr. 135, (Düsseldorf), (1987).

16. E. Arzt
Creep of dispersion strengthened materials - A critical assessment. Res Mechanica, 31, (1981), p.399.

17. V. Sklenicka, K. Kucharova, V. Foldyna, and J.Cadek
Interrelationship between creep deformation and creep rupture in a low alloy CrMoV steel after service. Proc. 3rd Inter. Conf. Creep and Fracture of Engng. Mater. Struct., The Institute of Metals, London, (1987), p.361.

18. P.K. Liaw, G.V. Rao and M.G. Burke
Creep fracture behaviour of 2.25Cr-1Mo welds from a 31-year-old fossil plant. Mater.Sci. Engg., A 131,(1991), p.187.

19. S.G.R. Brown
Extrapolation by creep curve shape analysis. Proc. Creep and Fracture of Engng. Mater. Struct., (eds) B. Wilshire and R.W. Evans. The Institute of Metals, London, (1987), p.829.

20. V.M. Radhakrishnan
Analysis of creep curve by constitutive equations. Mater.Sci.Tech., U.K., in press.

21. R.W. Evans and B. Wilshire
A new theoretical and practical approach to creep and creep fracture. Proc. 7th Int. Conf. on Strength of Metals and Alloys. (eds) H.J. McQueen, J.P. Bailon, J.I. Dicson, J.J. Jonas and M.G. Akbar. Pergamon Press, 2, (1985), p.1807.

22. V.M. Radhakrishnan
Characterization of creep deformation of a Ni-base superalloy by a constitutive equation. Proceedings of the 10th Congress on Materials Testing, GTE Scientific Society of Mech. Engrr., Budapest, Hungary, (Oct. 1991).

23. F.Dobes and K. Milicka
Met.Sci., 10, (1976), p.382

Table 1: Chemical composition of test materials, wt %

	Alloy 800H	1Cr0.5Mo new	1Cr0.5Mo service exp	Ni-base superalloy
Fe	bal	bal	bal	-
Cr	20.1	0.93	0.86	14.5
Ni	30.3	-	-	bal
C	0.065	0.13	0.16	0.12
Si	0.36	0.24	0.25	0.14
Mn	0.69	0.51	0.59	0.5
Ti	0.32	-	-	1.6
Al	0.30	-	-	1.8
Mo	-	0.62	0.56	4.8
Nb	-	-	-	0.8
W	-	-	-	2.3
S	0.003	0.008	0.011	-
P	0.010	0.02	0.025	-

- not determined

Table 2: **Values of the constants obtained by the ß-envelope method**

Alloy	Temp °C	n	m	q	$B_{20}\exp(-\frac{Q_2}{RT})$	$B_{30}\exp(-\frac{Q_3}{RT})$	B_2	B_3
800H	800	12.5	27.1	1/9.2	$1.8 \times 10^{-29.5}$	$8.16 \times 10^{-68.1}$	-	-
	850	9.2	21.6	1/7.2	$7.0 \times 10^{-23.2}$	$1.5 \times 10^{-54.6}$	-	-
	900	8.0	17.2	1/5.7	5.9×10^{-20}	$4.0 \times 10^{-46.2}$	-	-
1Cr0.5Mo new	530	-	-	-	$1 \times 10^{-13.36}$	$1 \times 10^{-31.22}$	0.010	0.020
	550	-	-	-	$1 \times 10^{-10.5}$	$1 \times 10^{-27.5}$	0.0068	0.0177
1Cr0.5Mo se	530	-	-	-	$1 \times 10^{-12.5}$	1×10^{-35}	0.0147	0.0434
	550	-	-	-	$1 \times 10^{-11.82}$	$1 \times 10^{-33.5}$	0.0140	0.0456
Ni-base Superalloy	777	15.5	26.4	1/8.8	$1 \times 10^{-40.7}$	$1 \times 10^{-71.1}$	-	-
	802	11.8	20.9	1/7.0	$1 \times 10^{-31.35}$	$1 \times 10^{-56.9}$	-	-
	827	8.75	15.0	1/5.0	1×10^{-24}	1×10^{-42}	-	-
	852	4.8	9.25	1/3.1	$1 \times 10^{-14.36}$	$1 \times 10^{-26.95}$	-	-

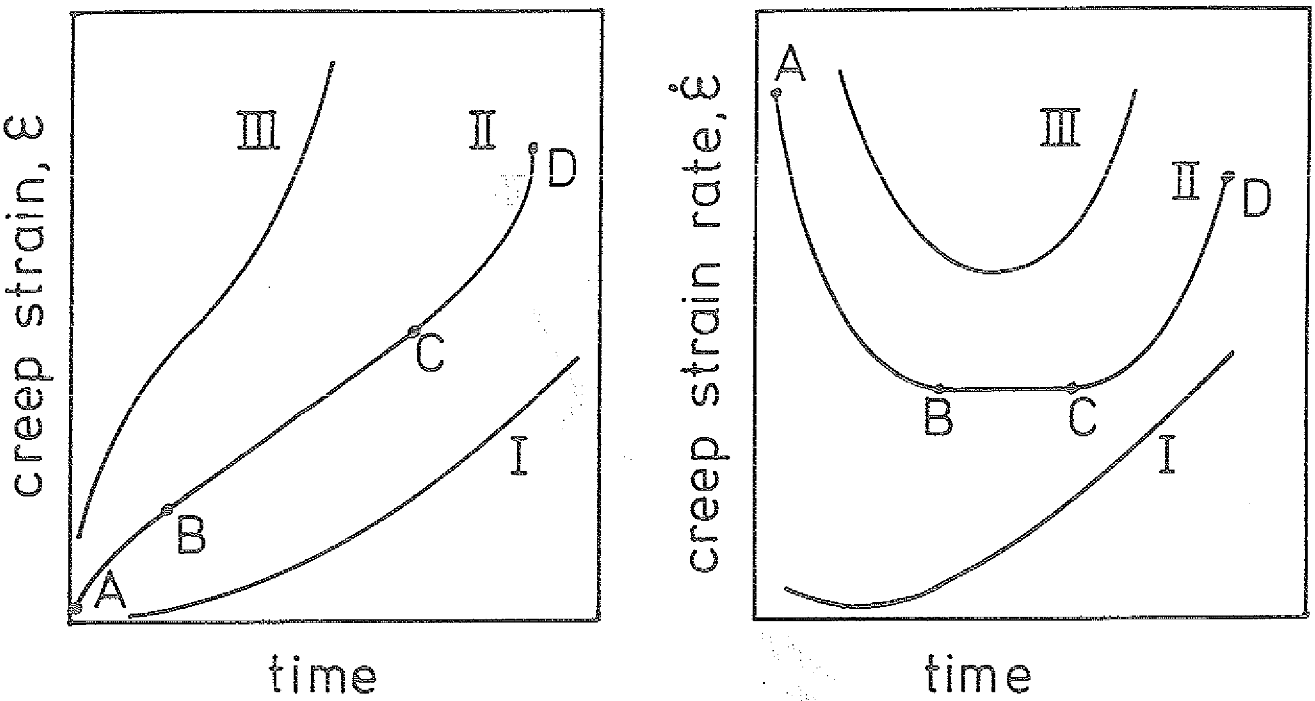

Fig. 1: Typical variation of creep strain and creep strain rate with time.

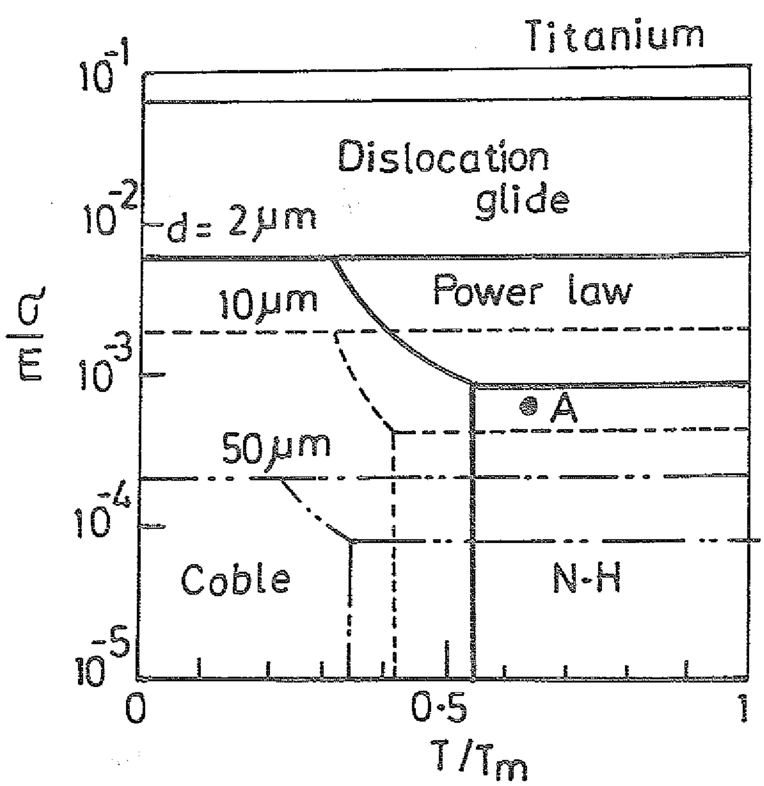

Fig. 2: Deformation diagram of titanium for different grain sizes /1/.

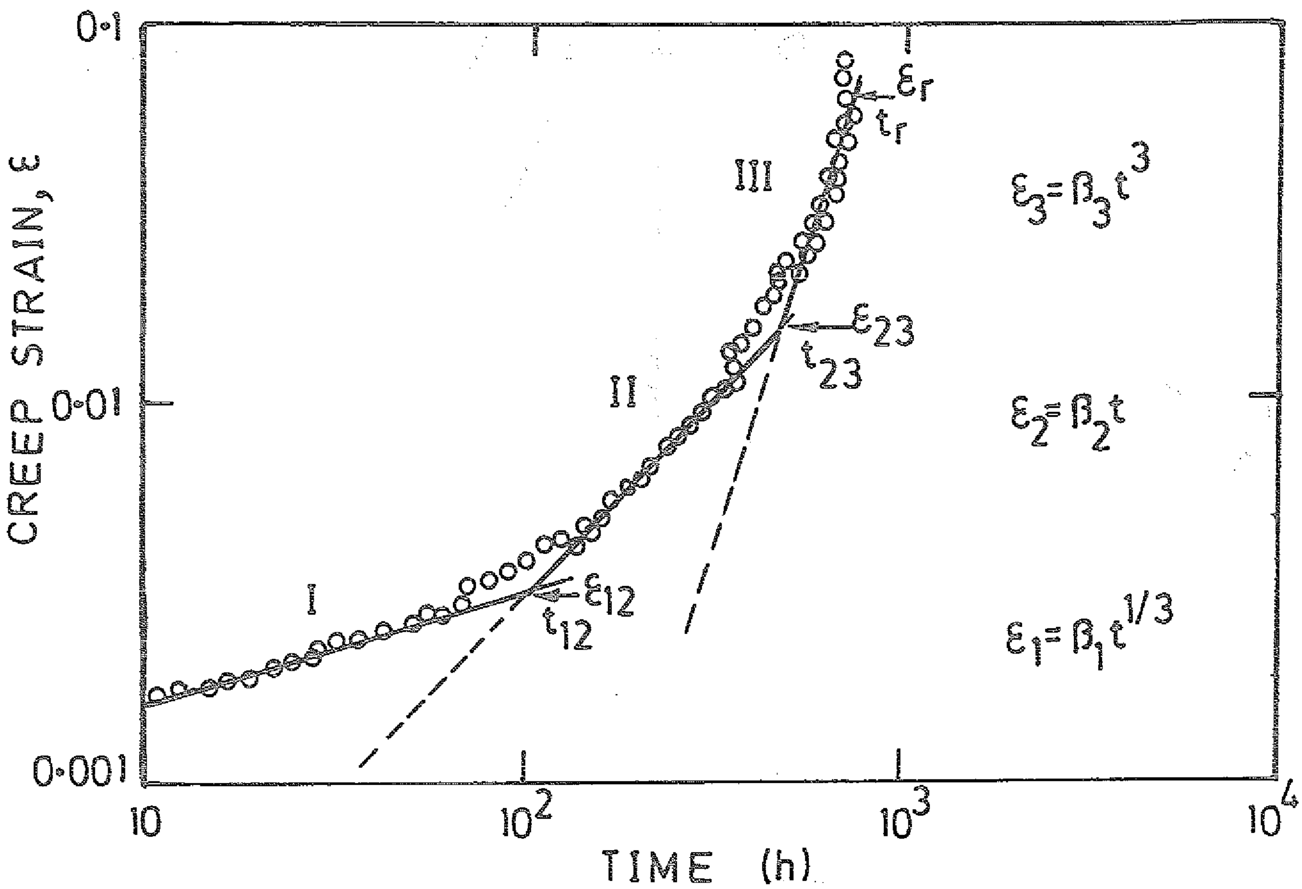

Fig. 3: Schematic representation of creep curve indicating the three stages of creep strain and the transition regions.

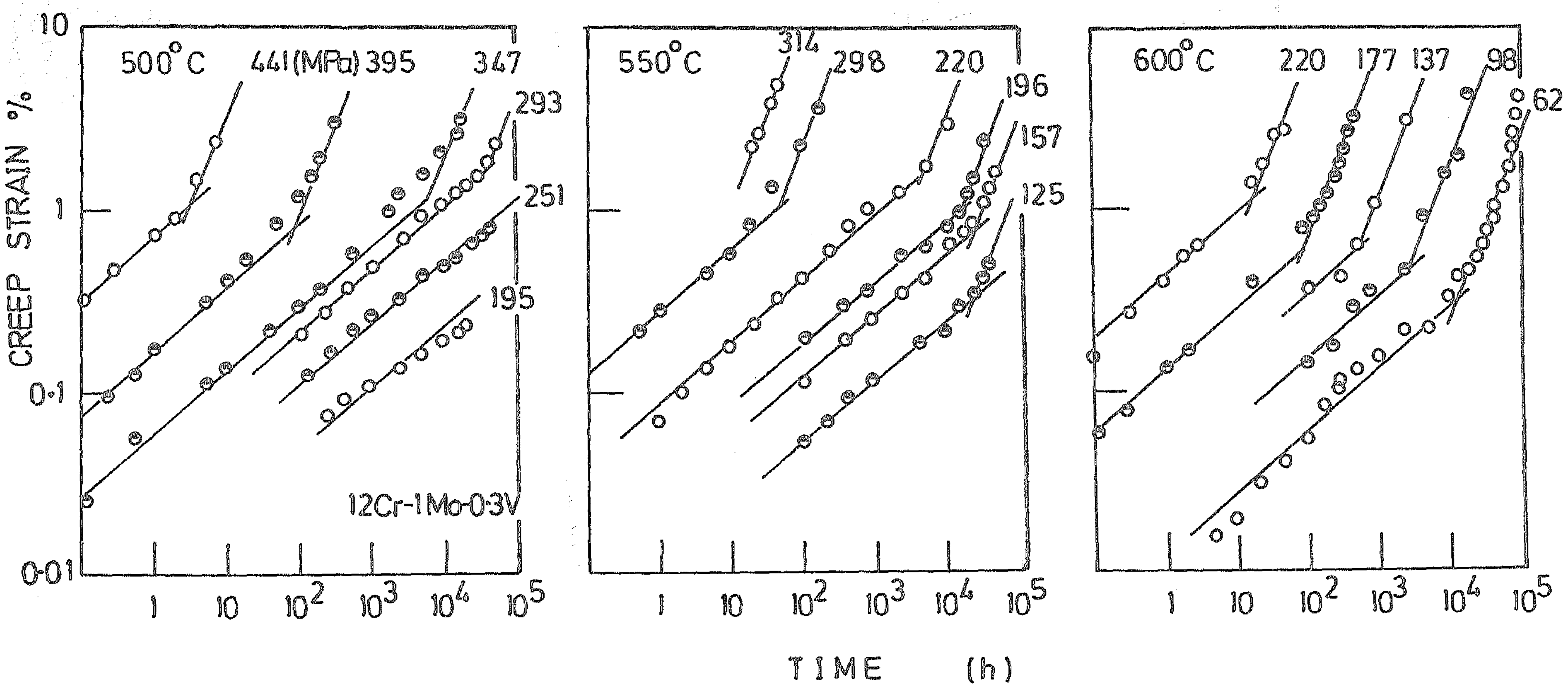

Fig. 4: Relation between creep strain and time for 12Cr-1Mo-0.3V steel at 500 °C, 550 °C and 600 °C. Only the first and the second stages are shown.

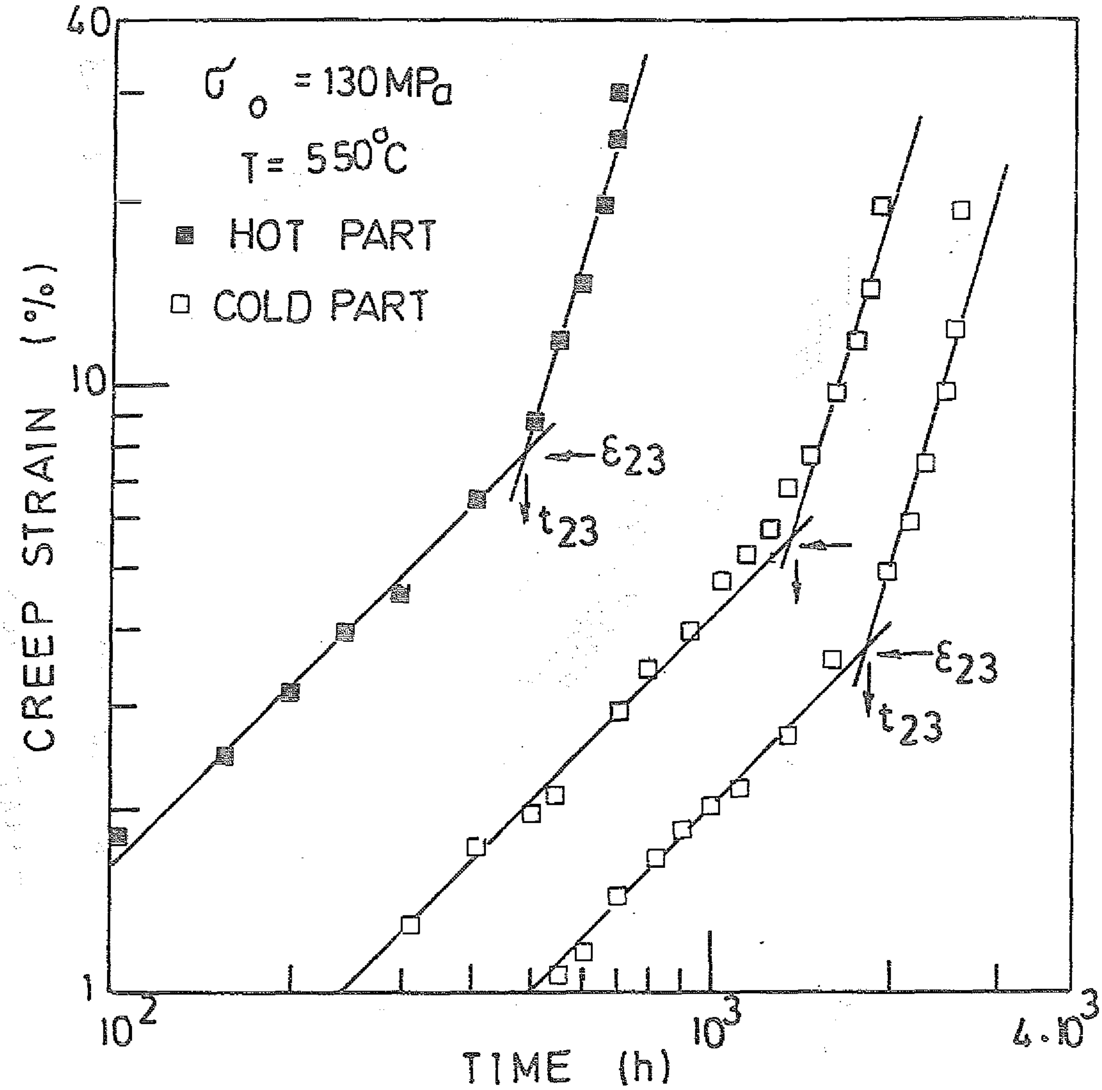

Fig. 5: Relation between creep strain and time for 1Cr-1Mo-0.25V steel exposed to 1.5 x 10^5 hours.

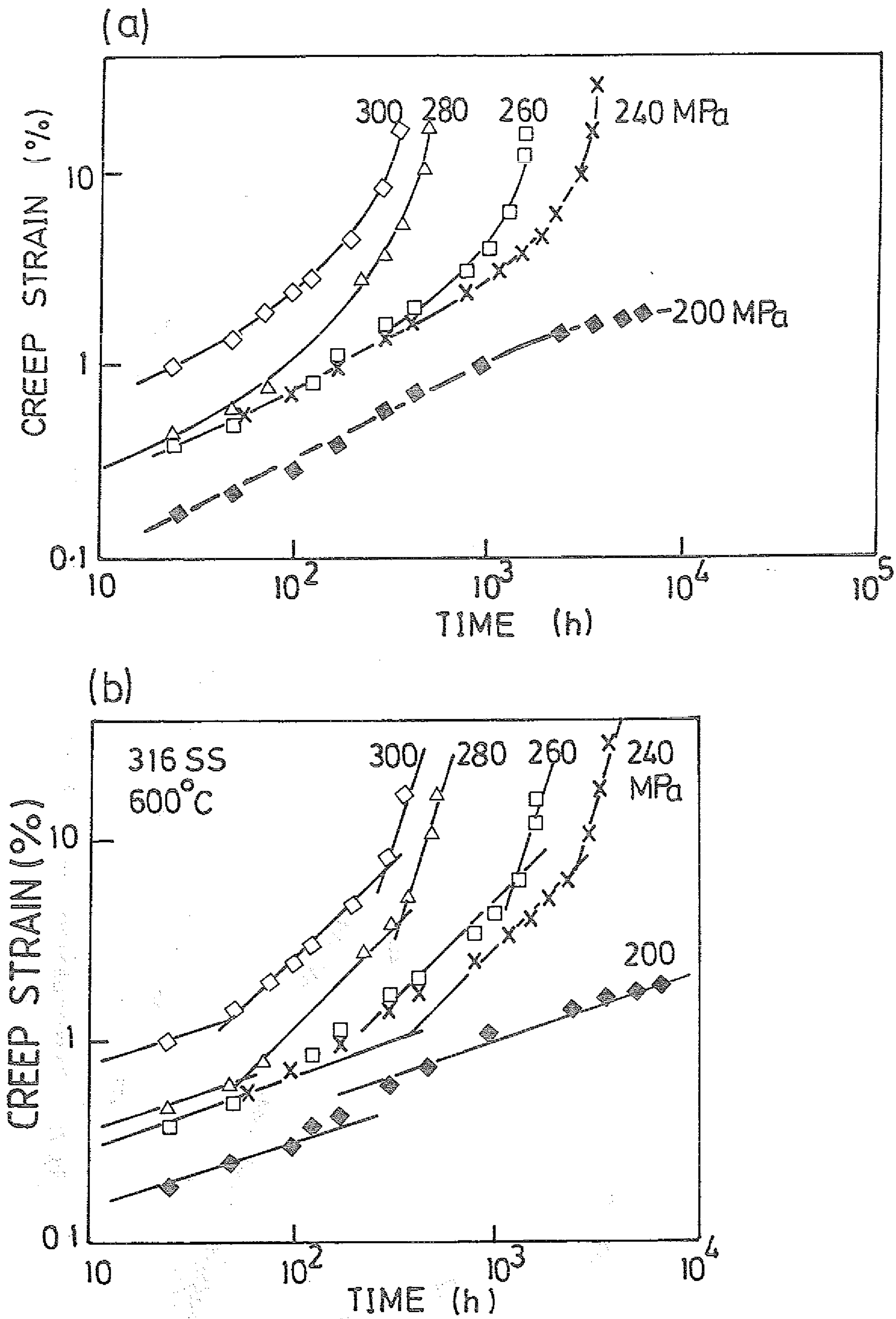

Fig. 6: Relation between creep strain and time for AISI 316SS at 600 °C:(a) as given in original paper, (b) ß-envelope method.

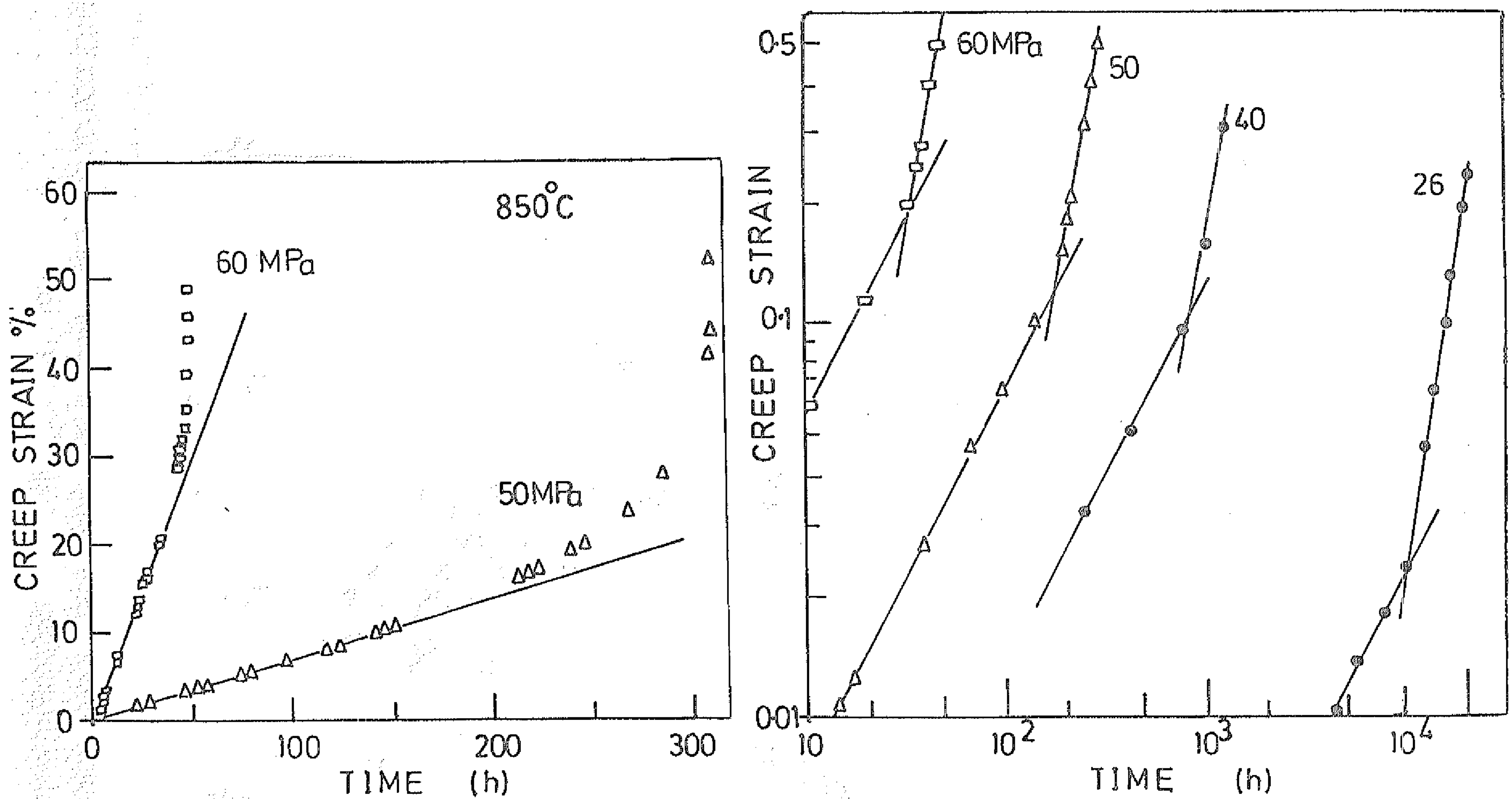

Fig. 7: Relation between creep strain and time for Alloy 800H at 850 °C. Note the negligible primary strain.

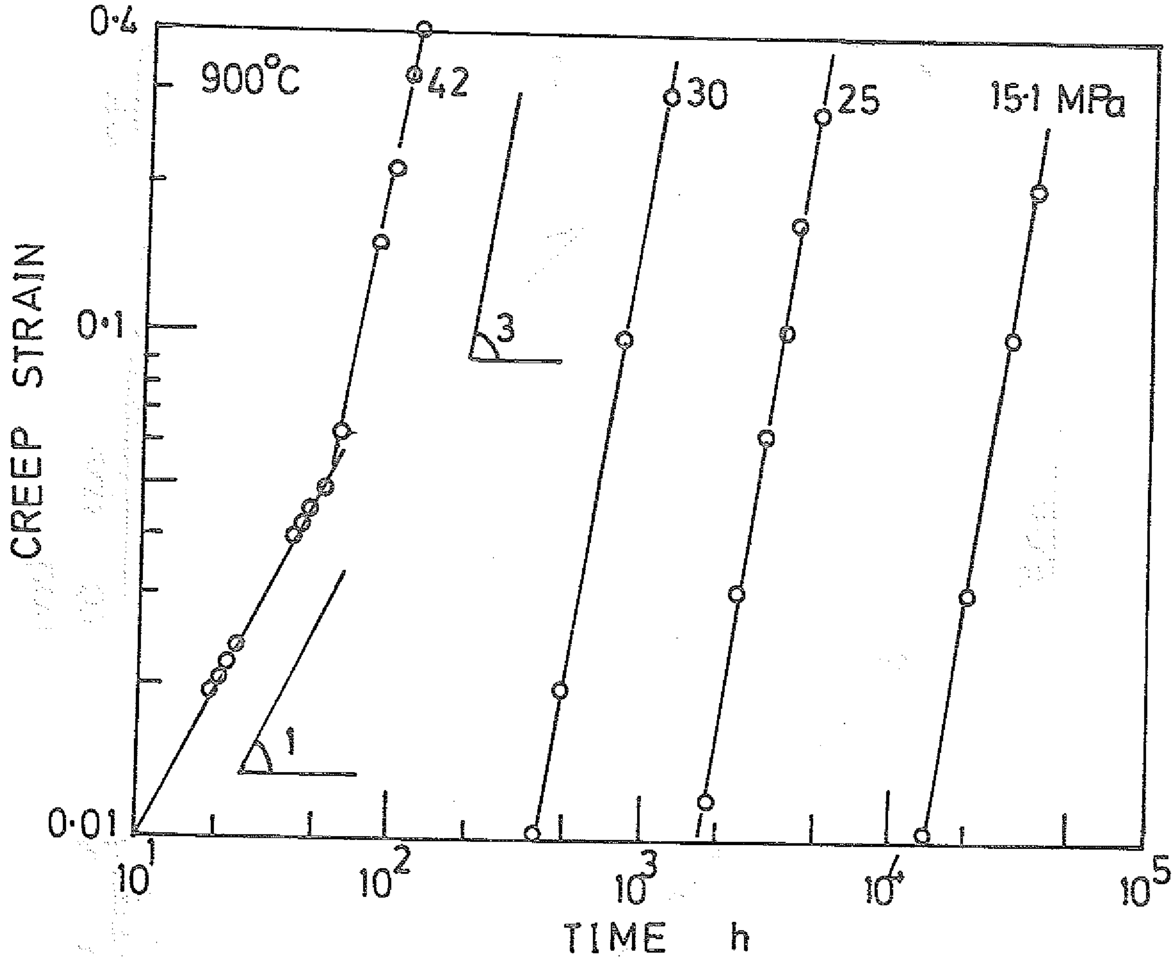

Fig. 8: Variation of creep strain with time for Alloy 800H at 900 °C.

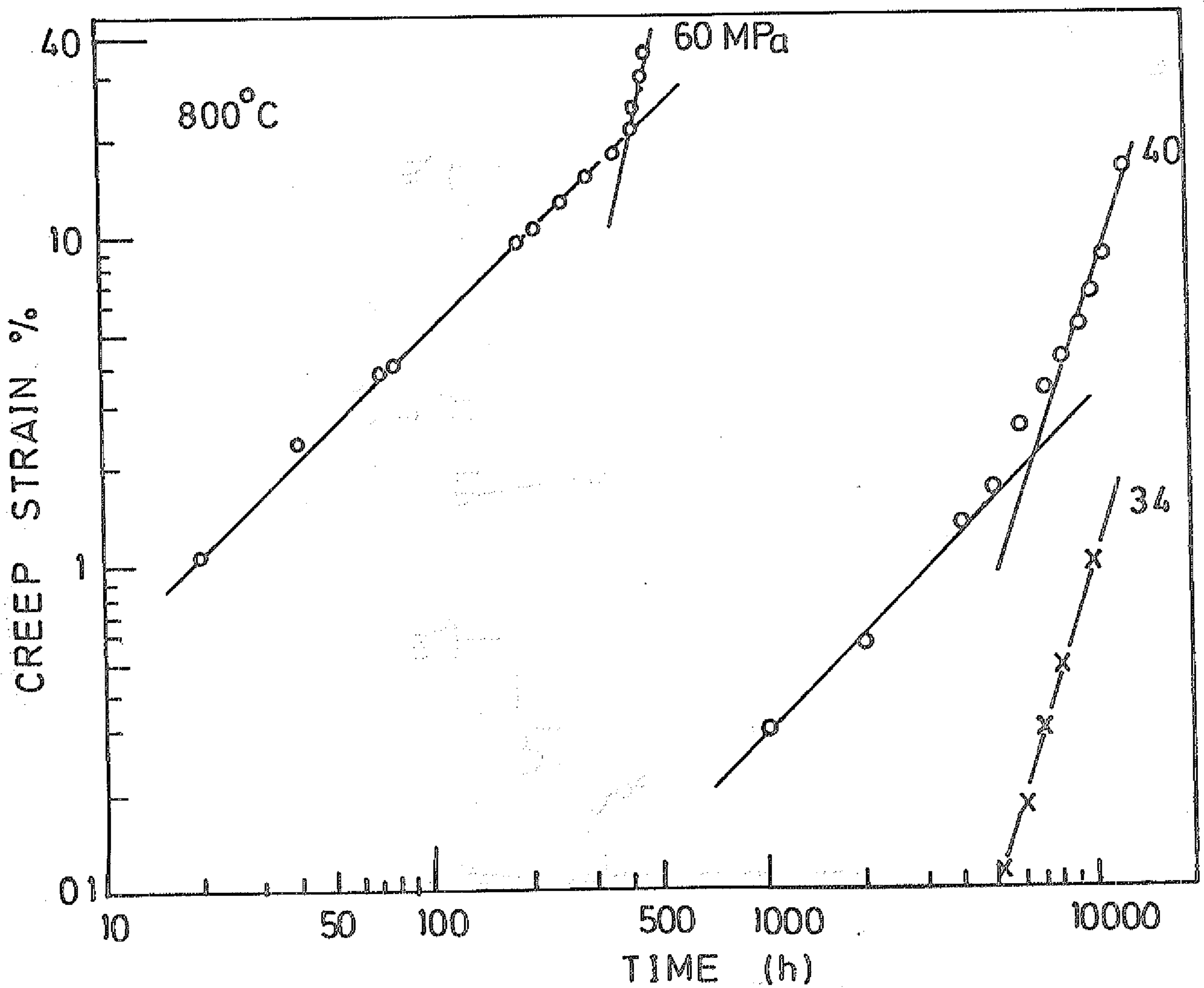

Fig. 9: Variation of creep strain with time for Alloy 800H at 800 °C.

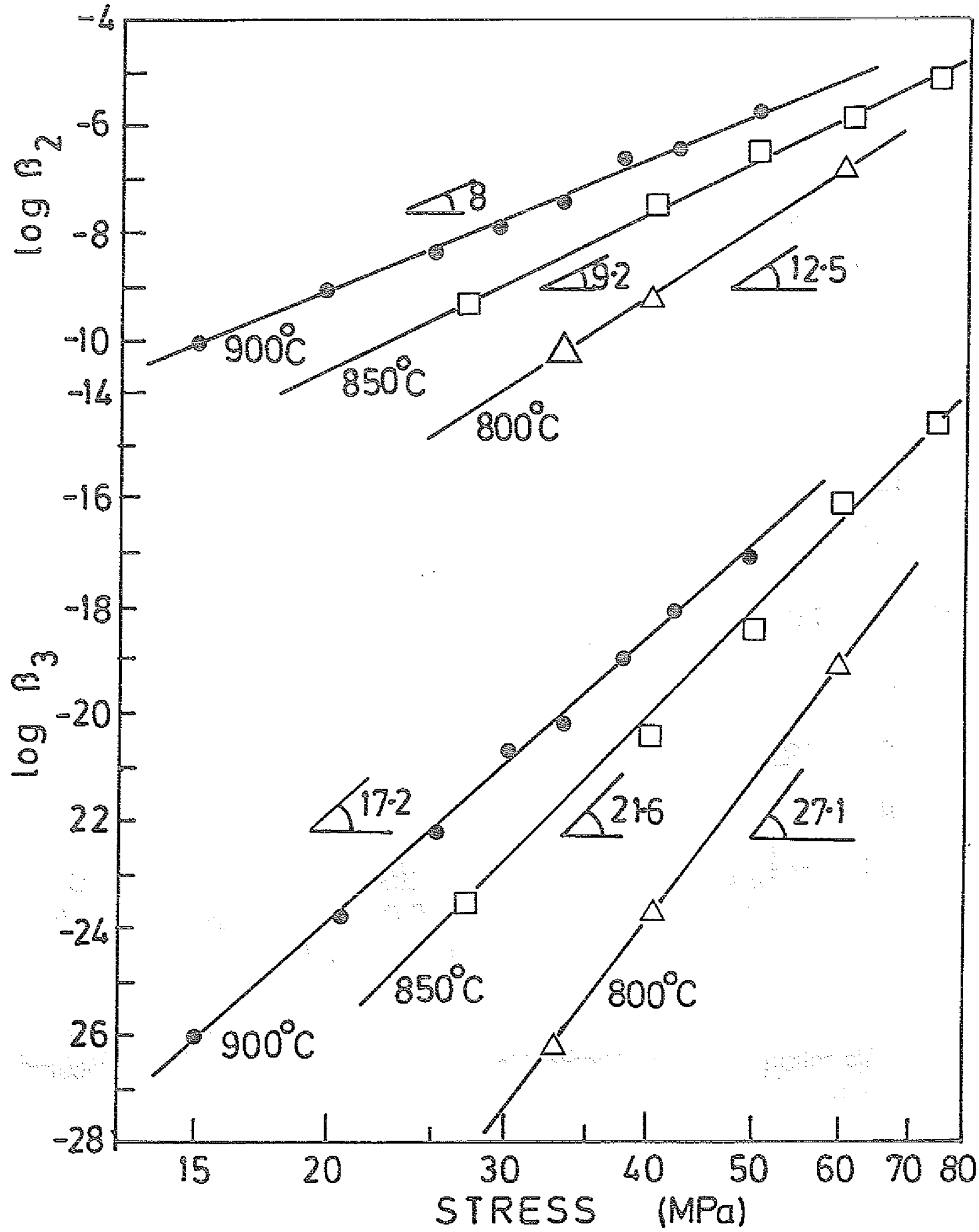

Fig. 10: Variations of the coefficients β_2 and β_3 with stress for Alloy 800H at 800, 850 and 900 °C.

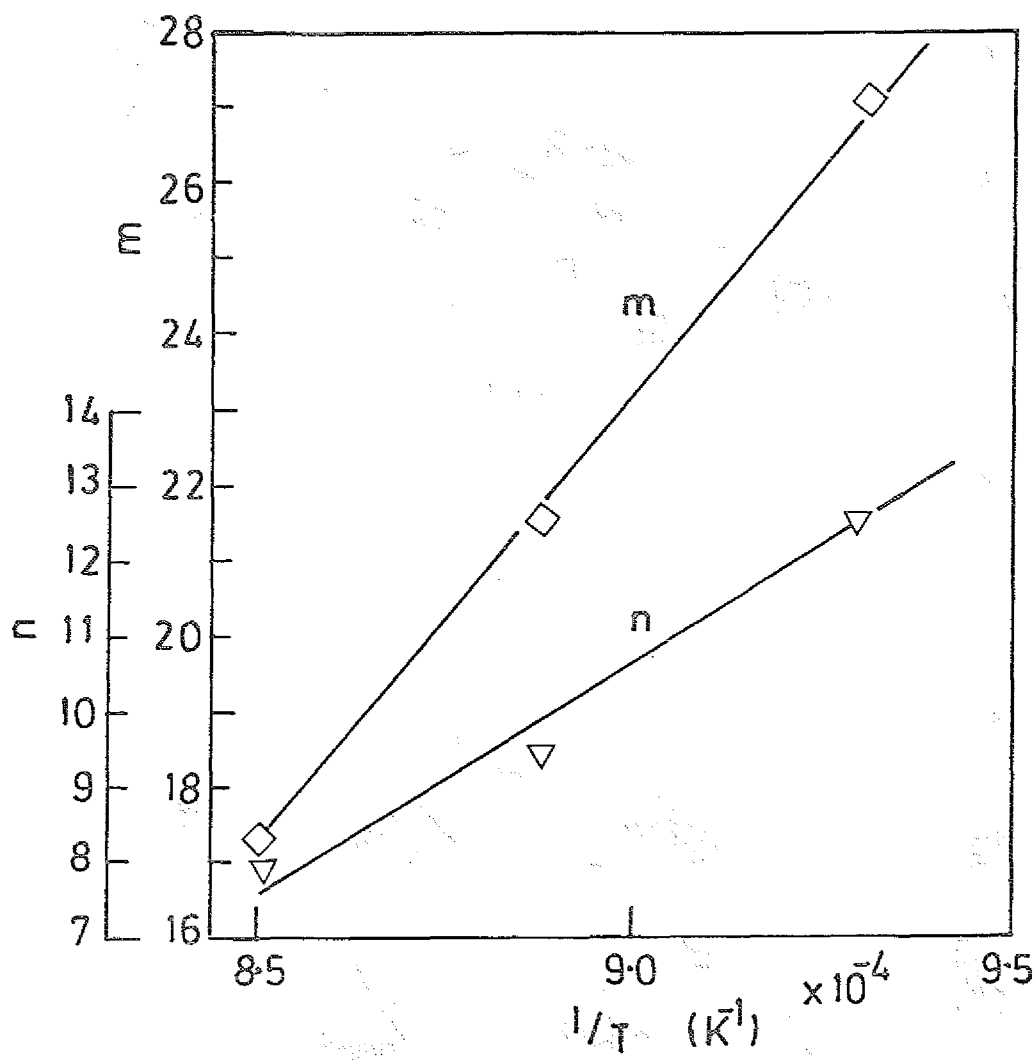

Fig. 11: Variation of the exponents n and m with the inverse of the temperature for Alloy 800H.

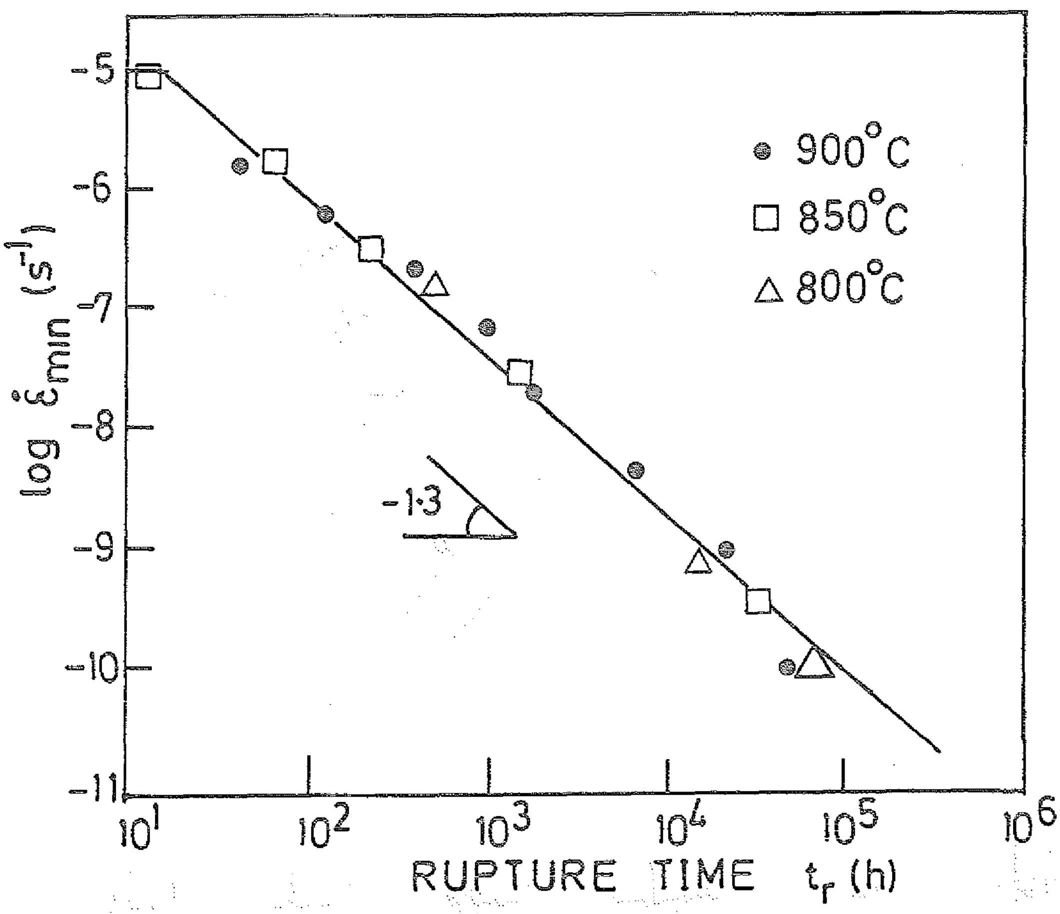

Fig. 12: Relation between the minimum creep rate and the rupture time for Alloy 800H.

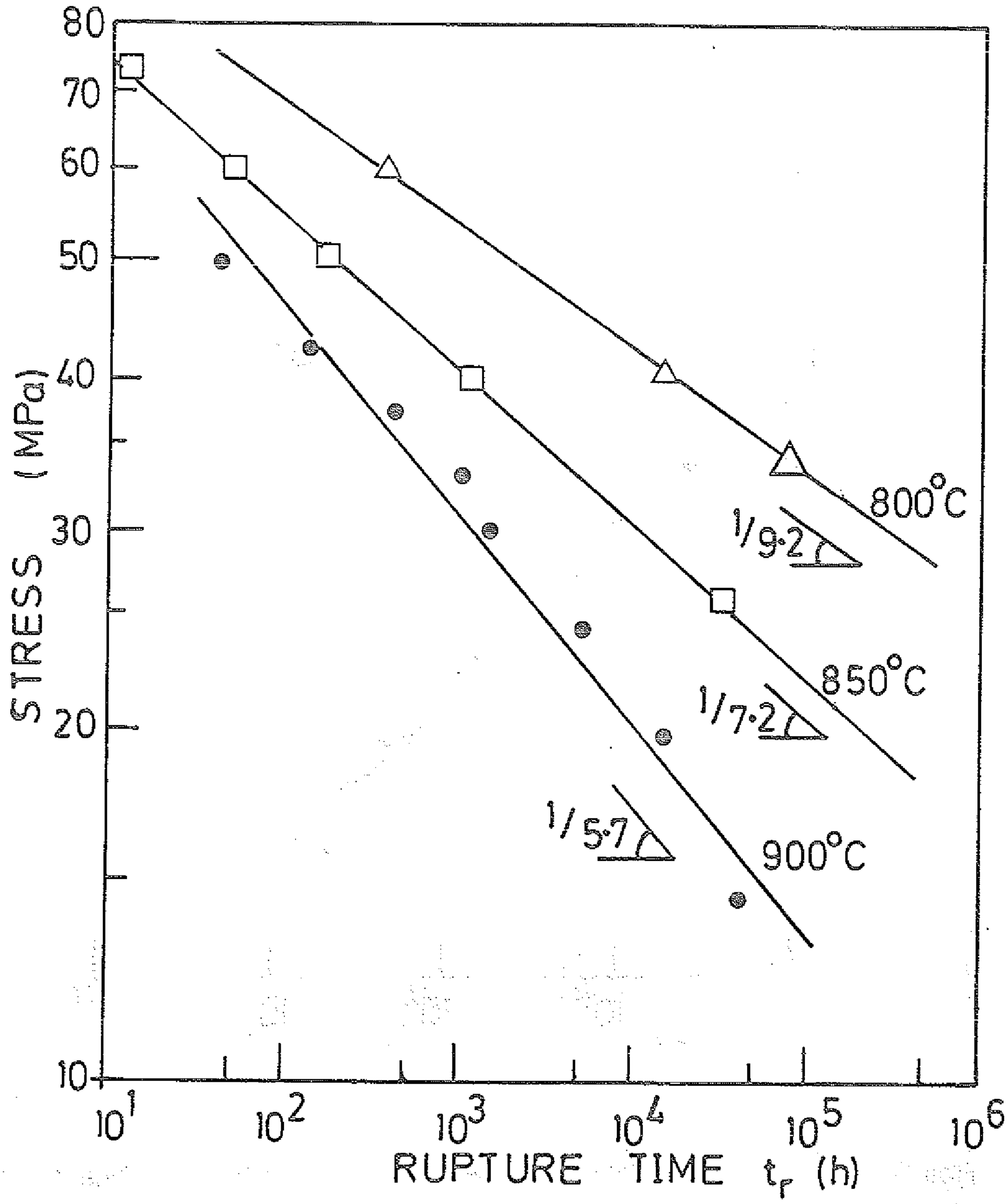

Fig. 13: Relation between stress and rupture time for Alloy 800H.

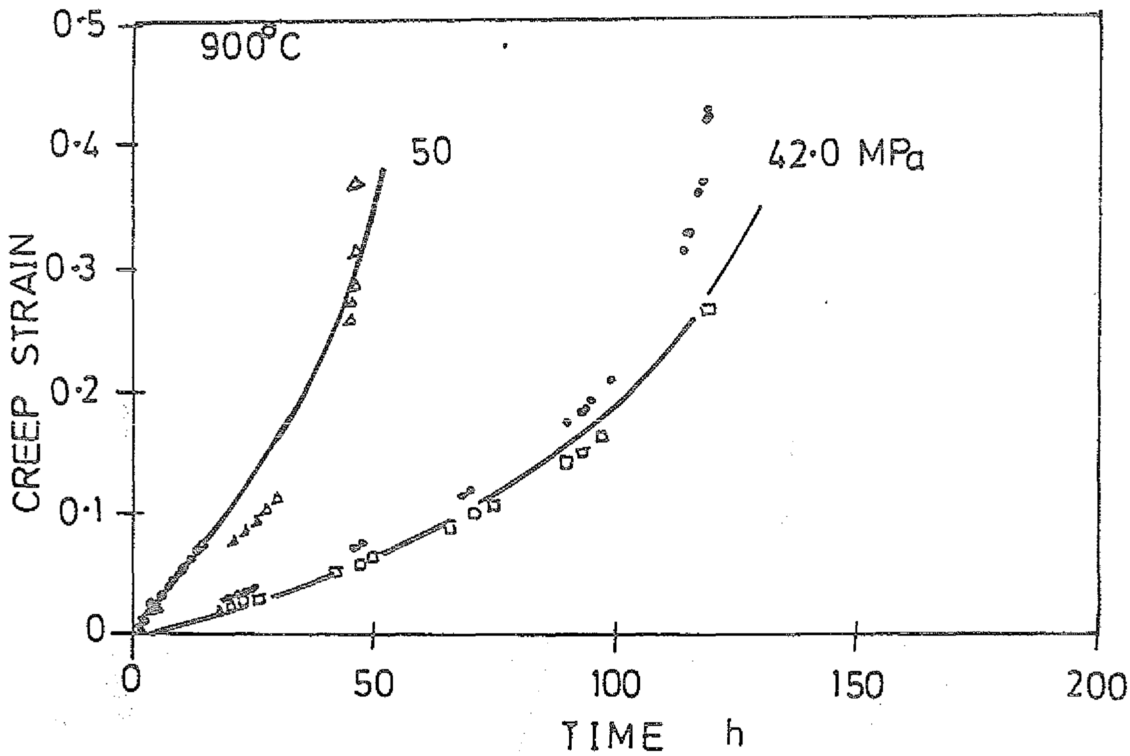

Fig. 14a: Relation between creep strain and time for Alloy 800H at 900 °C.

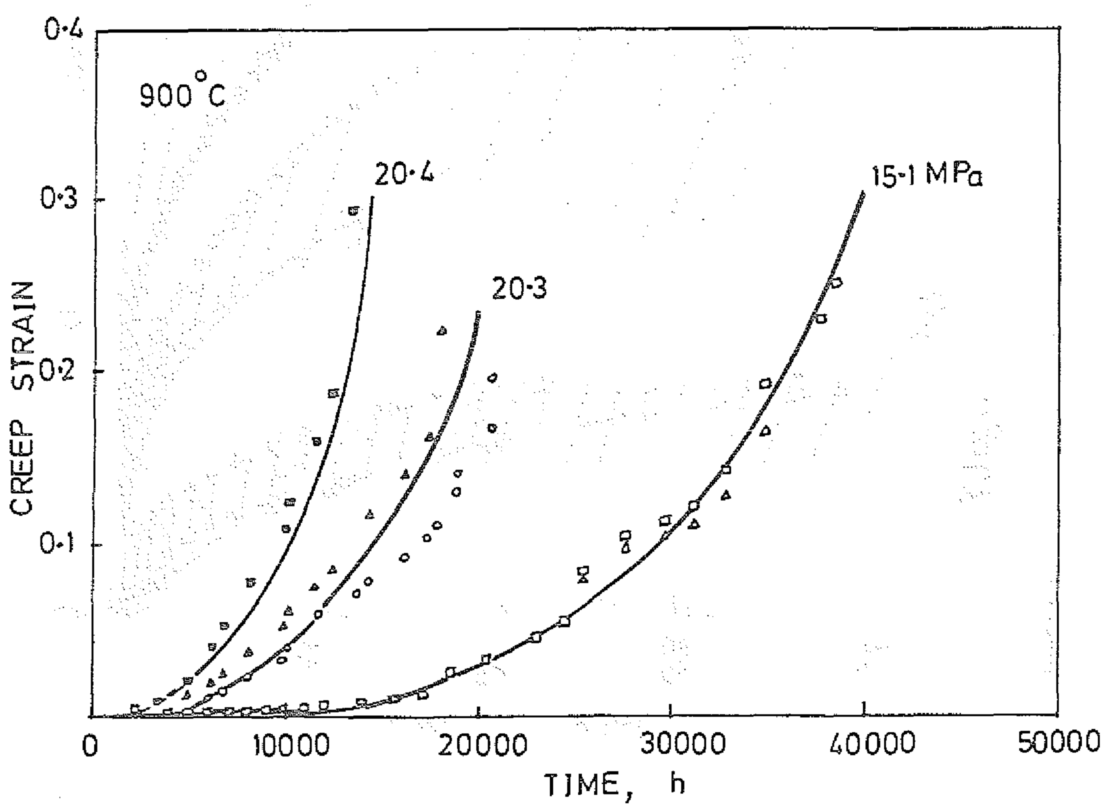

Fig. 14b: Relation between creep strain and time for Alloy 800H at 900 °C.

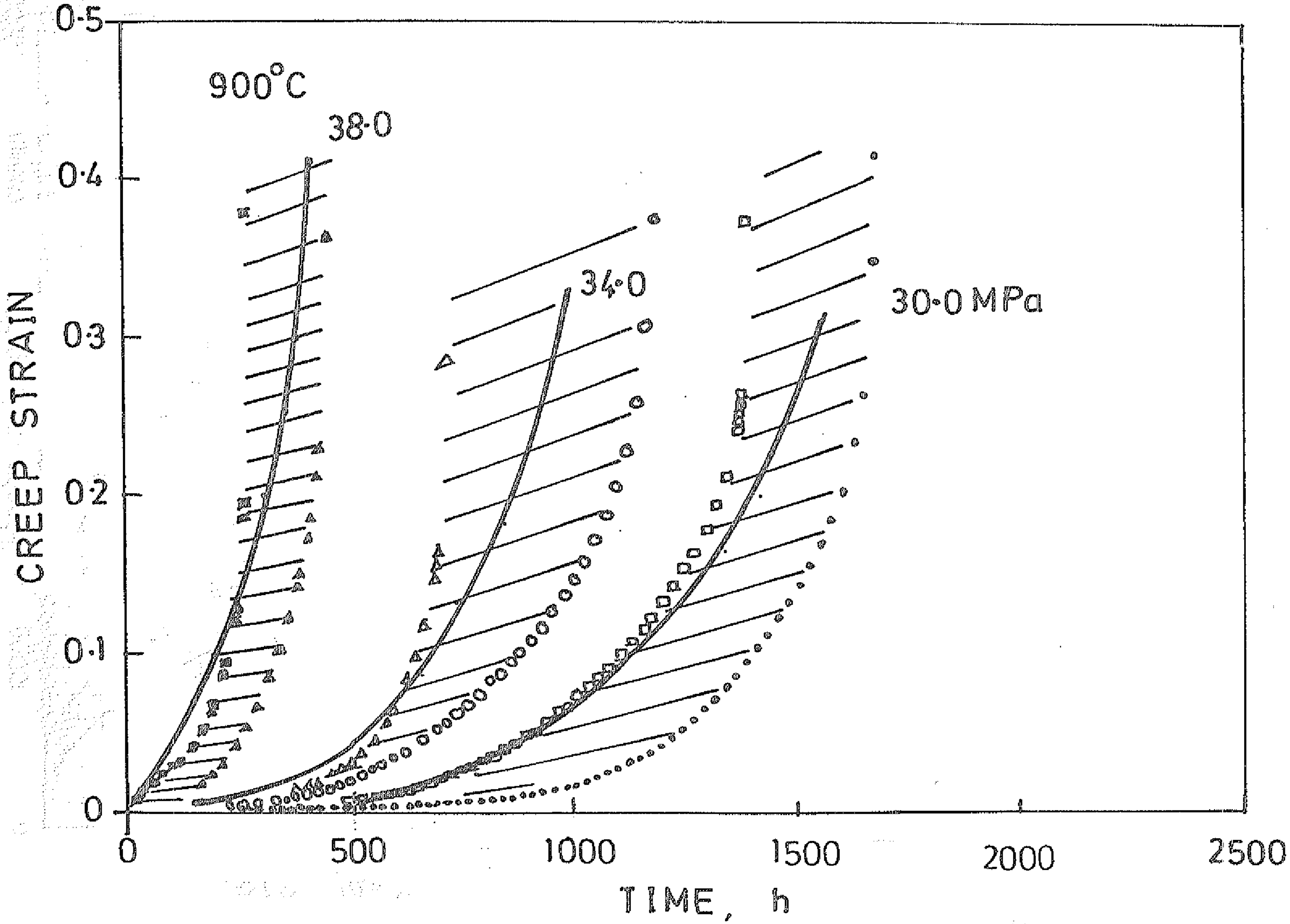

Fig. 14c: Variation of creep strain with time for Alloy 800H at 900 °C.

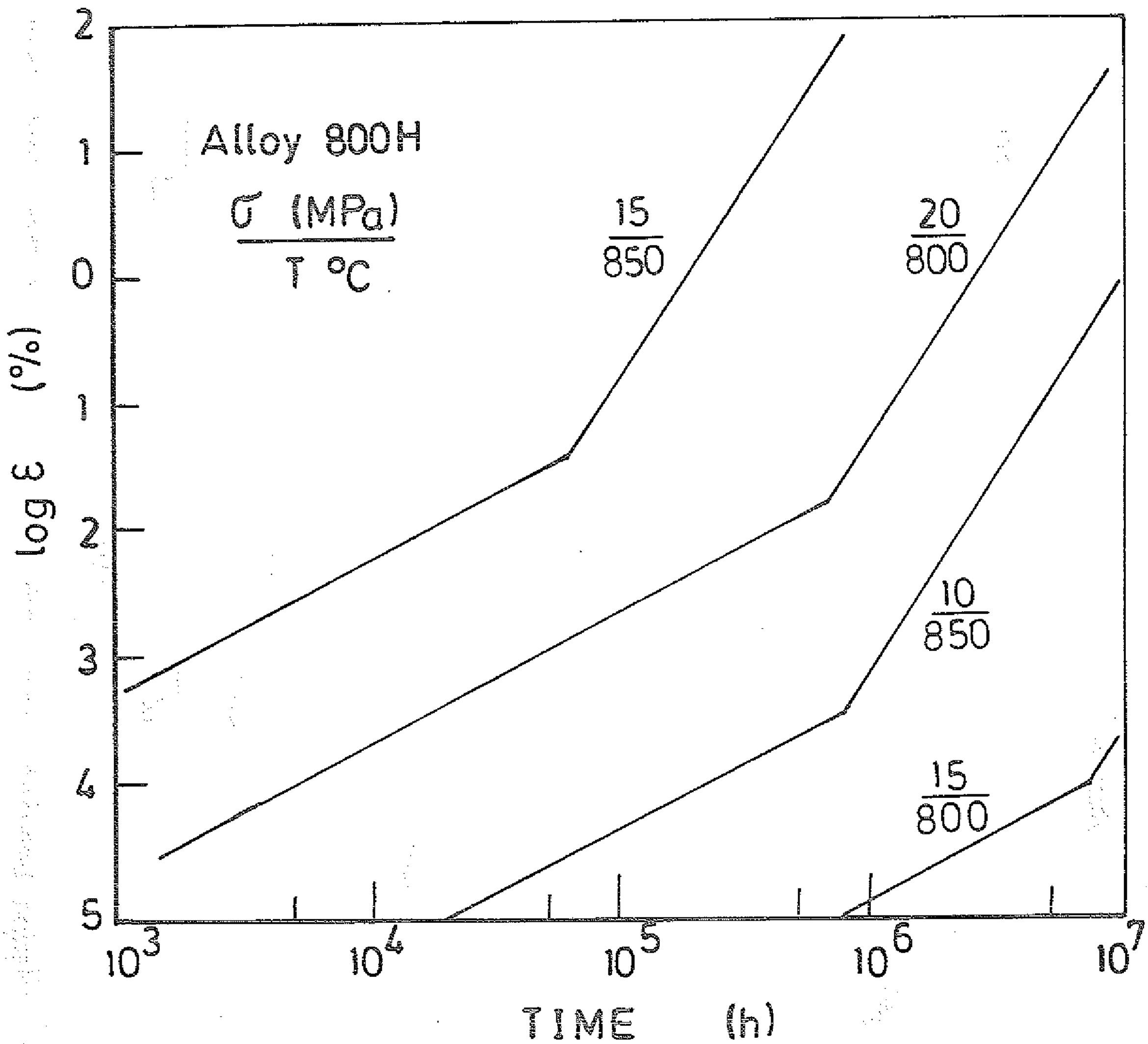

Fig. 15: Predicted variation of creep strain with time for Alloy 800H at the stress/temperature levels indicated.

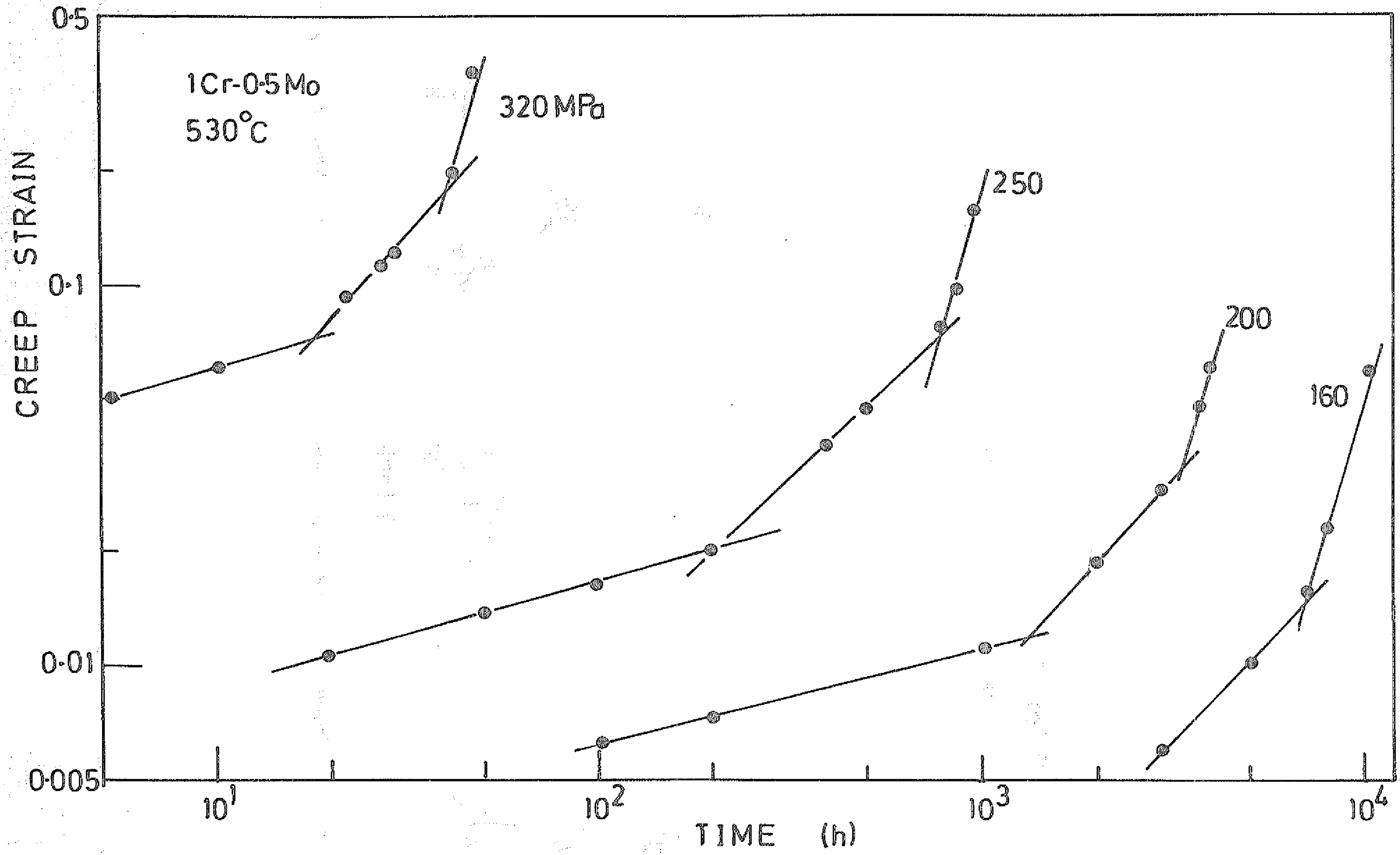

Fig. 16a: Relation between creep strain and time for 1Cr-0.5Mo steel (new) at 530 °C.

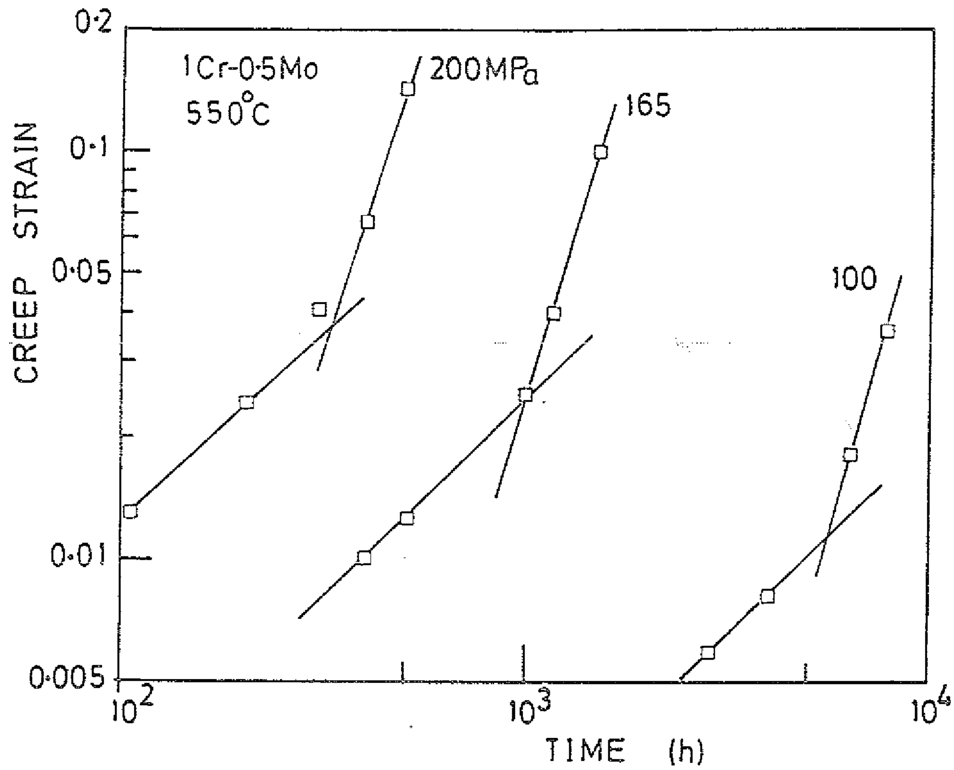

Fig. 16b: Relation between creep strain and time for 1Cr-0.5Mo steel (new) at 550 °C.

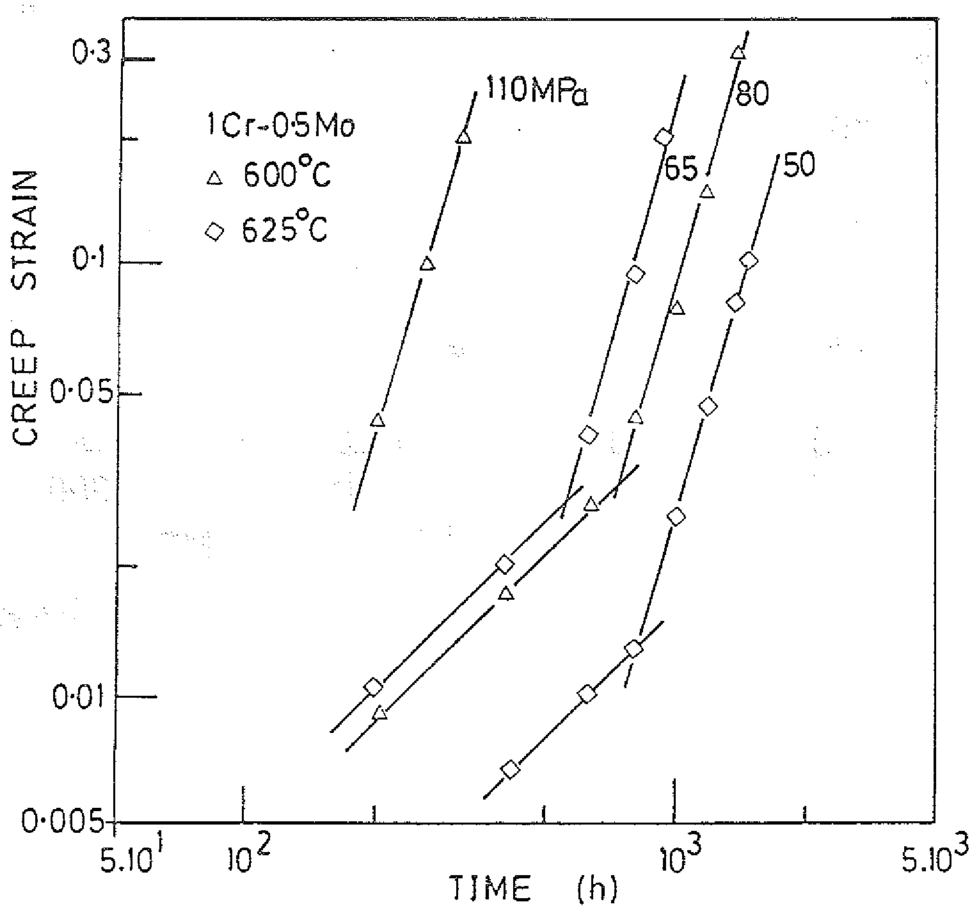

Fig. 16c: Relation between creep strain and time for 1Cr-0.5Mo steel (new) at 600 °C and 625 °C.

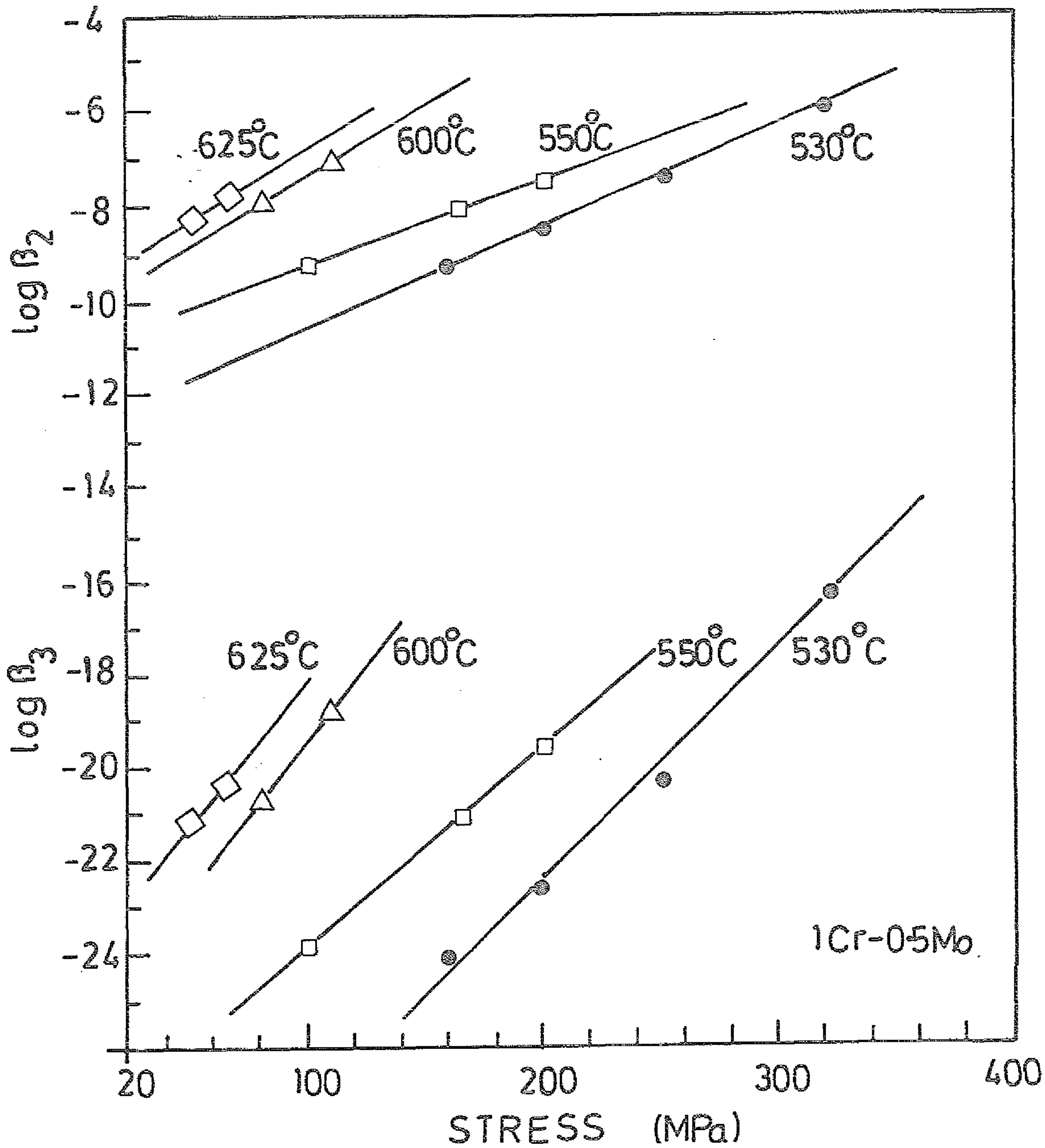

Fig. 17: Variation of β_2 and β_3 with stress for 1Cr-0.5 steel (new).

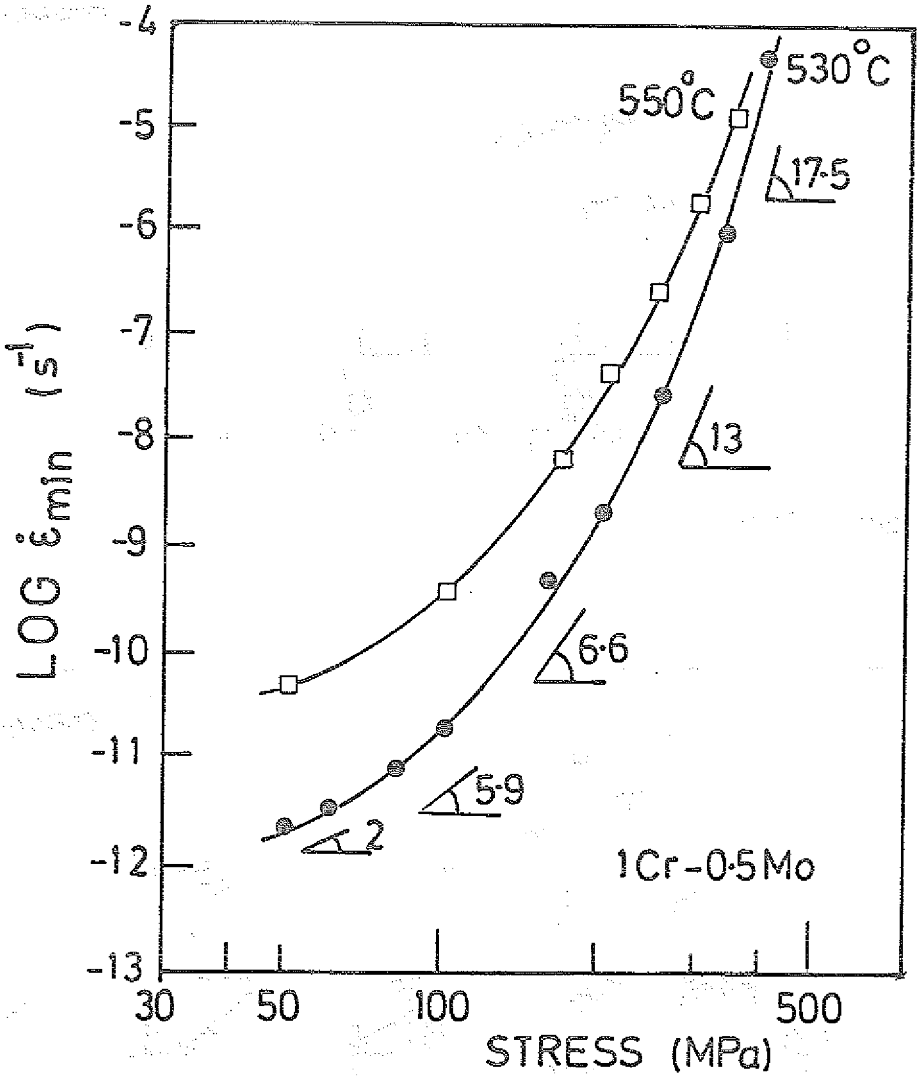

Fig. 18: Variation of log minimum creep rate with log stress for 1Cr-0.5Mo steel (new).

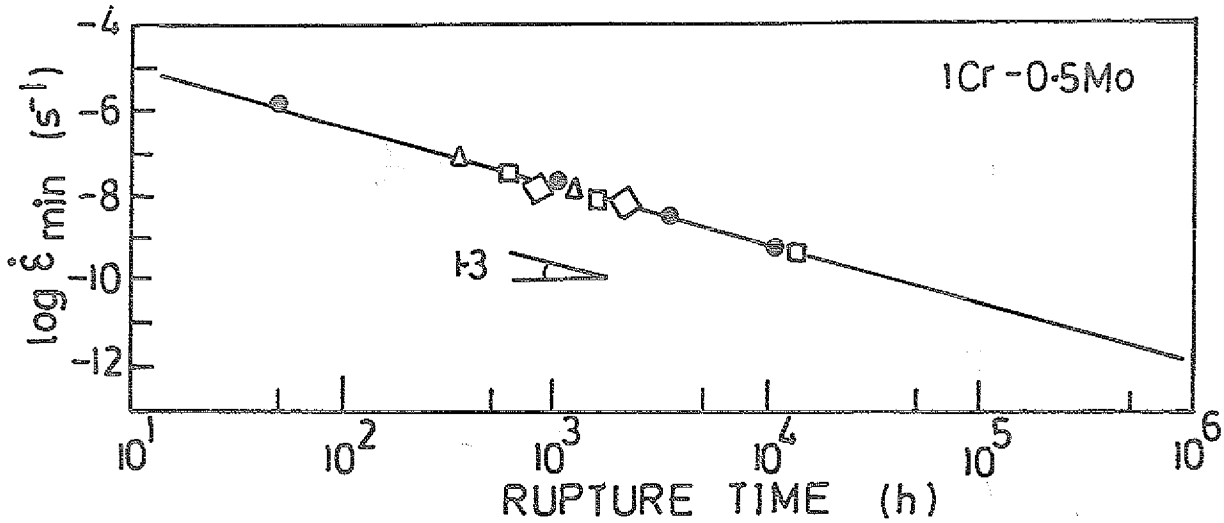

Fig. 19: Relation between minimum creep rate and rupture time for 1Cr-0.5Mo steel (new).

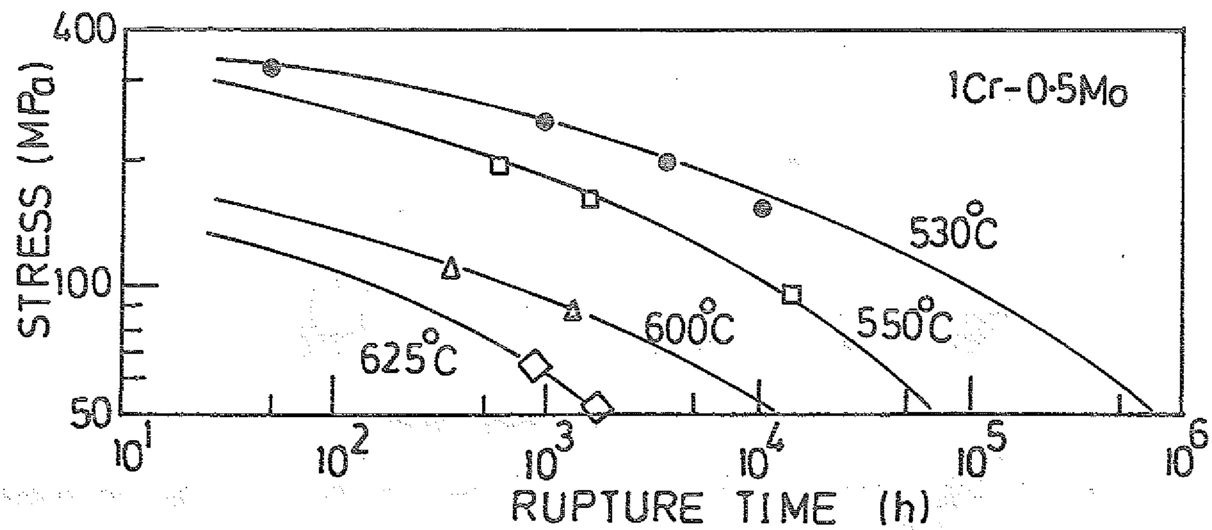

Fig. 20: Relation between creep strain and rupture time for 1Cr-0.5Mo steel (new)

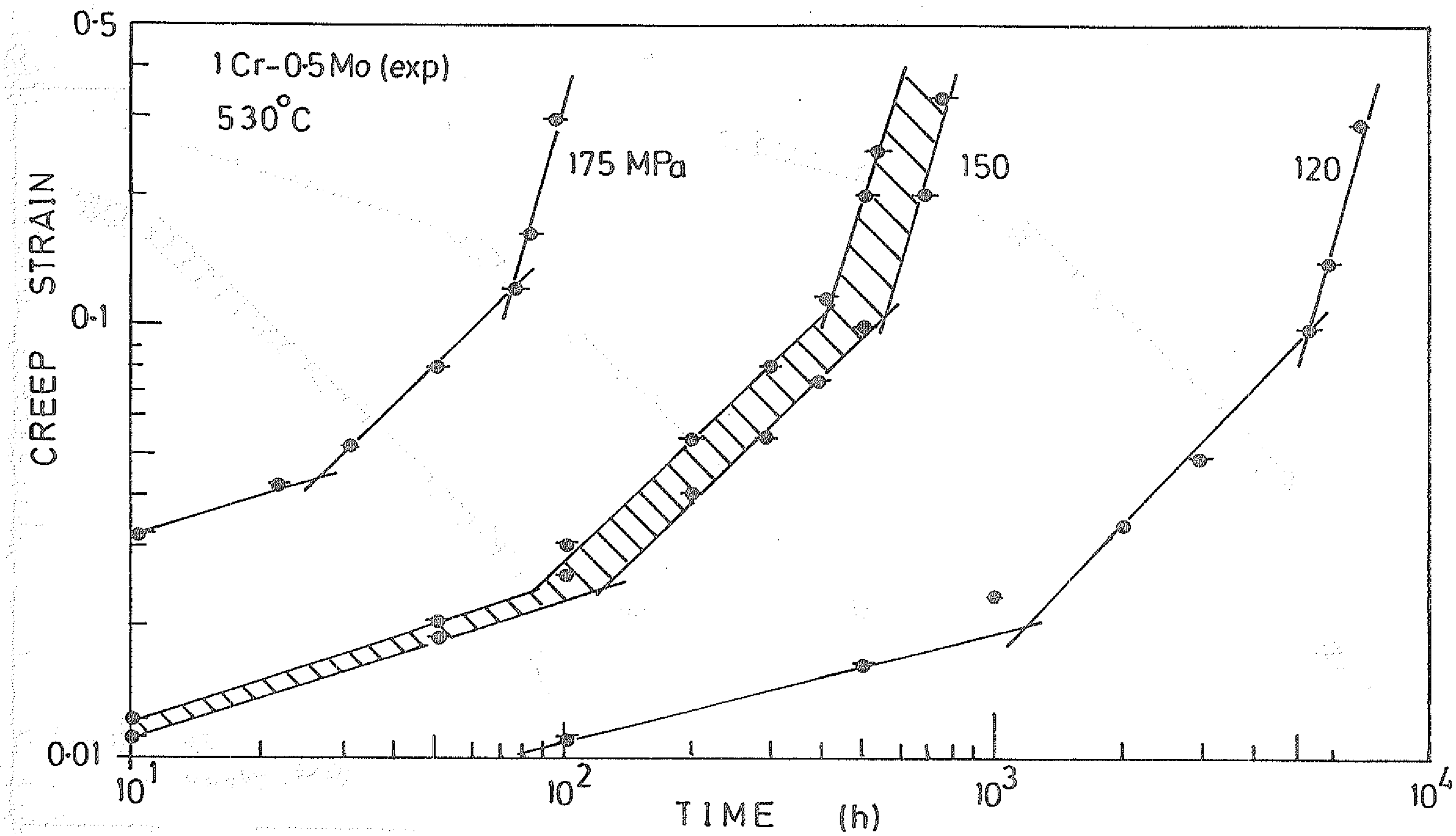

Fig. 21a: Variation of creep strain with time for 1Cr-0.5Mo steel (service exposed) at 530 °C.

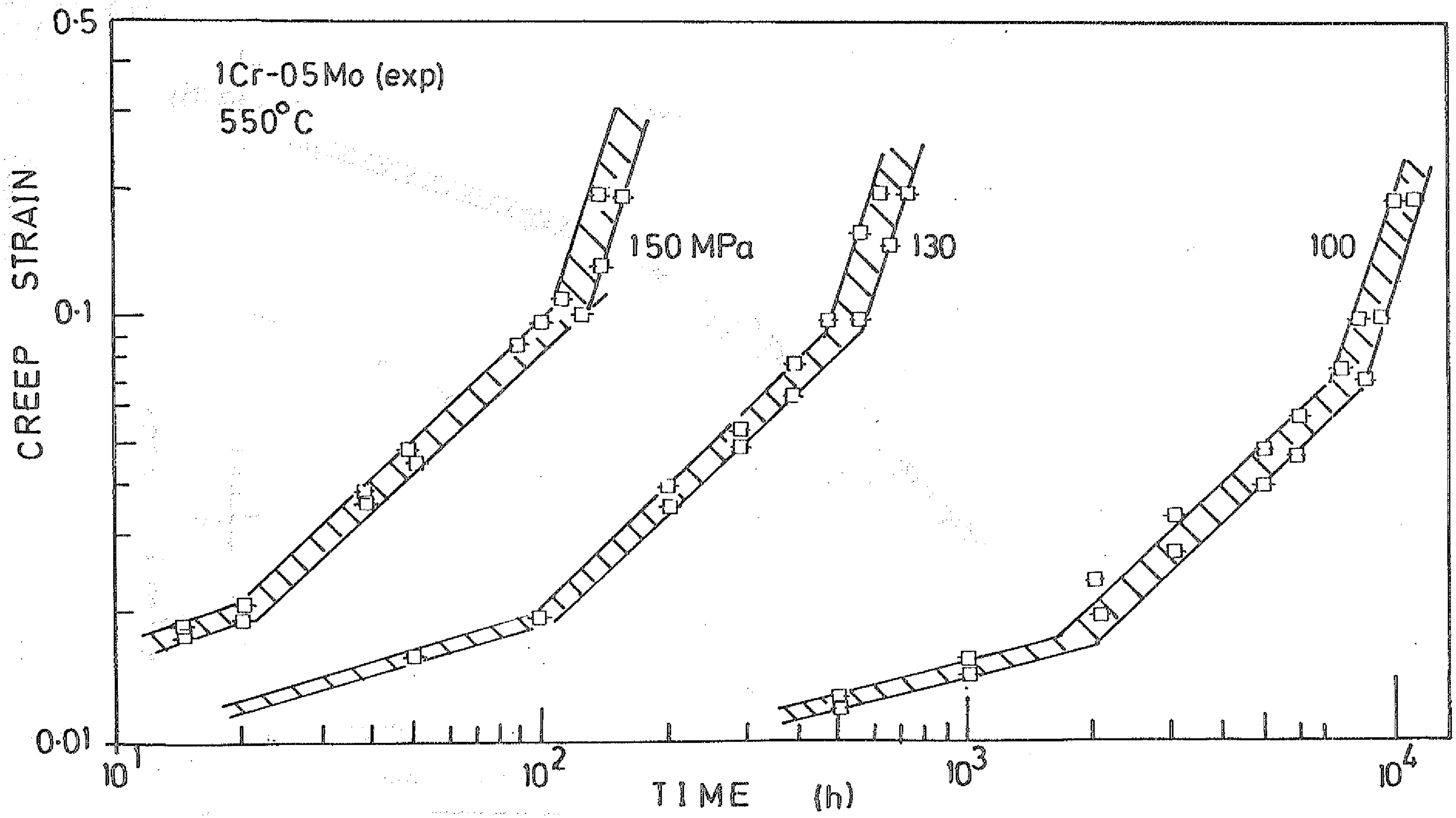

Fig. 21b: Variation of creep strain with time for 1Cr-0.5Mo steel (service exposed) at 550 °C.

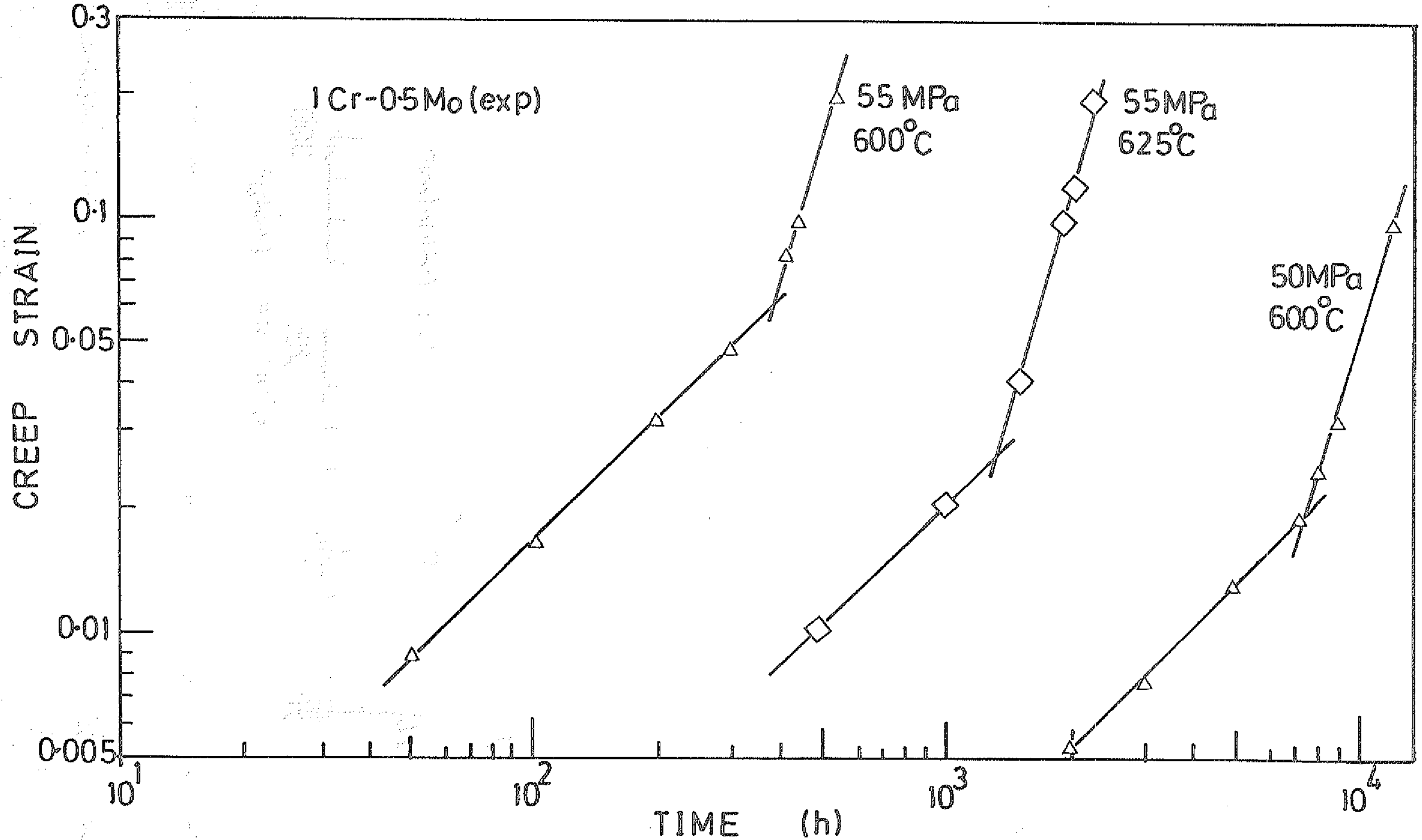

Fig. 21c: Variation of creep strain with time for 1Cr-0.5Mo steel (service exposed) at 600 °C and 625 °C.

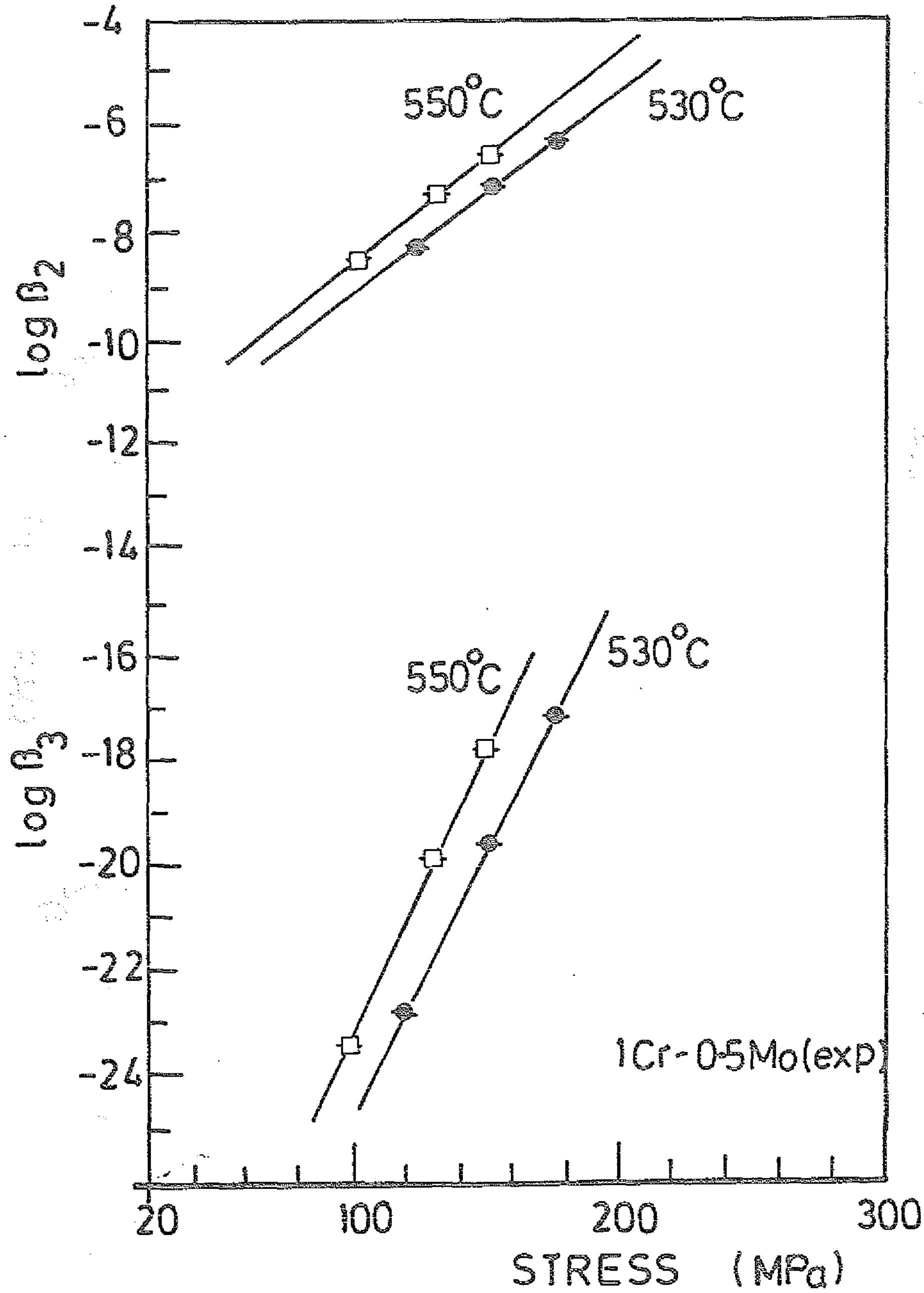

Fig. 22: Variation of $ß_2$ and $ß_3$ with stress for 1Cr-0.5Mo steel (service exposed).

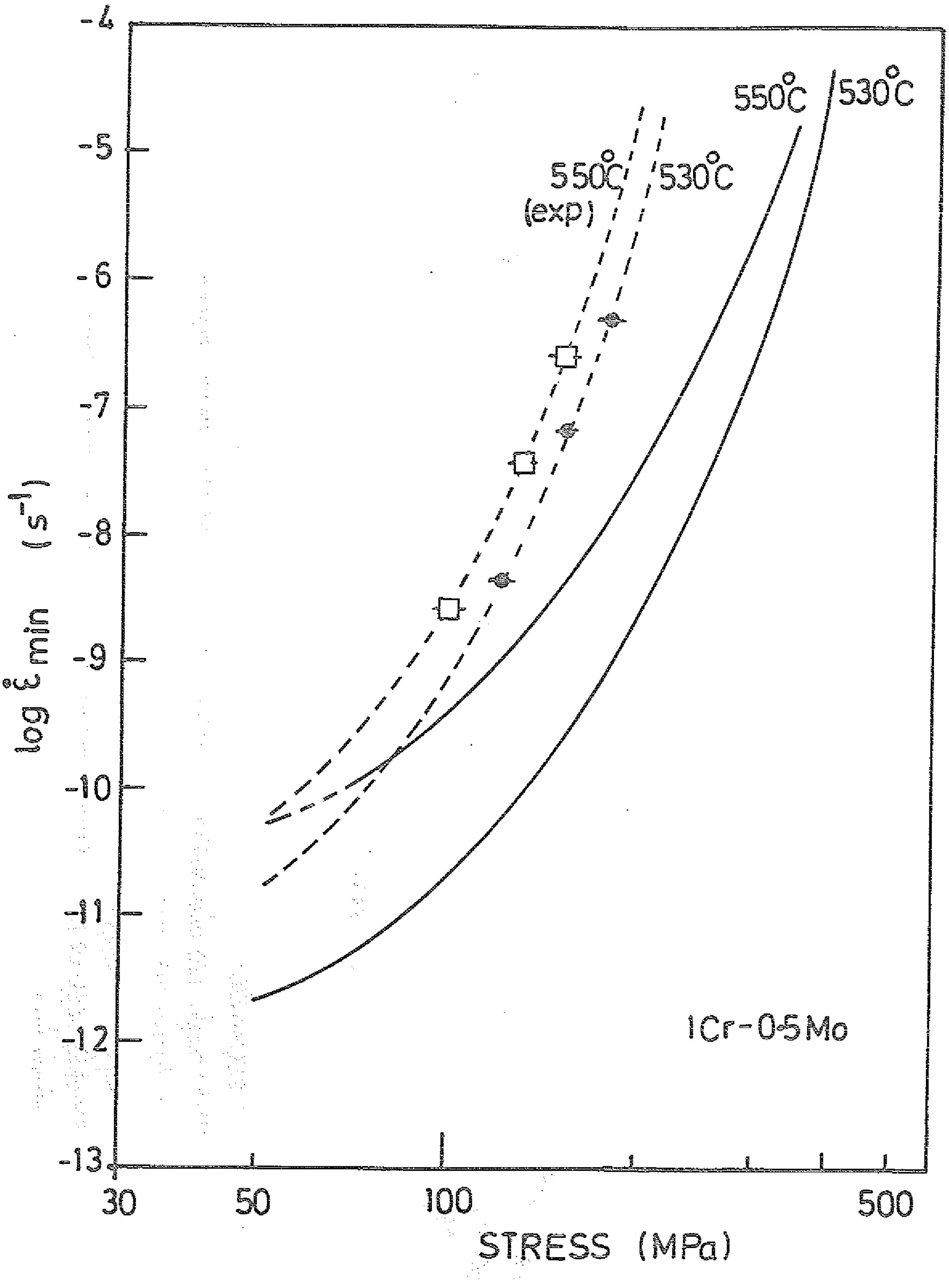

Fig. 23: Relation between log minimum creep rate and log stress for 1Cr-0.5Mo steel (service exposed). The full lines are for new material.

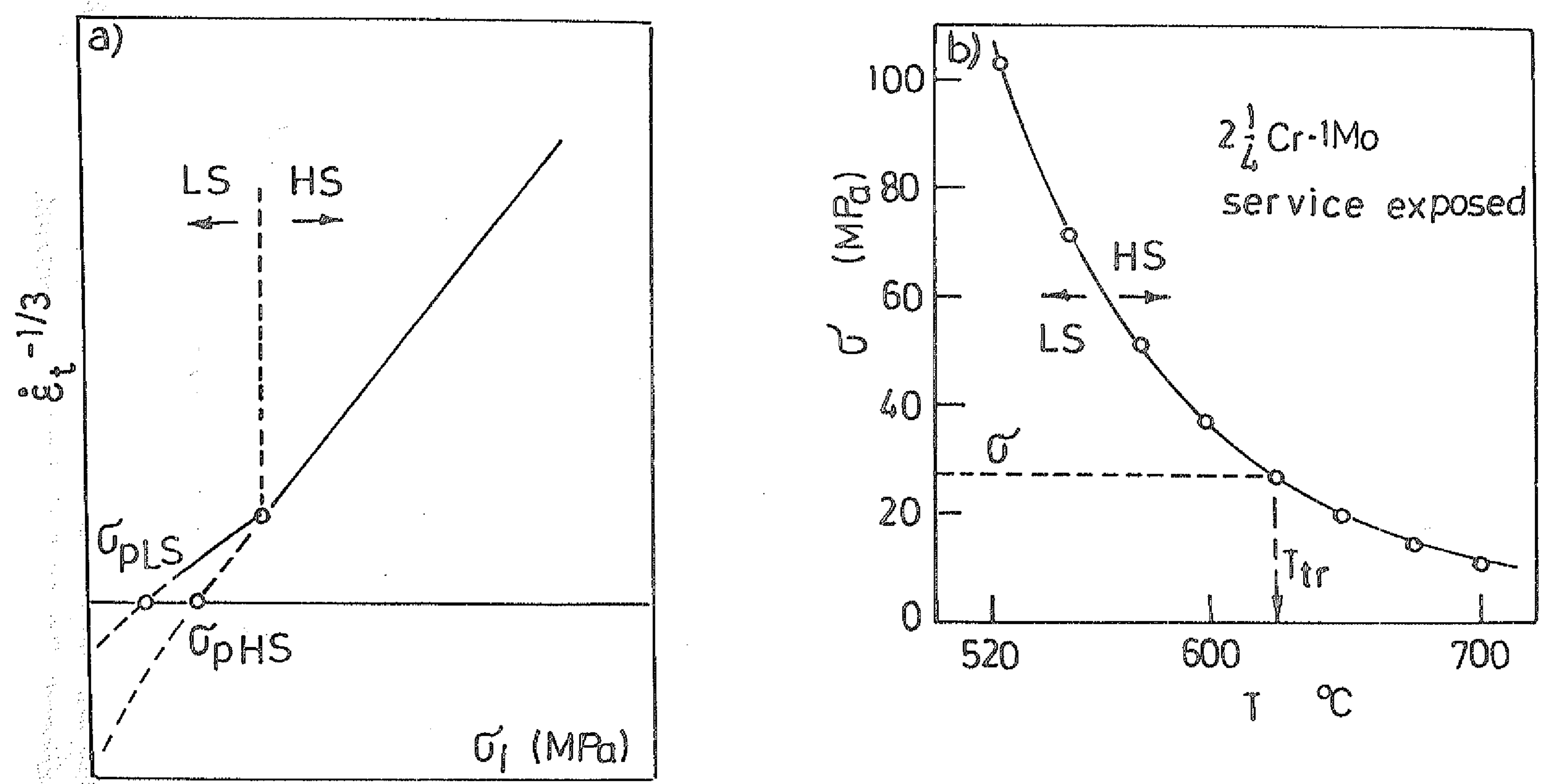

Fig. 24: For 2.25Cr-1Mo:

(a)Schematic representation of higher and intermediate stress regions where the deformation mechanisms are Orowan looping and dislocation climb respectively.

(b)Dependence of the boundary between high and low stress regions on temperature.

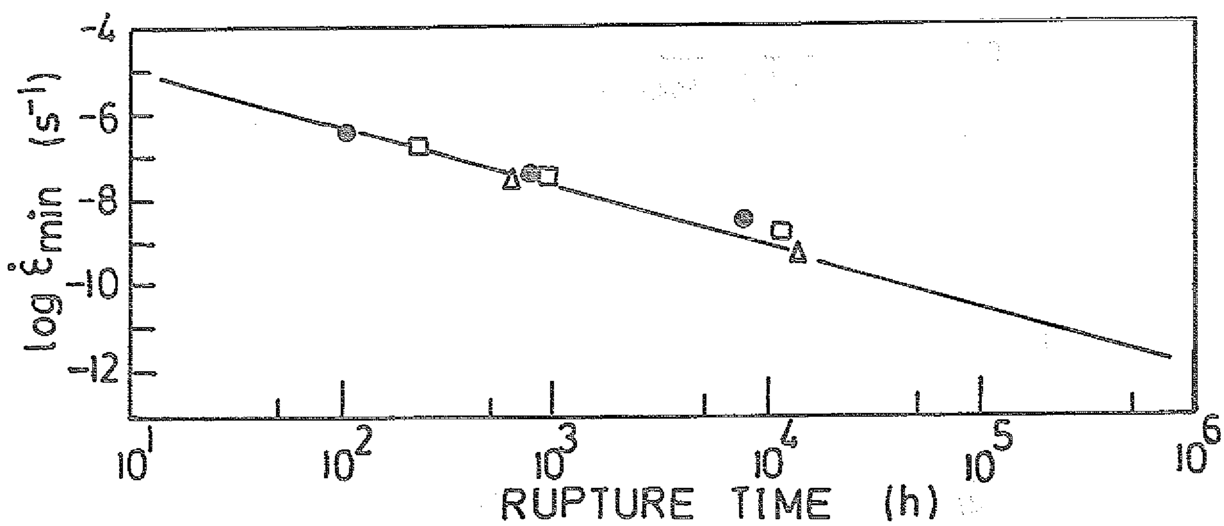

Fig. 25: Relation between minimum creep rate and rupture time for 1Cr0-0.5Mo steel (service exposed).

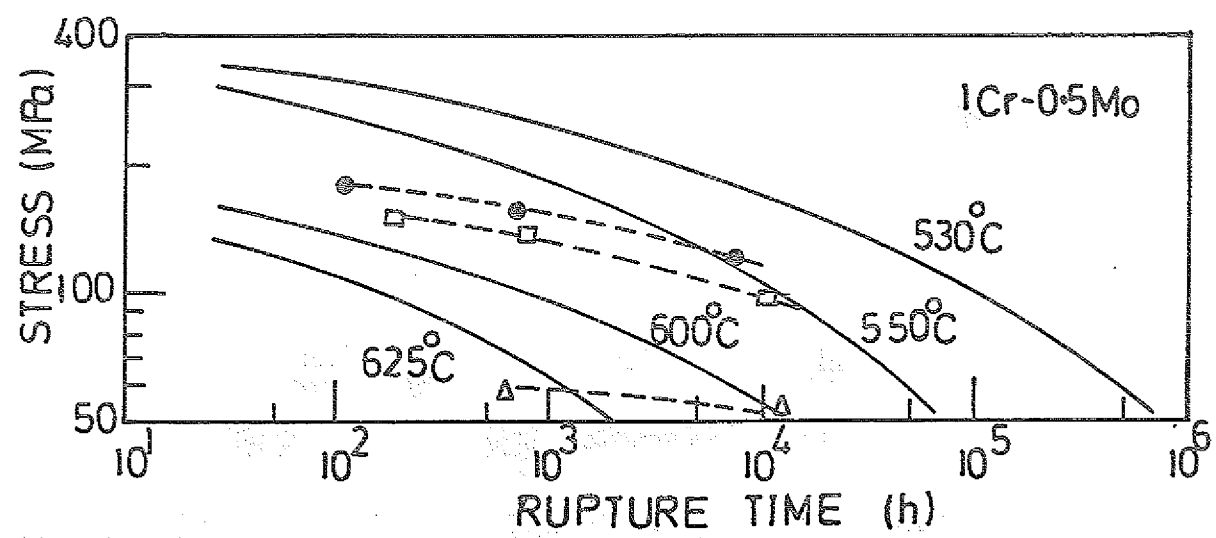

Fig. 26: Relation between minimum creep rate and rupture time for 1Cr0-0.5Mo steel (service exposed). Full lines are for new material.

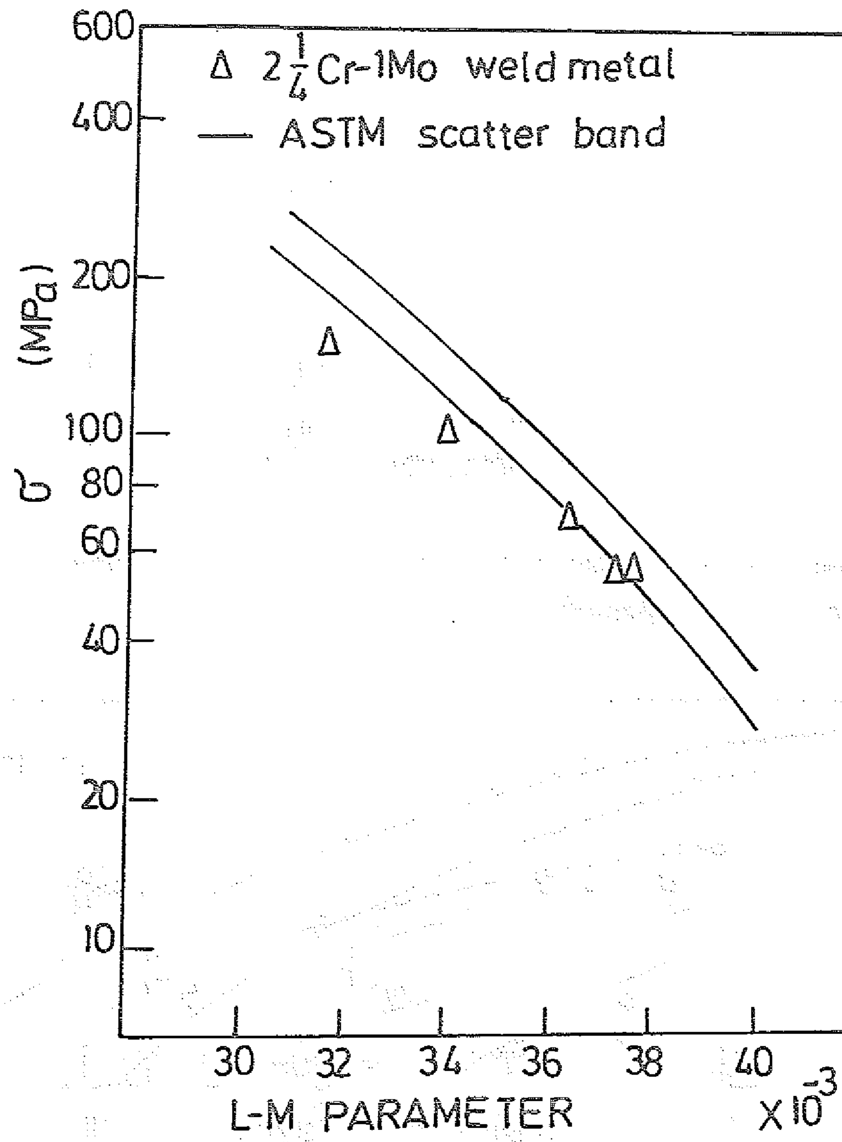

Fig. 27: ASTM scatterband of Larson-Miller parameter for 2.25Cr-1Mo. The data points are for service exposed weld metal.

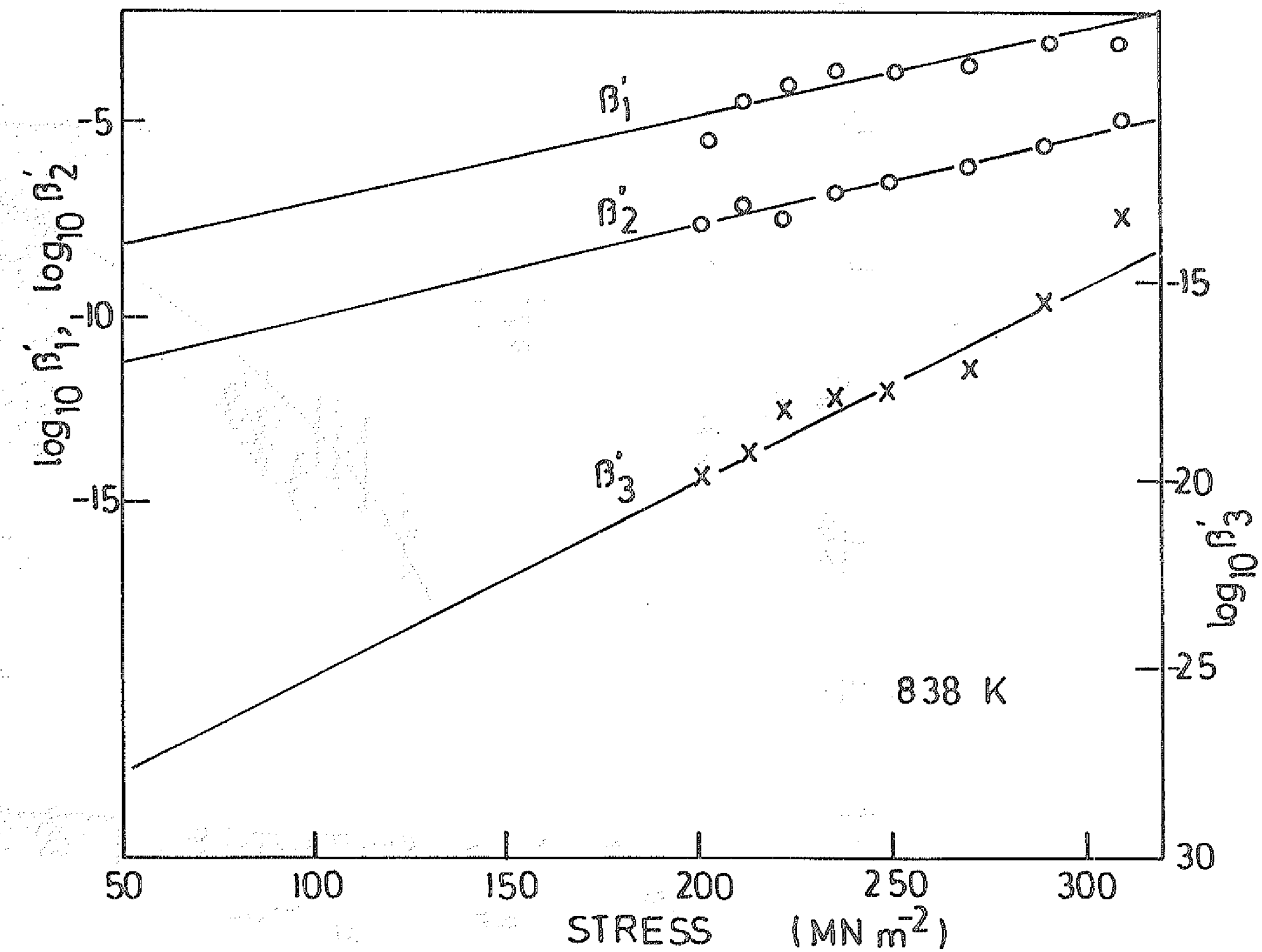

Fig. 28: Variation of the coefficients β'_1, β'_2, and β'_3 with stress for 0.5Cr-0.5-0.25V steel at 838K (565 °C).

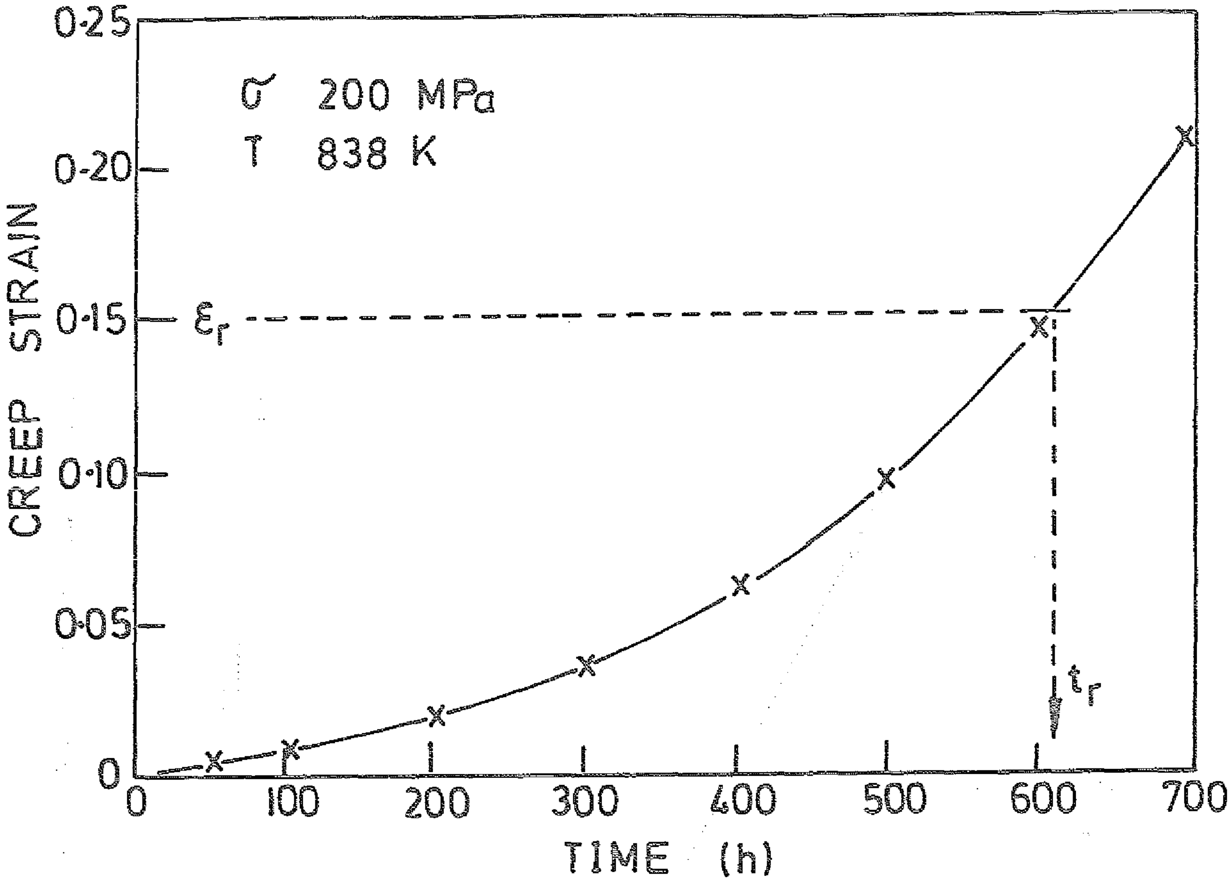

Fig. 29: Variation of creep strain with time for 0.5Cr-0.5Mo-0.25V steel at 838K (565 °C).

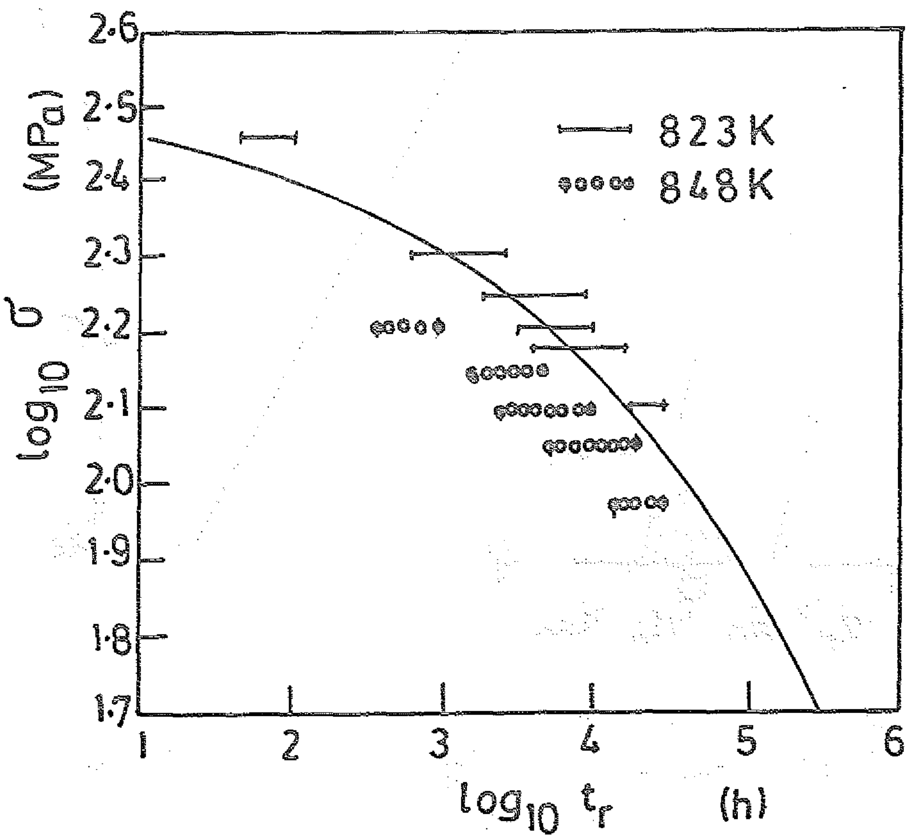

Fig. 30: Relation between stress and rupture time for 0.5Cr-0.5Mo-0.25V steel. The full line is for T = 838K (565 °C).

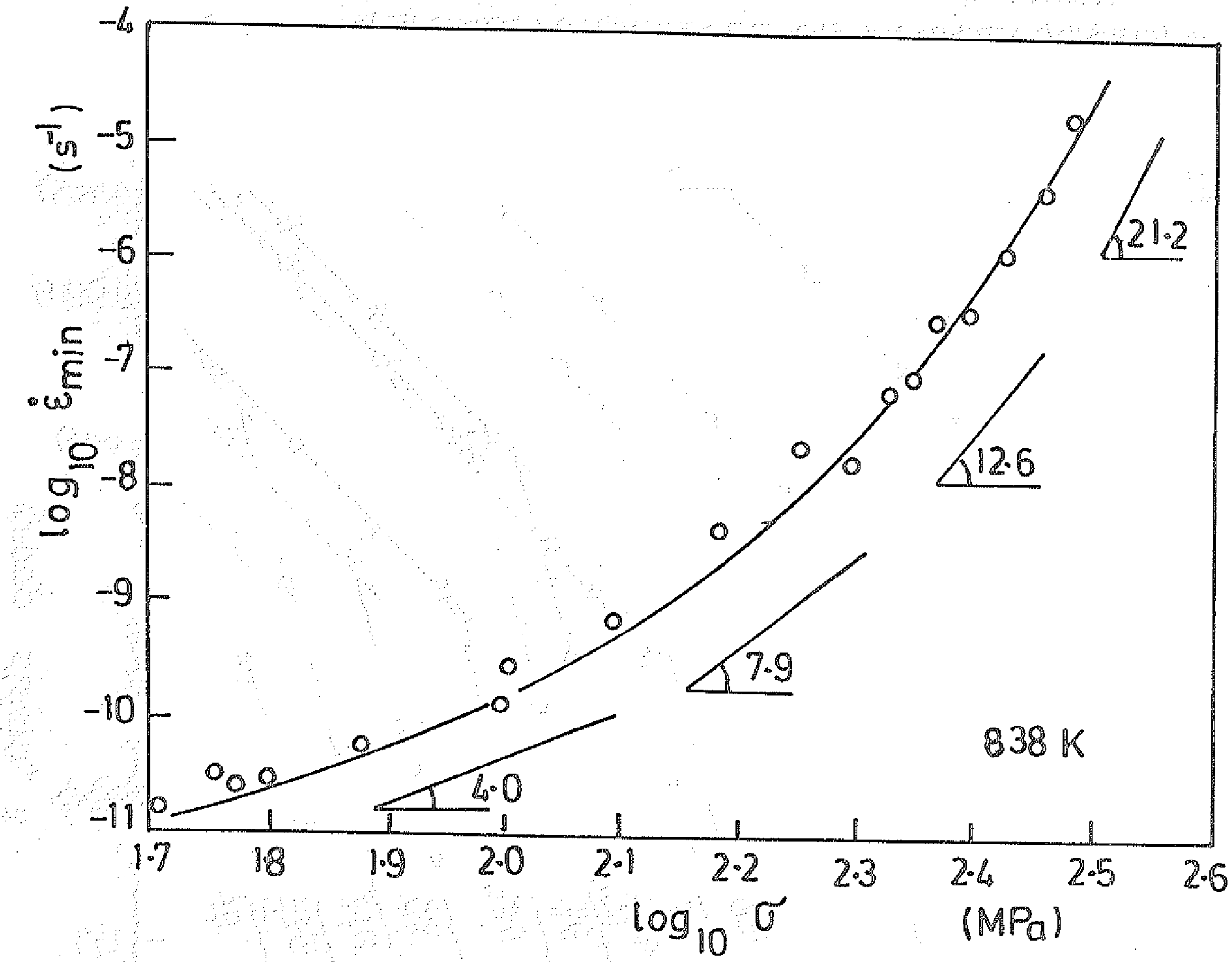

Fig. 31: Relation between the minimum creep rate and the stress for 0.5Cr-0.5Mo-0.25V steel at 838K (565 °C).

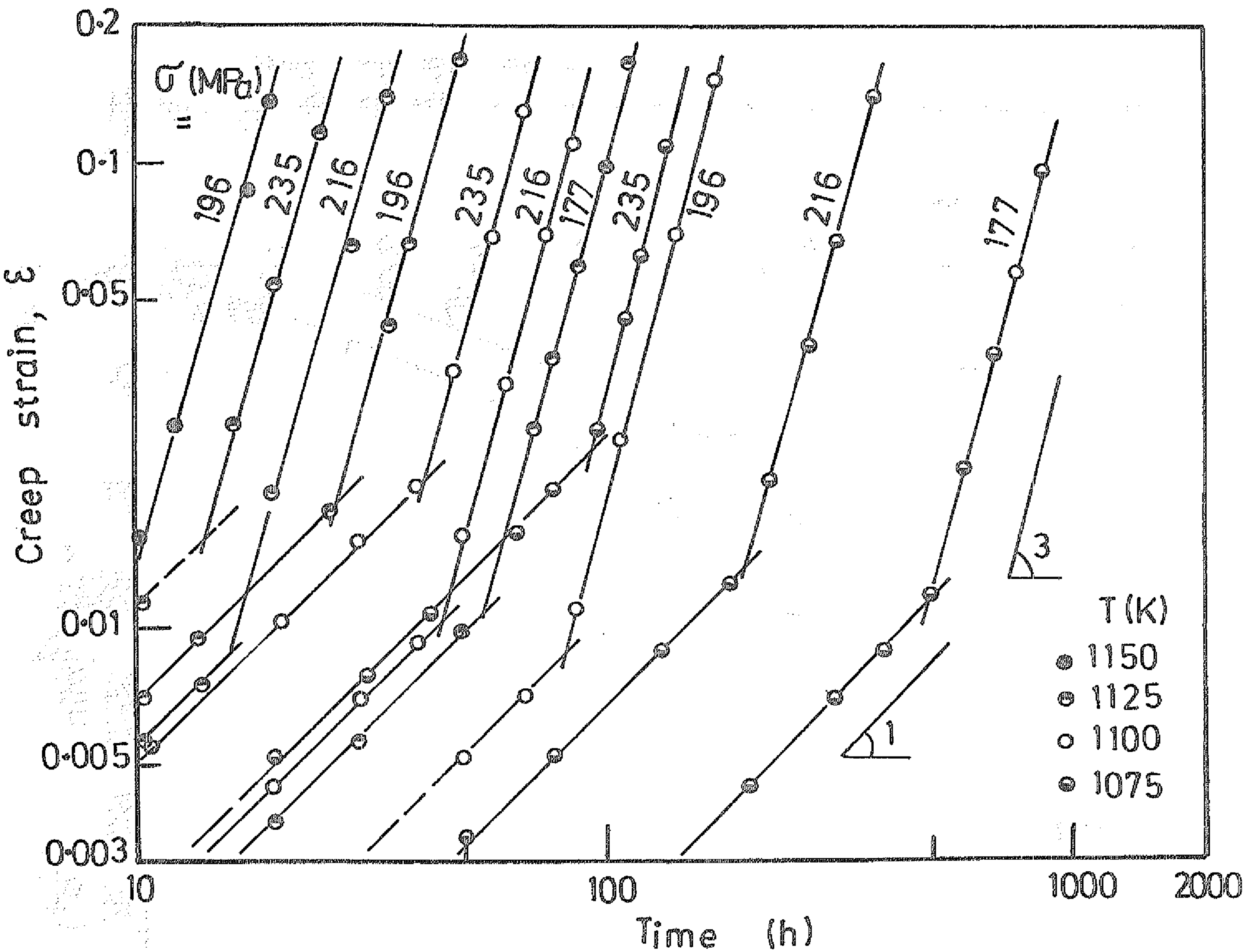

Fig. 32: Relation between creep strain and time of a Ni-base superalloy at 1075K (800 °C), 1100K (825 °C), 1125K (850 °C) and 1150K (875 °C).

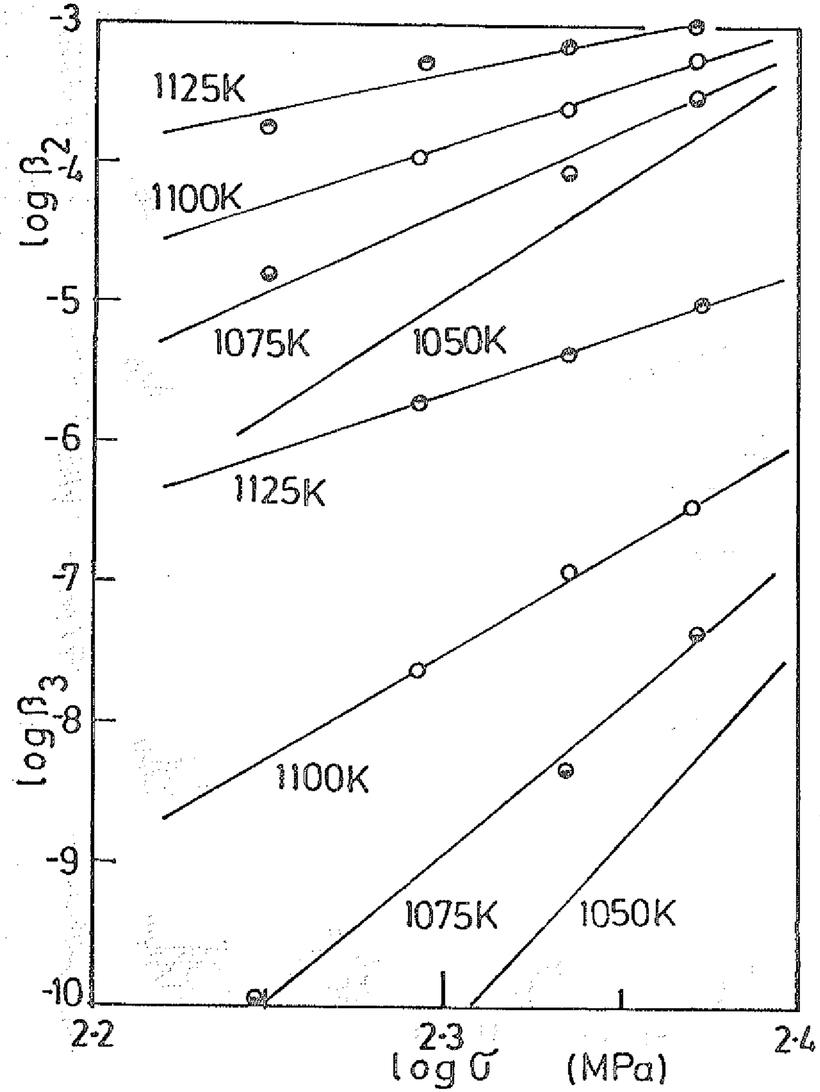

Fig. 33: Relation between stress and the parameters β_2 and β_3 for a Ni-base superalloy.

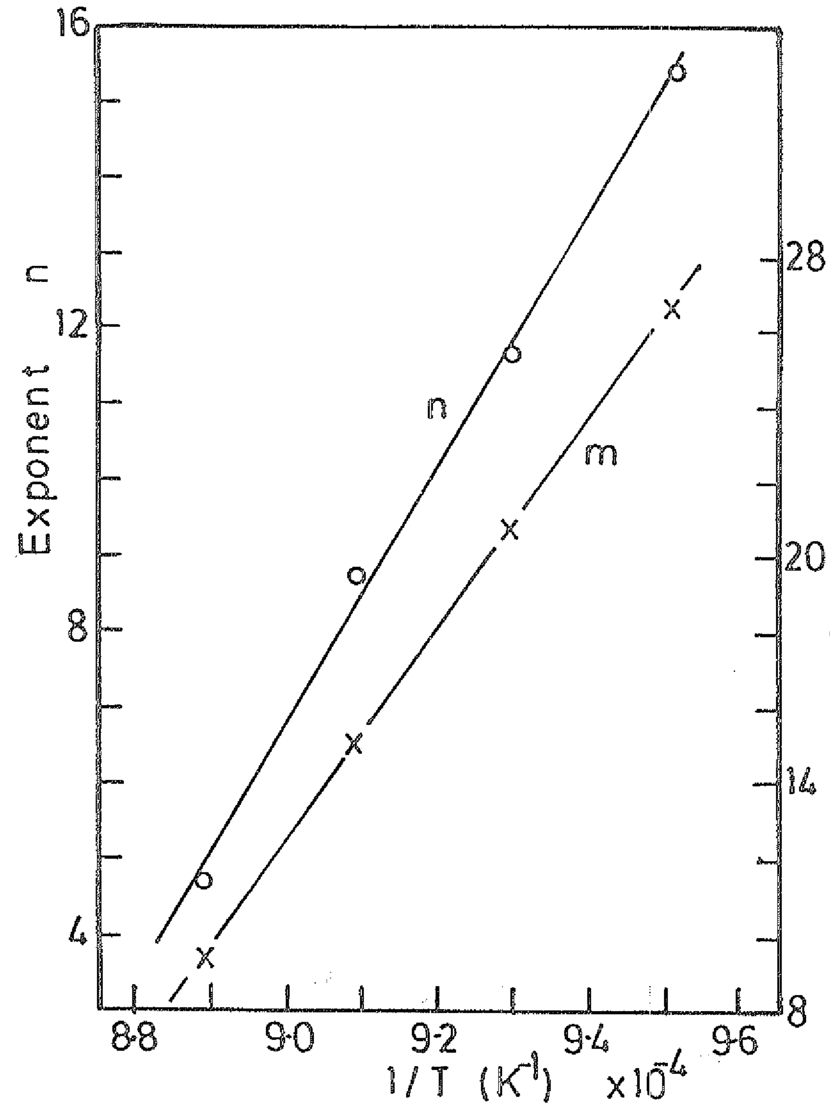

Fig. 34: Relation between the exponents n and m and the inverse temperature for Ni-base superalloy.

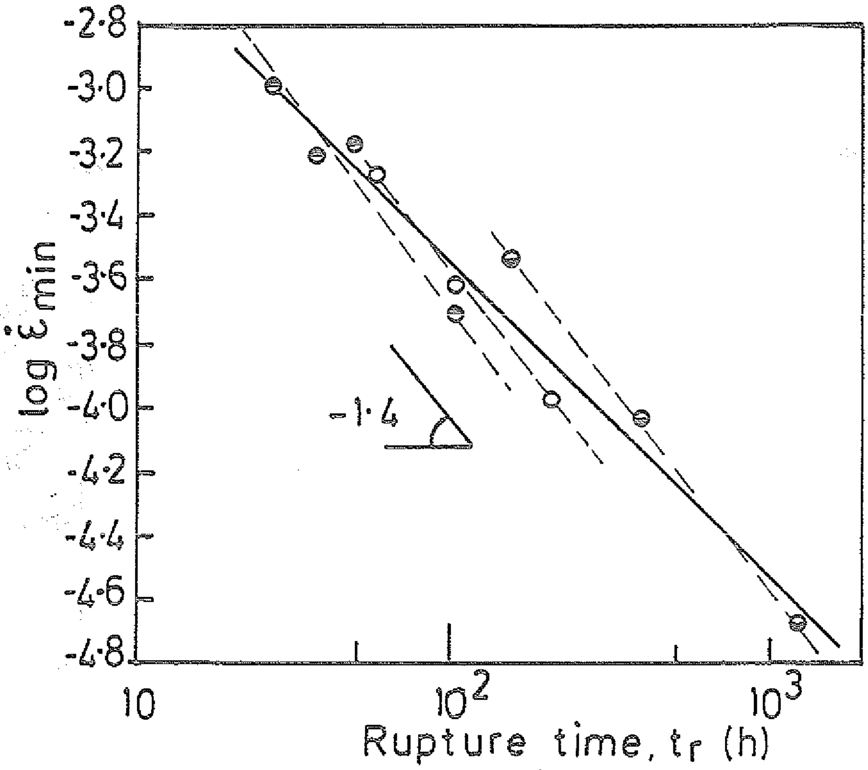

Fig. 35: Relation between minimum creep rate and rupture time for a Ni-base superalloy.

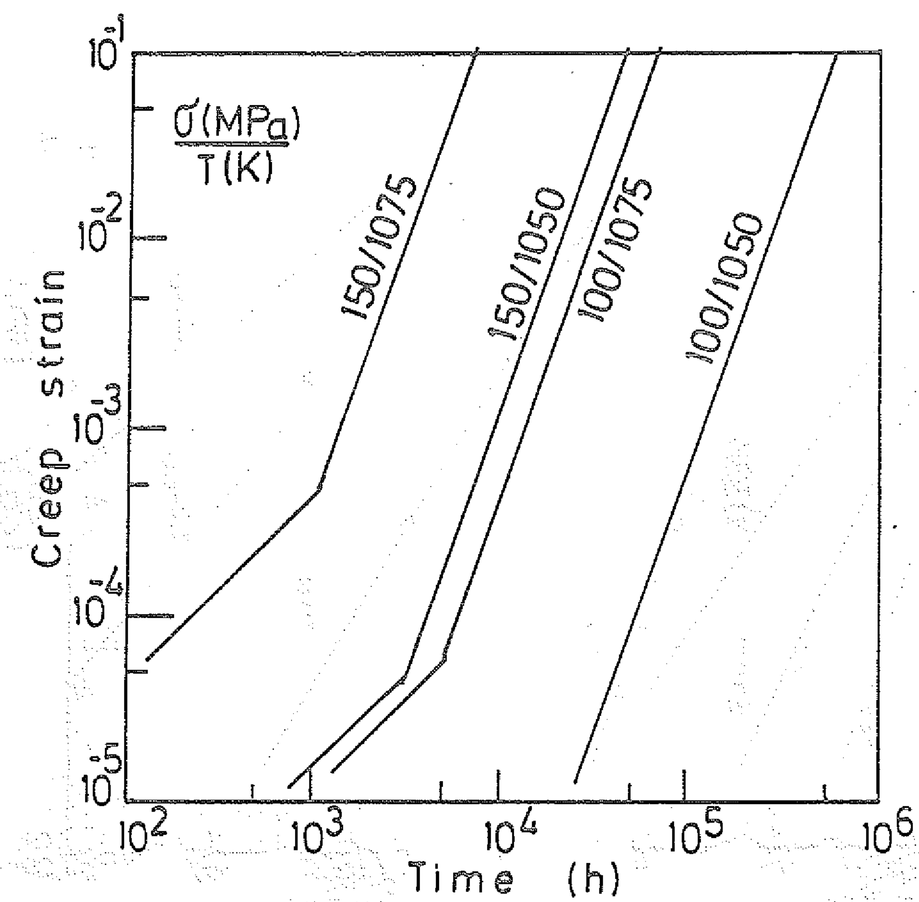

Fig. 36: Predicted variation creep strain with time for a Ni-base superalloy.

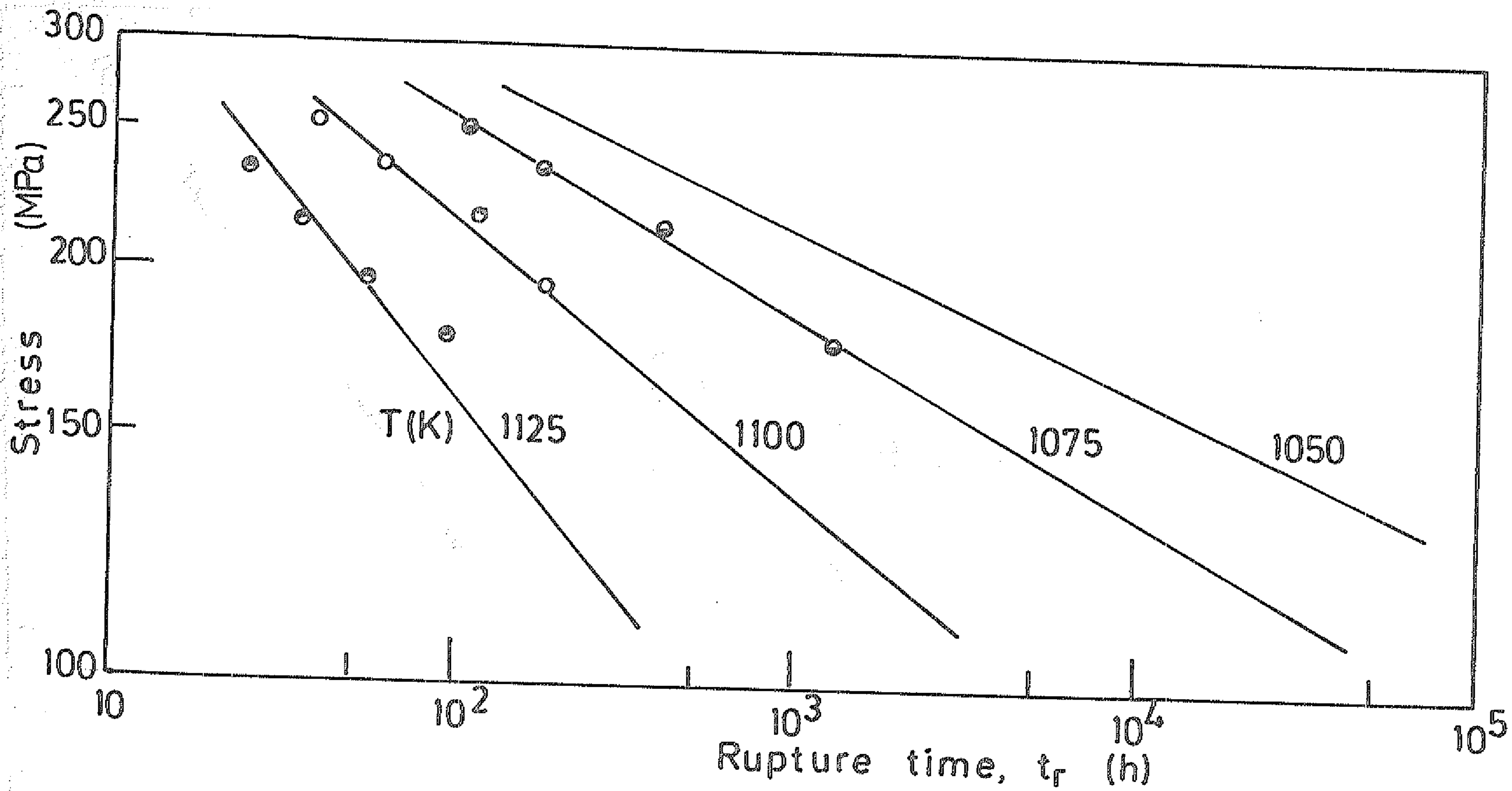

Fig. 37: Relation between stress and rupture time for a Ni-base superalloy.

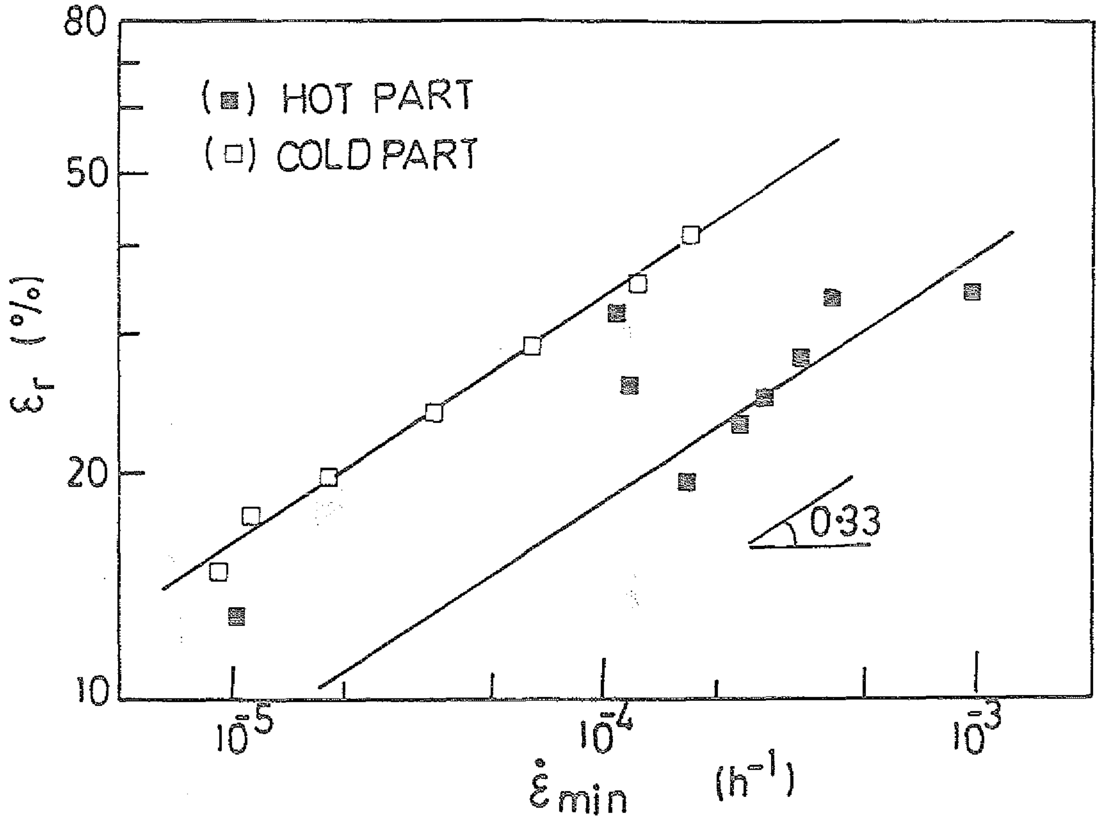

Fig. 38: Relation between minimum creep rate and rupture strain for hot and cold parts of a component of 1Cr-1Mo-0.25V steel at 550 °C.

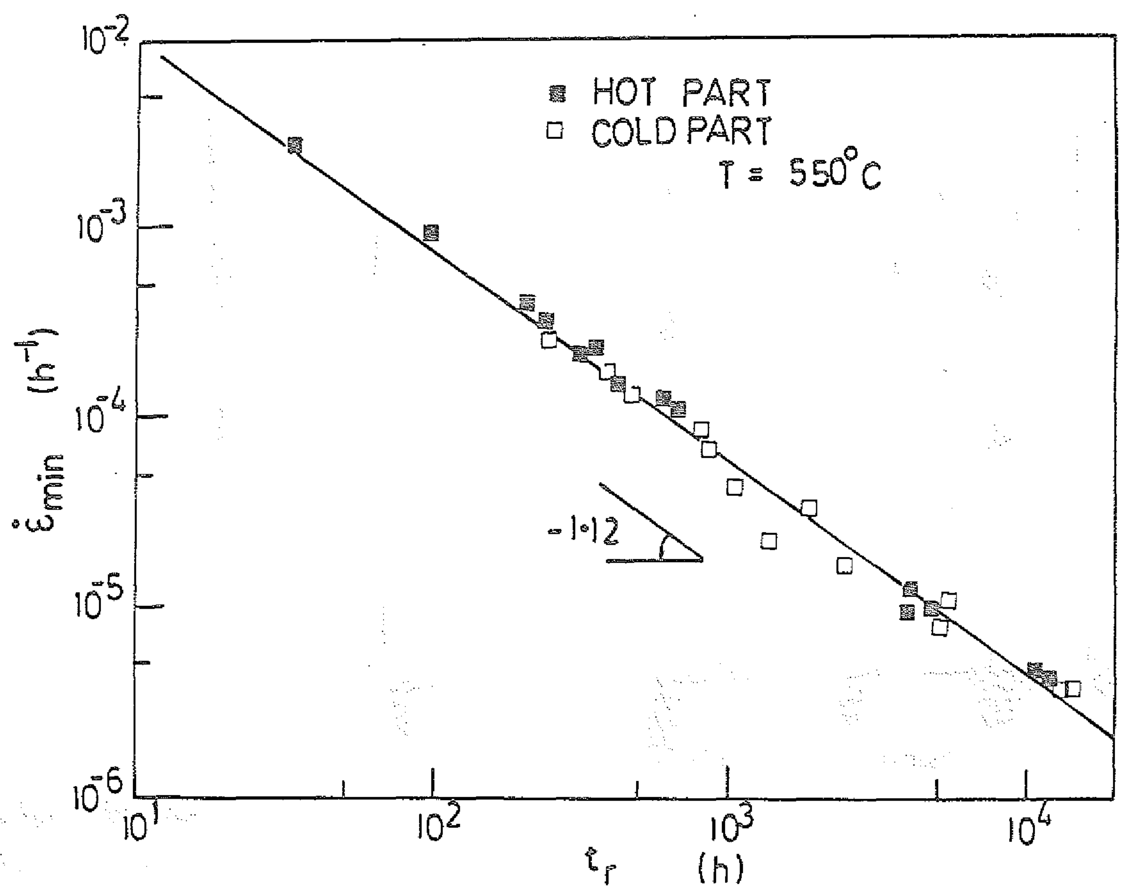

Fig. 39: Relation between minimum creep rate and rupture time of component of 1Cr-1Mo-0.25V steel at 550 °C.

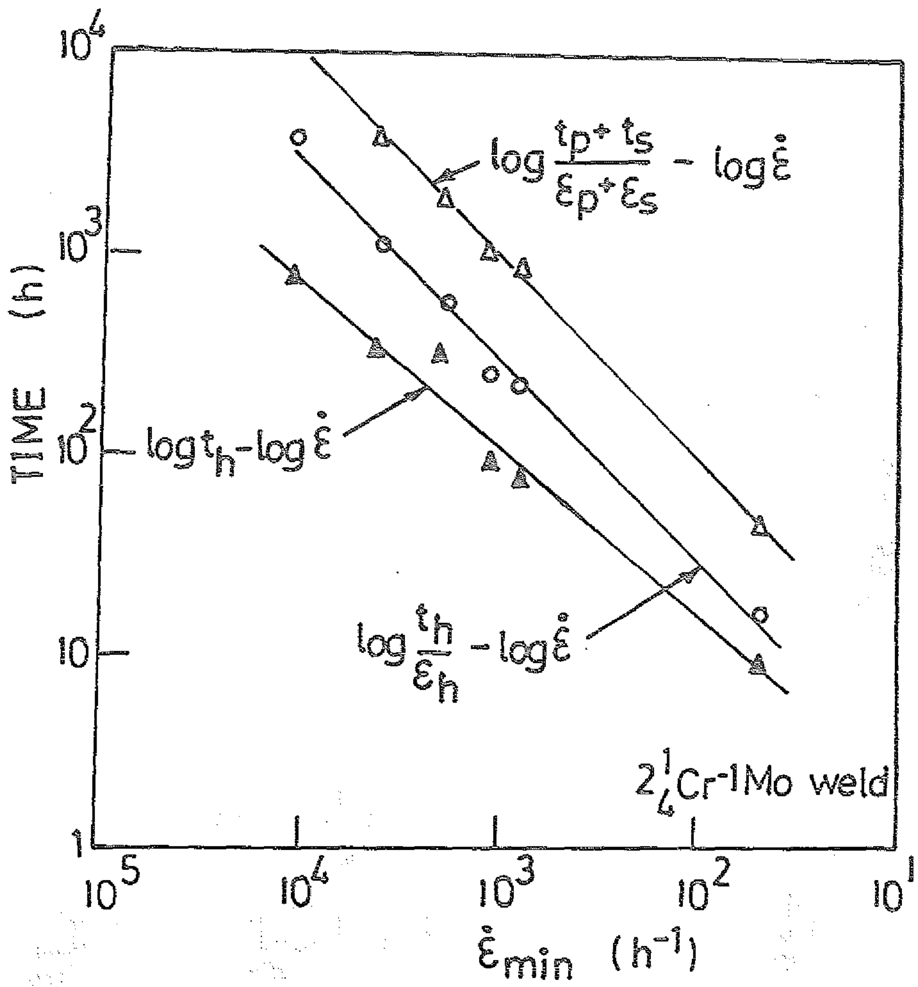

Fig. 40: Creep rate versus rupture time, normalized rupture time, t_n/ε_n and normalized primary and secondary creep time $(t_p+t_s)/\varepsilon_p+\varepsilon_s)$ for 2·25Cr-1Mo steam-pipe weld. Temperatures: 566, 632, 649 and 677 °C.

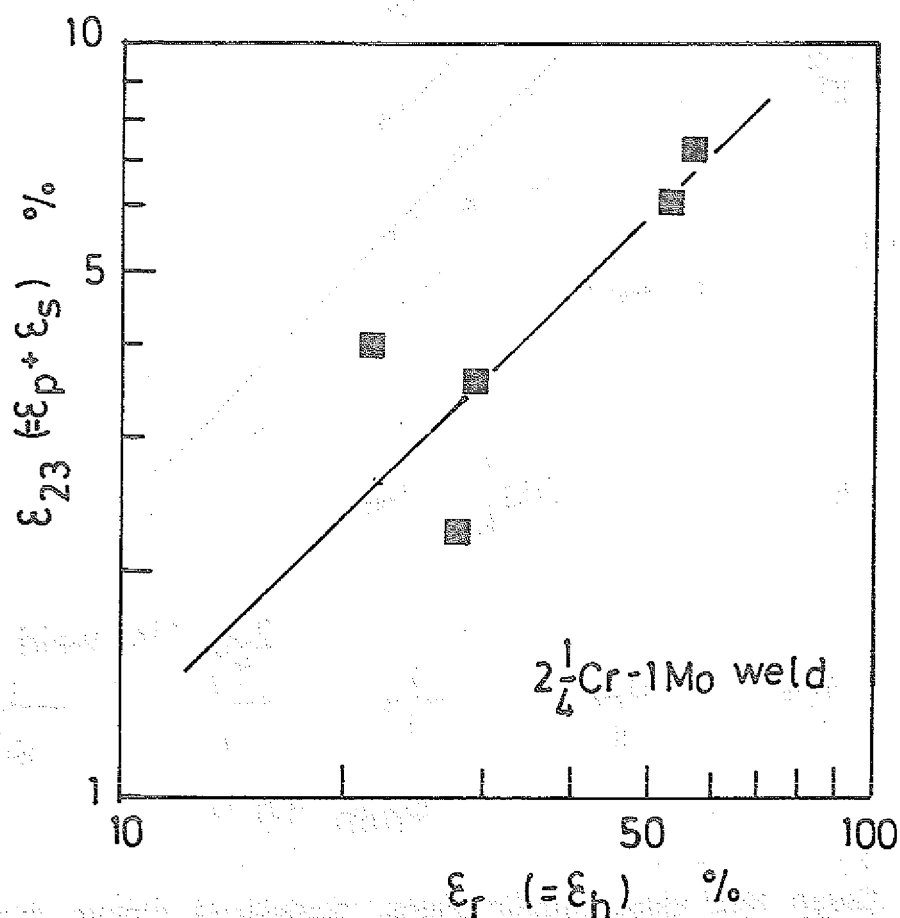

Fig. 41: Relation between the strain at the end of secondary stage and the rupture strain for 2·25Cr-1Mo steam-pipe weld. Temperatures: 566 °C, 632 °C, 649 °C and 677 °C.

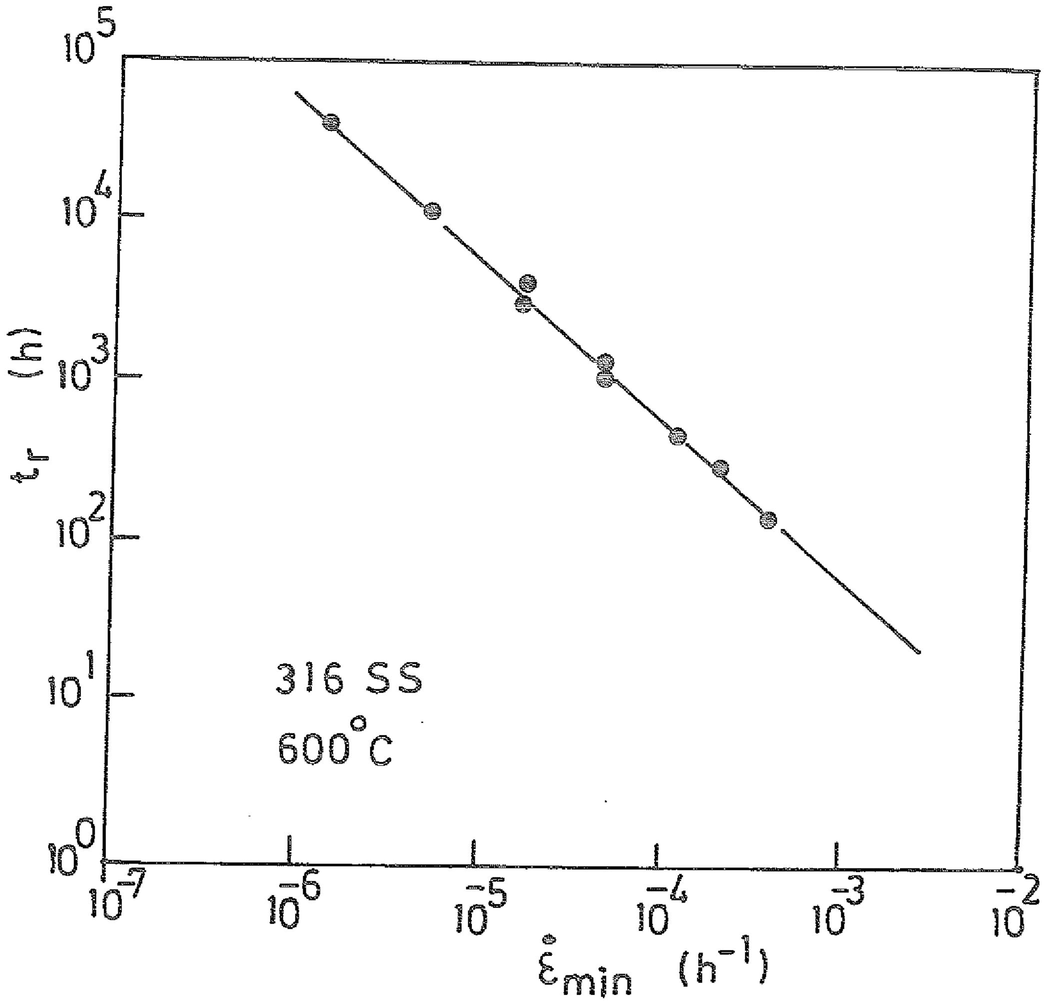

Fig. 42: Relation between the minimum creep rate and the rupture time for Type 316 stainless steel at 600 °C.

FORSCHUNGSZENTRUM JÜLICH GmbH

KFA

Jül-2535
Oktober 1991
ISSN 0366-0885